

**“ROLE OF DIFFUSION WEIGHTED MAGNETIC RESONANCE  
IMAGING AND APPARENT DIFFUSION COEFFICIENT VALUES  
IN DIFFERENTIATING BENIGN FROM MALIGNANT CERVICAL  
LYMPH NODES”**

By

**DR.K.N.MADAN KUMAR.**



**DISSERTATION SUBMITTED TO SRI DEVARAJ URS ACADEMY OF  
HIGHER EDUCATION AND RESEARCH, KOLAR, KARNATAKA**

**In partial fulfilment of the requirements for the degree of  
DOCTOR OF MEDICINE**

**IN**

**RADIODIAGNOSIS**

**Under the Guidance of**

**Dr. ANIL KUMAR SAKALECHA, MBBS, M.D  
PROFESSOR OF RADIODIAGNOSIS**

**&**

**Co-guidance of**

**Dr. HEMALATHA, MBBS, M.D  
PROFESSOR OF PATHOLOGY**



**DEPARTMENT OF RADIODIAGNOSIS, SRI DEVARAJ URS  
MEDICALCOLLEGE, TAMAKA, KOLAR-563101  
2023**

**SRI DEVARAJ URS ACADEMY OF HIGHER EDUCATION AND  
RESEARCH, TAMAKA, KOLAR, KARNATAKA**

**DECLARATION BY THE CANDIDATE**

I hereby declare that this dissertation entitled “**ROLE OF DIFFUSION WEIGHTED MAGNETIC RESONANCE IMAGING AND APPARENT DIFFUSION COEFFICIENT VALUES IN DIFFERENTIATING BENIGN FROM MALIGNANT CERVICAL LYMPH NODES**” is a bonafide and genuine research work carried out by me under the guidance of **Dr. ANIL KUMAR SAKALECHA**, Professor, Department of Radio-diagnosis, Sri Devaraj Urs Medical College, Kolar, in partial fulfilment of University regulation for the award “**M. D. DEGREE IN RADIODIAGNOSIS**”, the examination to be held in 2023 by SDUAHER. This has not been submitted by me previously for the award of degree from the university or any other university.

**Date:**

**DR. MADAN KUMAR.**

Postgraduate in Radiodiagnosis  
Sri Devaraj Urs Medical College  
Tamaka, Kolar.

**SRI DEVARAJ URS ACADEMY OF HIGHER EDUCATION AND  
RESEARCH, TAMAKA, KOLAR, KARNATAKA**

**CERTIFICATE BY THE GUIDE**

This is to certify that the dissertation entitled **“ROLE OF DIFFUSION WEIGHTED MAGNETIC RESONANCE IMAGING AND APPARENT DIFFUSION COEFFICIENT VALUES IN DIFFERENTIATING BENIGN FROM MALIGNANT CERVICAL LYMPH NODES”** is a bonafide research work done by **DR. MADAN KUMAR**, under my direct guidance and supervision at Sri Devaraj Urs Medical College, Kolar, in partial fulfilment of the requirement for the degree of **“M.D. RADIODIAGNOSIS”**.

**Date:**

**Dr. ANIL KUMAR SAKALECHA, MBBS, MD**

**Place: Kolar**

Professor and HOD,  
Department of Radiodiagnosis  
Sri Devaraj Urs Medical College  
Tamaka, Kolar

**SRI DEVARAJ URS ACADEMY OF HIGHER EDUCATION AND  
RESEARCH, TAMAKA, KOLAR, KARNATAKA**

**CERTIFICATE BY THE HEAD OF DEPARTMENT**

This is to certify that the dissertation entitled **“ROLE OF DIFFUSION WEIGHTED MAGNETIC RESONANCE IMAGING AND APPARENT DIFFUSION COEFFICIENT VALUES IN DIFFERENTIATING BENIGN FROM MALIGNANT CERVICAL LYMPH NODES”** is a bonafide research work done by **DR. MADAN KUMAR**, under my supervision at Sri Devaraj Urs Medical College, Kolar, in partial fulfilment of the requirement for the degree of **“M.D. RADIODIAGNOSIS”**.

**Date:**

**Dr. ANIL KUMAR SAKALECHA, MBBS, MD**

**Place: Kolar**

Professor & HOD

Department Of Radiodiagnosis

Sri Devaraj Urs medical college & hospital  
Tamaka, Kolar.

**SRI DEVARAJ URS ACADEMY OF HIGHER EDUCATION AND  
RESEARCH, TAMAKA, KOLAR, KARNATAKA**

**ENDORSEMENT BY THE HEAD OF THE DEPARTMENT AND  
PRINCIPAL**

This is to certify that the dissertation entitled, “**ROLE OF DIFFUSION WEIGHTED MAGNETIC RESONANCE IMAGING AND APPARENT DIFFUSION COEFFICIENT VALUES IN DIFFERENTIATING BENIGN FROM MALIGNANT CERVICAL LYMPH NODES**” is a bonafide research work done by **Dr. MADAN KUMAR.** under the direct guidance and supervision of **Dr. ANIL KUMAR SAKALECHA,** HOD & Professor, Department of Radio-diagnosis, Sri Devaraj Urs Medical College, Kolar, in partial fulfilment of University regulation for the award “**M.D. DEGREE IN RADIODIAGNOSIS**”.

**Dr. ANIL KUMAR SAKALECHA**

Professor & HOD

Department Of Radiodiagnosis,  
Sri Devaraj Urs Medical College,  
Tamaka, Kolar.

**DR. P.N.SREERAMULU**

Principal,

Sri Devaraj Urs Medical College,  
Tamaka,  
Kolar.

**Date:**

**Place: Kolar**

**Date:**

**Place: Kolar**

**SRI DEVARAJ URS ACADEMY OF HIGHER EDUCATION AND RESEARCH  
TAMAKA, KOLAR, KARNATAKA**

**ETHICAL COMMITTEE CERTIFICATE**

This is to certify that the Ethical committee of Sri Devaraj Urs Medical College, Tamaka,  
Kolar has unanimously approved

**DR. MADAN KUMAR.**

**Post-Graduate student in the subject of**

**RADIODIAGNOSIS at Sri Devaraj Urs Medical College, Kolar**

**to take up the Dissertation work entitled**

**“ROLE OF DIFFUSION WEIGHTED MAGNETIC RESONANCE IMAGING  
AND APPARENT DIFFUSION COEFFICIENT VALUES IN  
DIFFERENTIATING BENIGN FROM MALIGNANT CERVICAL LYMPH  
NODES”**

to be submitted to the

**SRI DEVARAJ URS ACADEMY OF HIGHER EDUCATION AND  
RESEARCH, TAMAKA, KOLAR, KARNATAKA.**

**Date:**  
**Place: Kolar**

Signature of Member Secretary  
Ethical Committee

**SRI DEVARAJ URS ACADEMY OF HIGHER EDUCATION AND  
RESEARCH TAMAKA, KOLAR, KARNATAKA**

**COPY RIGHT DECLARATION BY THE CANDIDATE**

I hereby declare that Sri Devaraj Urs Academy of Higher Education and Research, Kolar, Karnataka shall have the rights to preserve, use and disseminate this dissertation/thesis in print or electronic format for academic/research purpose.

**Date:**

**Place: Kolar**

**DR. MADAN KUMAR**

Postgraduate

Department of Radio-diagnosis

Sri Devaraj Urs Medical College

Tamaka, Kolar

## **ACKNOWLEDGEMENT**

*I owe debt and gratitude to my parents **K.NAMASIVAYAM & N.SUMATHI**, My brother **K.N.HARSHATH KUMAR** for their moral support and constant encouragement during the study.*

*With humble gratitude and great respect, I would like to thank my teacher, mentor and guide, **DR. ANIL KUMAR SAKALECHA**, Professor, Department of Radiodiagnosis, Sri Devaraj Urs Medical College, Kolar, for his able guidance, constant encouragement, immense help and valuable advices which went a long way in moulding and enabling me to complete this work successfully. Without his initiative and constant encouragement this study would not have been possible. His vast experience, knowledge, able supervision and valuable advices have served as a constant source of inspiration during the entire course of my study.*

*I would like to express my sincere thanks to **Dr. HEMALATHA.**, Professor Department of Pathology, Sri Devaraj Urs Medical College for her valuable support, guidance and encouragement throughout the study.*

*I would also like to thank **DR.DEEPTI NAIK** Professor, **Dr. RAJESWARI** Asso. Prof. **Dr. HARINI BOPAIAH** Asso. Prof. **DR.ANEES** Asst. prof. and **Dr. RAHUL DEEP** Asst. prof. Department of Radio-diagnosis, Sri Devaraj Urs Medical College for their whole hearted support and guidance.*

*I would like to thank **Dr.DARSHAN, Dr.PARAMESHWAR KEERTHI, Dr. VINEELA, Dr. AASHISH, Dr. MONISHA V, Dr. CHAITANYA, Dr. YASHAS ULLAS Dr. VARSHITHA G.R.** and all my teachers of Department of Radio diagnosis, Sri Devaraj Urs Medical College and Research Institute, Kolar, for their constant guidance and encouragement during the study period.*

*I am extremely grateful to the patients who volunteered for this study, without them this study would just be a dream.*

*I am thankful to my postgraduates **Dr. ARUN, Dr. NIKHIL, Dr. SANDEEP Dr. UHASAI, Dr. LYNN JOY, Dr. MAHIMA KALE, Dr. PRAVEEN, Dr. REVANTH, Dr. GURU YOGENDRA, Dr. SIVA, Dr. KRISHNA, Dr. MANNAN, Dr. GAURAV, Dr. RISHI, Dr. POOJA and Dr. SHANTALA** for having rendered all their co-operation and help to me during my study.*

*I am also thankful to **Mr. RAVI, and Mr. SUBRAMANI** with other **technicians** of Department of Radiodiagnosis, R.L Jalappa Hospital & Research Centre, Tamaka, Kolar for their help. My sincere thanks to **Mr. SUNIL, Mrs. NASEEBA, Mrs. HAMSA** and rest of the computer operators.*

## Turnitin Originality Report

Document Viewer

Processed on: 30-Jan-2023 15:12 IST  
ID: 2002399511  
Word Count: 8904  
Submitted: 1

*Madan*  
**Professor & Head**  
**Dept. of Radio-Diagnosis,**  
**tri Devaraj Urs Medical College**  
**Tamaka KOLAR-563 101**

**ROLE OF DIFFUSION  
WEIGHTED MAGNETIC  
RESONANCE... By Madan  
Kumar**

*30/1/23*  
**University Library**  
**Learning Resource Centre**  
**SDUAHER, Tamaka**  
**KOLAR-563103**

Similarity Index

9%

Similarity by Source

Internet Sources:	7%
Publications:	9%
Student Papers:	1%

☐ include quoted ☐ include bibliography ☐ excluding matches < 14 words

mode:

1% match (Internet from 23-Dec-2015)

<http://www.egms.de>

1% match (Internet from 26-Dec-2022)

<https://cyberleninka.org/article/n/364671>

1% match ()

[Febin Ross Joseph Jeyamony, "Role of Magnetic Resonance Imaging Diffusion Weighted and Apparent Diffusion Coefficient Evaluation in Brain Infarction", 2020](#)

&lt;1% match (Internet from 08-Mar-2022)

[https://assets.cureus.com/uploads/original\\_article/pdf/83892/20220218-4408-1iqd88k.pdf](https://assets.cureus.com/uploads/original_article/pdf/83892/20220218-4408-1iqd88k.pdf)

&lt;1% match (Internet from 16-Nov-2022)

[https://assets.cureus.com/uploads/original\\_article/pdf/85315/20220409-641-11ncx7b.pdf](https://assets.cureus.com/uploads/original_article/pdf/85315/20220409-641-11ncx7b.pdf)

&lt;1% match (Internet from 09-Apr-2022)

[https://link.springer.com/article/10.1007/s00330-020-07587-x?code=7060ef51-e1f2-4331-8a5e-eb320b4c5334&error=cookies\\_not\\_supported](https://link.springer.com/article/10.1007/s00330-020-07587-x?code=7060ef51-e1f2-4331-8a5e-eb320b4c5334&error=cookies_not_supported)

<1% match (Head & Neck Cancer Current Perspectives Advances and Challenges, 2013.)

[Head & Neck Cancer Current Perspectives Advances and Challenges, 2013.](#)

<1% match ("Radiological Imaging in Hematological Malignancies", Springer Science and Business Media LLC, 2004)

["Radiological Imaging in Hematological Malignancies", Springer Science and Business Media LLC, 2004](#)

&lt;1% match (Internet from 08-Dec-2017)

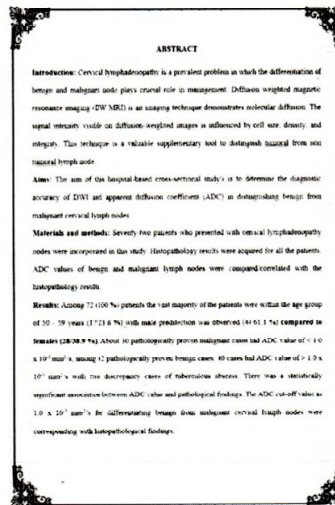



## Digital Receipt

This receipt acknowledges that Turnitin received your paper. Below you will find the receipt information regarding your submission.

The first page of your submissions is displayed below.

Submission author: Madan Kumar  
Assignment title: ROLE OF DIFFUSION WEIGHTED MAGNETIC RESONANCE IMA...  
Submission title: ROLE OF DIFFUSION WEIGHTED MAGNETIC RESONANCE IMA...  
File name: DWMRI\_plag\_-\_1.docx  
File size: 11.73M  
Page count: 96  
Word count: 8,904  
Character count: 49,147  
Submission date: 30-Jan-2023 03:11PM (UTC+0530)  
Submission ID: 2002399511



  
30/1/23  
University Library  
Learning Resource Centre  
SDUAHER, Tamaka  
KOLAR-563103





**SRI DEVARAJ URS ACADEMY OF HIGHER EDUCATION & RESEARCH**  
Tamaka, Kolar 563103


**Certificate of Plagiarism Check**


<b>Title of the Thesis/Dissertation</b>	ROLE OF DIFFUSION WEIGHTED MAGNETIC RESONANCE IMAGING AND APPARENT DIFFUSION COEFFICIENT VALUES IN DIFFERENTIATING BENIGN FROM MALIGNANT CERVICAL LYMPH NODES
<b>Name of the Student</b>	Dr. K.N.MADAN KUMAR
<b>Registration Number</b>	20RD1026
<b>Name of the Supervisor / Guide</b>	Dr. ANIL KUMAR SAKALECHA
<b>Department</b>	RADIOLOGY
<b>Acceptable Maximum Limit (%) of Similarity</b> (PG Dissertation /Ph.D. Thesis)	10%
<b>Similarity</b>	9 %
<b>Software used</b>	Turnitin
<b>Paper ID</b>	2002399511
<b>Submission Date</b>	30/01/2023

  
Signature of Student

  
Signature of Guide/Supervisor

  
HOD Signature  
Prof. & HOD  
Dept. of Radiodiagnosis  
Sri Devaraj Urs Medical College  
Tamaka, Kolar-563101.

  
University Librarian  
Library  
Learning Resource Centre  
SDUAHER, Tamaka  
KOLAR-563103

  
Coordinator UG and PG Program  
Co-Ordinator,  
UG&PG Program ,Faculty of Medicine,  
Sri Devarj Urs Medical College ,  
Tamaka, Kolar- 563103

## LIST OF ABBREVIATIONS

GLOSSARY	ABBREVIATIONS
TB	Tuberculosis
DWI	Diffusion-weighted MR imaging
ADC	Apparent Diffusion Coefficient
DW-MRI	Diffusion-Weighted Magnetic Resonance Imaging
IJV	Internal Jugular Vein
MALT	Mucosa-Associated Lymphoid Tissue
EBV	Epstein Barr Virus
CMV	Cytomegalovirus
HIV	Human Immunodeficiency Virus
SCC	Squamous Cell Carcinoma
MUO	Metastasis from Unknown Origin
TNM	Tumor, Node, and Metastasis
CDI	Colour Doppler Imaging
RI	Resistivity Index
PI	Pulsatility Index
SWE	Shear Wave Elastography
ARFI	Acoustic Radiation Force Impulse
VTI	Virtual Touch Tissue Imaging
CT	Computed Tomography
CTP	CT Perfusion Imaging
BF	Blood Flow
BV	Blood Volume
MTT	Mean Transit Time

## ABSTRACT

**Introduction:** Cervical lymphadenopathy is a prevalent problem in which the differentiation of benign and malignant node plays crucial role in management. Diffusion weighted magnetic resonance imaging (DW MRI) is an imaging technique demonstrates molecular diffusion. The signal intensity visible on diffusion-weighted images is influenced by cell size, density, and integrity. This technique is a valuable supplementary tool to distinguishing benign from malignant lymph node.

**Aims:** The aim of this hospital-based cross-sectional study's is to determine the diagnostic accuracy of DWI and apparent diffusion coefficient (ADC) in distinguishing benign from malignant cervical lymph nodes.

**Materials and methods:** Seventy-two patients who presented with cervical lymphadenopathy nodes were included in this study. Histopathology results were obtained for all the patients. ADC values of benign and malignant lymph nodes were correlated with the histopathology results.

**Results:** Among 72 (100 %) patients the vast majority of the patients were within the age group of 50 – 59 years (17/23.6 %) with male predilection was observed (44/61.1 %) compared to females (28/38.9 %). About 30 pathologically proven malignant cases had ADC value of  $< 1.0 \times 10^{-3} \text{ mm}^2/\text{s}$ , among 42 pathologically proven benign cases, 40 cases had ADC value of  $> 1.0 \times 10^{-3} \text{ mm}^2/\text{s}$  with two discrepancy cases of tuberculous abscess. There was a statistically significant association between ADC value and pathological findings. The ADC cut-off value as  $1.0 \times 10^{-3} \text{ mm}^2/\text{s}$  for differentiating benign from malignant cervical lymph nodes were corresponding with histopathological findings.

The difference in the proportion of pathological findings between ADC values of benign and malignant lesions was statistically significant ( $P < 0.001$ ). The ADC cut-off value of  $1.0 \times 10^{-3} \text{ mm}^2/\text{s}$  for cervical lymph nodes had overall sensitivity and specificity of 100 % & 95.24 % with excellent positive and negative predictive validity of 93.75 % & 100 % and the total diagnostic accuracy was 97.22 %.

**Conclusions:** MRI is an excellent modality for diagnosing and characterising cervical lymph nodes at various levels. In adjunct with conventional MRI, diffusion weighted imaging and ADC is an important supportive and diagnostic tool in differentiating between benign and malignant cervical lymph nodes.

**Key words:** Diffused Weighted MRI, Cervical Lymphadenopathy, ADC.



## TABLE OF CONTENTS

S. NO	TOPIC	PAGE NO
1.	INTRODUCTION	1
2.	AIMS & OBJECTIVES	3
3.	REVIEW OF LITERATURE	4
4.	MATERIALS & METHODS	52
5.	RESULTS	56
6.	IMAGES	68
7.	DISCUSSION	77
8.	CONCLUSION	84
9.	SUMMARY	85
10.	LIMITATIONS AND RECOMMENDATIONS	88
11.	BIBLIOGRAPHY	89
12.	ANNEXURE	99

## LIST OF TABLES

S.NO	TABLE DESCRIPTION	PAGE NO
1.	Classification of head and neck group of lymph nodes	12
2.	Infective causes of cervical lymphadenopathy	24
3.	Immunologic disorders causing cervical lymphadenopathy	26
4.	Metabolic disorders causing cervical lymphadenopathy	27
5.	First echelon lymph nodes for various primary sites	31
6.	Clinical N staging	32
7.	Age wise distribution of patients	56
8.	Gender wise distribution of patients	57
9.	Distribution of patients based on side of lymph node	58
10.	Distribution of patients based on size of lymph node	59
11.	Distribution of patients based on number of lymph node	60
12.	Distribution of patients based on level of lymph nodes	61
13.	Distribution of patients based on margin of lymph nodes	62
14.	Distribution of patients based on shape of lymph nodes	63
15.	Distribution of patients based on pathological diagnosis	64
16.	Distribution of patients based on restricted diffusion	65
17.	Comparison of ADC and pathological findings	66
18.	Validity of ADC	67
19.	Validity of DWMRI, ADC and pathology diagnosis	67

## LIST OF FIGURES

<b>S.NO</b>	<b>FIGURE DESCRIPTION</b>	<b>PAGE NO.</b>
1.	Lymph sacs	5
2.	Development of thoracic duct and right lymphatic duct	6
3.	Anatomy of lymph node	8
4.	Histology of lymph node	9
5.	Structures of the neck with its lymphatic drainage	10
6.	Sub mental and anterior compartment group of lymph nodes	14
7.	Levels of cervical lymph nodes	18
8.	Levels of lymph nodes on MRI sagittal section	20
9.	Superficial and deep lymphatic node groups of head & neck	21
10.	Ultrasound appearance of normal cervical lymph node	33
11.	Elastogram patterns of lymph node on strain elastography	36
12.	Contrast-enhanced CT image of lymph nodes at suprahyoid, hyoid and infrahyoid levels	39
13.	CECT neck of metastatic lymph nodes with vascular invasion	41
14.	CT and fused PET/CT image of bilateral level II lymph node	42
15.	Conventional MRI appearance of cervical lymph node	43
16.	DWMRI images of cervical lymph nodes	47
17.	MR Scanner 1.5 Tesla, 18 channel	55
18.	Age wise distribution of patients	56
19.	Gender wise distribution of patients	57

20.	Bar graph showing distribution of patients based on side of lymph node involvement	58
21.	Bar graph showing distribution of patients based on size of lymph node	59
22.	Bar graph showing distribution of patients based on number of lymph node	60
23.	Distribution of Patients Based on Level of Lymph Nodes	61
24.	Distribution of patients based on margin of lymph nodes	62
25.	Distribution of patients based on shape of lymph nodes	63
26.	Distribution of Patients Based on Pathological Diagnosis	64
27.	Distribution of patients based on restricted diffusion	65
28.	DWI image showing shape of lymph nodes	68
29.	DWI imageshowing margins of lymph nodes	69
30.	DWI imageshowing number of lymph nodes	70
31.	DWI imageshowing side of lymph nodes	71
32.	DWI imageshowing size of lymph nodes	72
33.	DWI imageshowing levels of lymph nodes	73
34.	Figure showing benign lymph node of tuberculous lymphadenitis	74
35.	Figure showing malignant lymph node of Non-Hodgkin's lymphoma	75
36.	Figure showing malignant lymph node of metastatic squamous cell carcinoma	76

# INTRODUCTION



---

## INTRODUCTION

Lymph is a derivative of interstitial fluid that flows into the lymphatics. The system of lymphatic flow is a major route for absorption of nutrients, proteins and also the bacteria from the interstitial tissue. This systemic flow of lymph in the cervical region has 300 nodes out of the total of 800 nodes in the entire body.<sup>1</sup>

“Lymphadenopathy” is defined as an abnormality in size and/or alteration in consistency of the lymph nodes. It is proven to result from various etiologies, including infections, autoimmune disorders and malignancies (metastatic or lymphomas).<sup>1</sup>

Cervical lymph nodes are prone to be involved in several pathological conditions. They are common sites for lymphoma, metastasis, and reactive enlargement in a number of conditions including tuberculosis (TB).<sup>1</sup> Differentiation between benign and malignant lymph nodes usually tends to affect the patient prognosis and plays a vital part in formulating a therapeutic approach in malignancy suspected patients.<sup>2</sup> However, the differentiation between benign and malignant lymph nodes remains challenging.<sup>3</sup>

Conventional MRI diagnose malignancy based on morphological characteristics such as lymph node size, shape, vascularity, extracapsular dissemination, calcifications, and necrosis. These factors are insufficient to distinguish between benign and malignant lymph nodes.<sup>4</sup> Diffusion-weighted MR imaging (DW-MRI) is a non-invasive functional technique for the identification and characterization of lymph nodes; it highlights both normal and pathological lymph nodes and enables measuring diffusion in lymph nodes by means of apparent diffusion coefficient (ADC).<sup>5, 6</sup>

---

Normal lymph nodes have a relatively restricted diffusion (low ADC) because of their high cellular density. Metastatic lymph nodes may have increased cellular density or necrotic areas, which further restrict or increases diffusion, respectively.<sup>7, 8</sup> The detection of nodal necrosis in patients with a primary head and neck tumour is the most reliable sign of a metastatic node.<sup>9, 10</sup>

DW-MRI is helpful in differentiating epidermoid carcinoma and malignant lymphoma, staging neck nodal disease, and distinguishing radiotherapy-induced tissue changes from persistent or recurrent cancer. The creation of an ADC map is an excellent method for differentiation between the viable and necrotic parts of head and neck tumours. Thus, the ADC map can be used to select the best biopsy site and to detect tumour viability in the post-treatment follow-up of patients after radiation therapy. Hence, this study mainly focuses on detecting and distinguishing benign from malignant cervical lymph nodes without invasive studies and risk of exposure to radiation.<sup>11, 12</sup>

# **AIMS AND OBJECTIVES**



---

## **AIMS AND OBJECTIVES**

- 1.** To determine apparent diffusion coefficient (ADC) values by using diffusion weighted magnetic resonance imaging (DWMRI).
- 2.** To derive ADC cut-off values to differentiate benign from malignant cervical lymph nodes.
- 3.** To correlate DWMRI and ADC findings with pathological findings.

# **REVIEW OF LITERATURE**

---

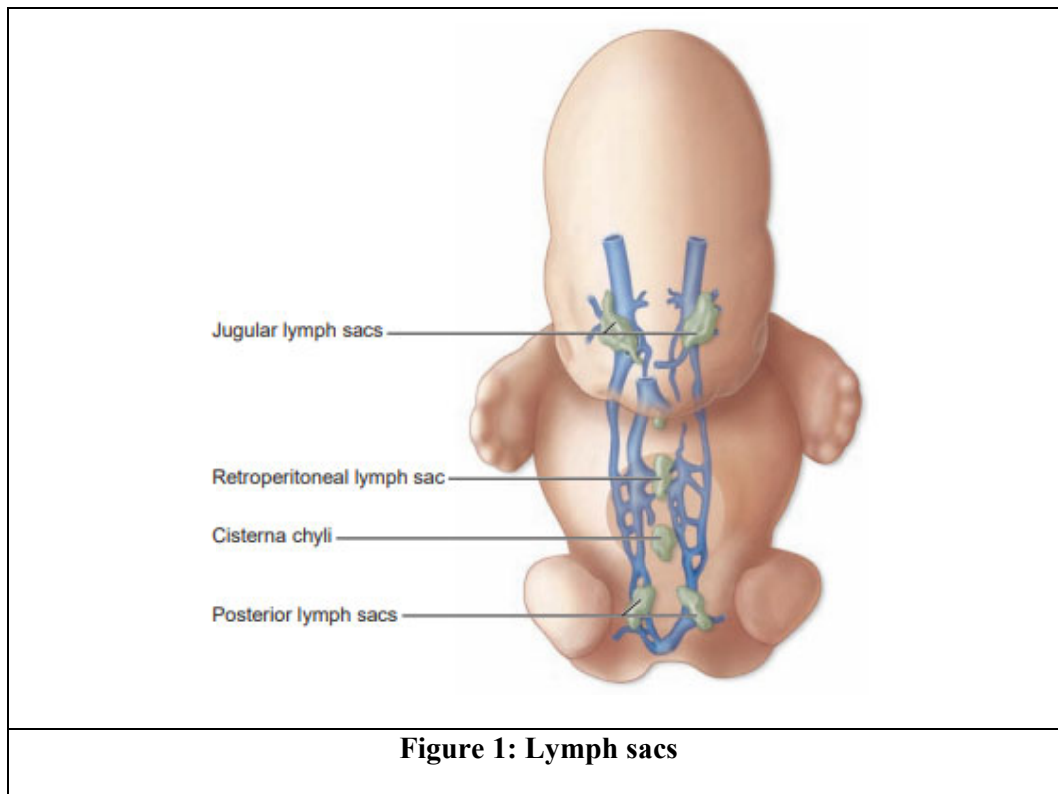
## REVIEW OF LITERATURE

### EMBRYOLOGY OF LYMPHATIC SYSTEM AND LYMPH NODES

Lymph nodes are essential component of the lymphatic system and adaptive immune system. They are located throughout the body in relation to lymphatic vessels.<sup>13</sup> Lymphatic system development starts approximately at 5<sup>th</sup> week of intrauterine gestation. Lymph nodes develop from lymphatic sacs.<sup>14, 15</sup> Different theories exist regarding lymphatic system development. One school of thought is that, there is budding of endothelial cells from veins into lymph sacs. Another theory suggested that lymph sacs develop from mesenchyme followed by budding of endothelial cells into lymph sacs. The first theory is widely recognized and is supported by subsequent studies<sup>15, 16</sup>.

Lymph sacs develop adjacent to blood vessels. Hence, lymph nodes and lymphatic system which evolve from lymph sacs are closely related to the vascular system. They form a functional anastomosis between lymph vessels and blood vessels<sup>17</sup>.

Developing foetus has six major groups of lymph sacs. Jugular sacs and iliac sacs are paired, whereas retroperitoneal and cisterna chyli are unpaired. Jugular sacs are the first ones to appear adjacent to the junction of anterior cardinal vein and subclavian veins<sup>18, 19</sup>. Bilateral iliac sacs are found around common iliac veins. Retroperitoneal sac lies near root of the mesentery. Cisterna chyli lies in the midline dorsal to the retroperitoneal sac.<sup>20, 21</sup> (Figure 1)

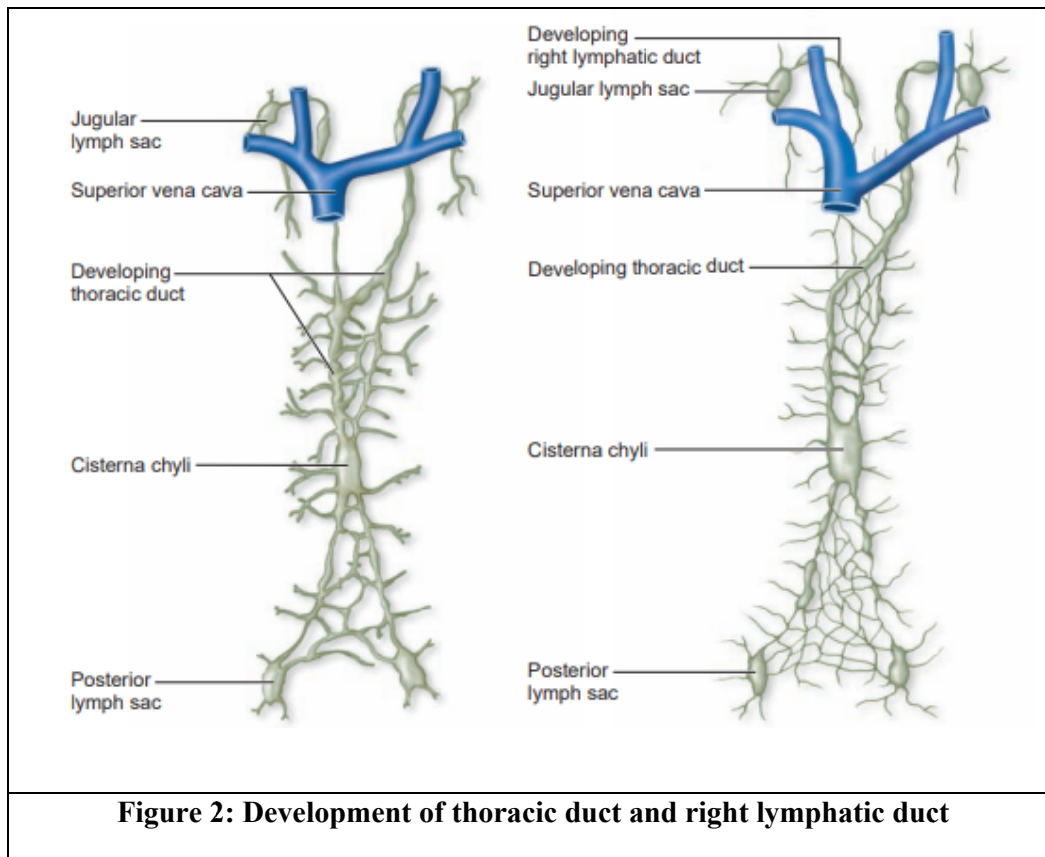


All the lymph sacs are interconnected to each other with multiple channels which drain lymph from the head and neck region, limbs and body wall. Jugular sacs and cisterna chyli are joined by two main channels (right and left thoracic channels) and anastomosis forms between these channels. Formation and development of jugular lymph sacs plays a crucial role in diagnosing aneuploidy fetuses. Thickening of nuchal translucency on ultrasound between 11 to 14 weeks is seen in approximately 75 % of trisomy foetus. Increase in accumulation of tissue fluid between the skin and soft tissues manifests as thickening of nuchal translucency. It tends to resolve beyond 14 weeks of gestation because of development of lymphatic system.<sup>14,22</sup>

The thoracic duct develops from the caudal portion of the right channel, the anastomosis between right and left channel, and the cranial portion of the left channel.

---

Cranial portion of the right channel forms right lymphatic duct. Right and left thoracic duct drains lymph into the junction of the internal jugular vein (IJV) and subclavian vein. Eventually, connective tissue and lymphocytes invade all the sacs except the cisterna chyli forming groups of lymph nodes.<sup>22</sup>



Transcription factor PROX1 upregulates genes of lymphatic vessel and it also downregulates genes of blood vessel, thus making the lineage specific for the lymphatic system. VEGFR3 gene is the receptor for paracrine factor VEGFC and is upregulated by PROX1. VEGFC protein acts on endothelial cells and initiates growth of lymphatic vessels.<sup>22</sup>

---

Mesenchymal cells invade into lymph sacs. Lymph nodes are formed from these condensed mesenchymal areas which eventually bulge into the lymphatic vessels. Further development leads to differentiation into cortex and medulla. Early lymph nodes develop around 15 to 17 weeks of intrauterine gestation and late lymph nodes develop around 18 to 24 weeks of intrauterine gestation. Cortico-medullary differentiation becomes apparent at around 25 to 38 weeks.<sup>23</sup>

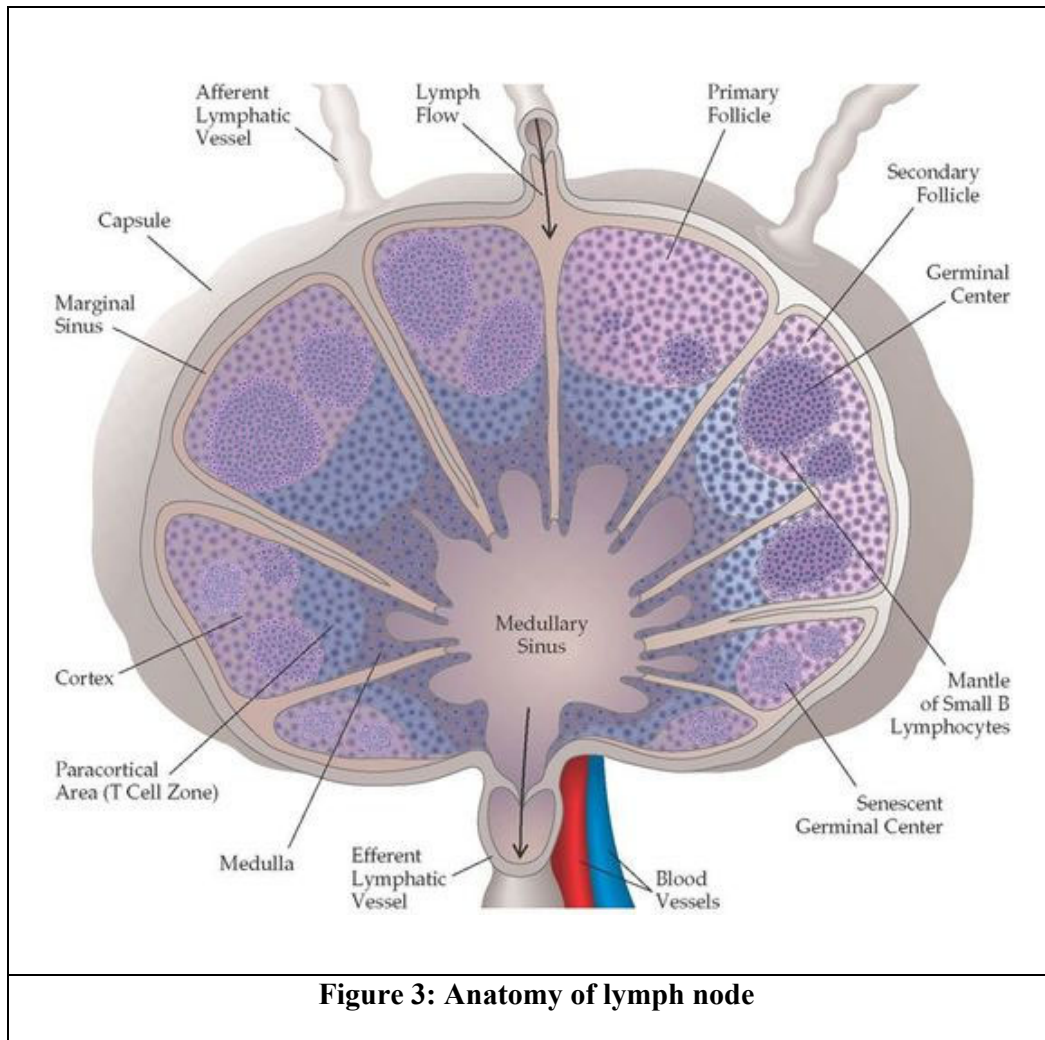
There are two types of lymphocytes, B-cells and T-cells. Embryologically, T-lymphocytes originate from primitive stem cells of mesenchyme of yolk sac. B-cells originate from marrow and lymphatic tissue associated with gut and spleen.<sup>13</sup> (Figure 2)

Lymphopoietic stem cells which are precursors of T lymphocytes migrate to thymus from bone marrow. These lymphopoietic stem cells differentiate in thymus and are ultimately released into circulation. Immature lymphocytes derived from thymus reach lymphoid organs. Thymus is the source of lymphocytes in lymph nodes before birth. After birth mesenchymal cells in lymph nodes modify into lymphocytes. Lymphocytes are not produced in lymph nodule or germinal centres until just before or after birth.<sup>13</sup>

## **ANATOMY OF LYMPH NODES**

Lymphoid tissue is classified into primary and secondary lymphoid organs. Primary lymphoid organs (ex: bone marrow and thymus) are site for de novo synthesis and maturation of lymphocytes. Secondary lymphoid organs (ex: lymph nodes, Peyer's patch tonsils, spleen, and MALT (mucosa-associated lymphoid tissue) are responsible for activation of lymphocytes and initiation of immune response. Lymph nodes are part of

secondary lymphoid organs. They are located throughout the body along lymphatic vessels. Human body of a young adult has approximately 450 - 500 lymph nodes predominantly located in abdominopelvic region followed by thorax and head and neck region.<sup>14</sup>



The nodes in the neck region are small bean shaped structures. A noticeable depression is seen in the midline on one side termed hilus, from where the blood vasculature enters (afferent) and leaves the node (efferent). It has an outer cortex, middle paracortex and inner medulla. The cortex is deficient at the hilus. The efferent vessels directly originate from the inner medulla while the afferent vessels have a drainage into the outer cortex.<sup>24</sup>

---

The capsule, made up of “collagen fibers” and some “elastic fibers”, forms the external cover. The paracortex acts as a transitional area for the lymphocytes to reach back to its parent system from the vascular anatomy. Lymphoid follicles form the cortex. The central medulla contains the trabeculae, cords and the sinuses.<sup>24</sup> (Figure 4)

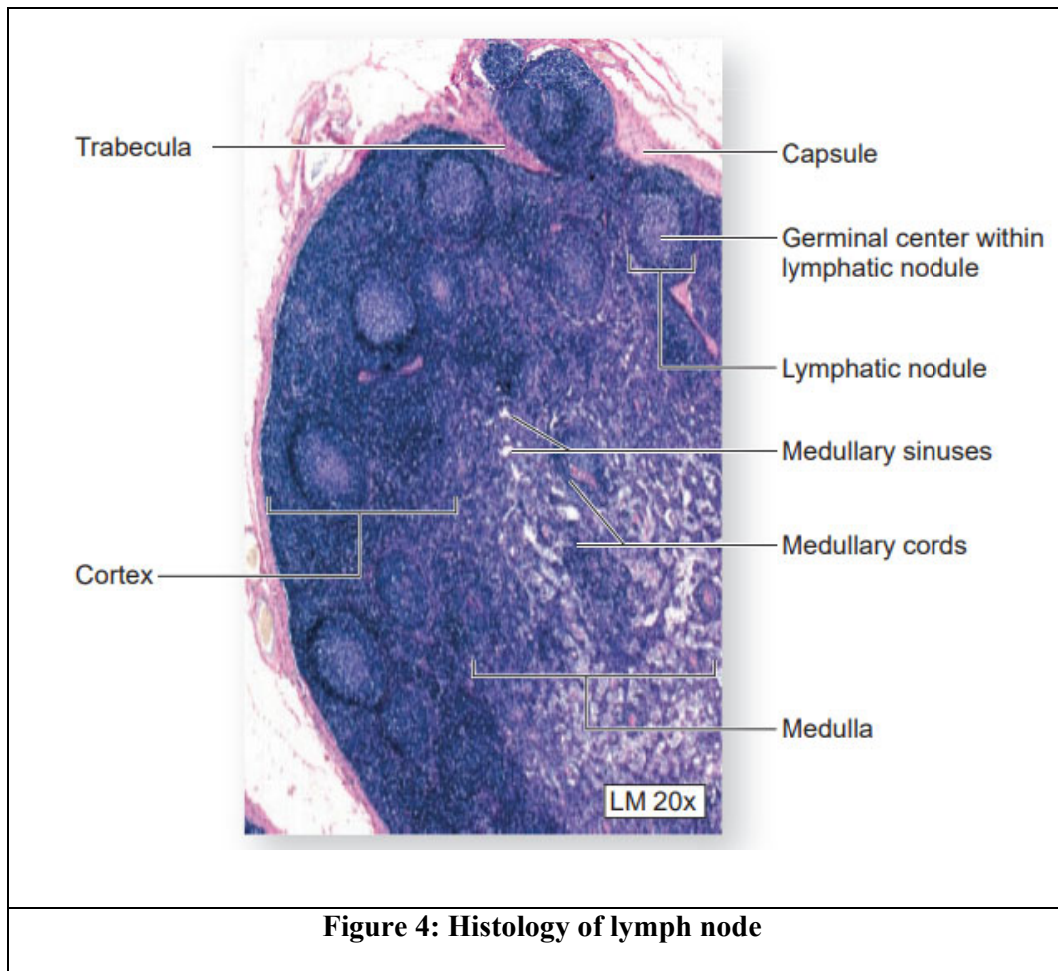


**Figure 4: Histology of lymph node**

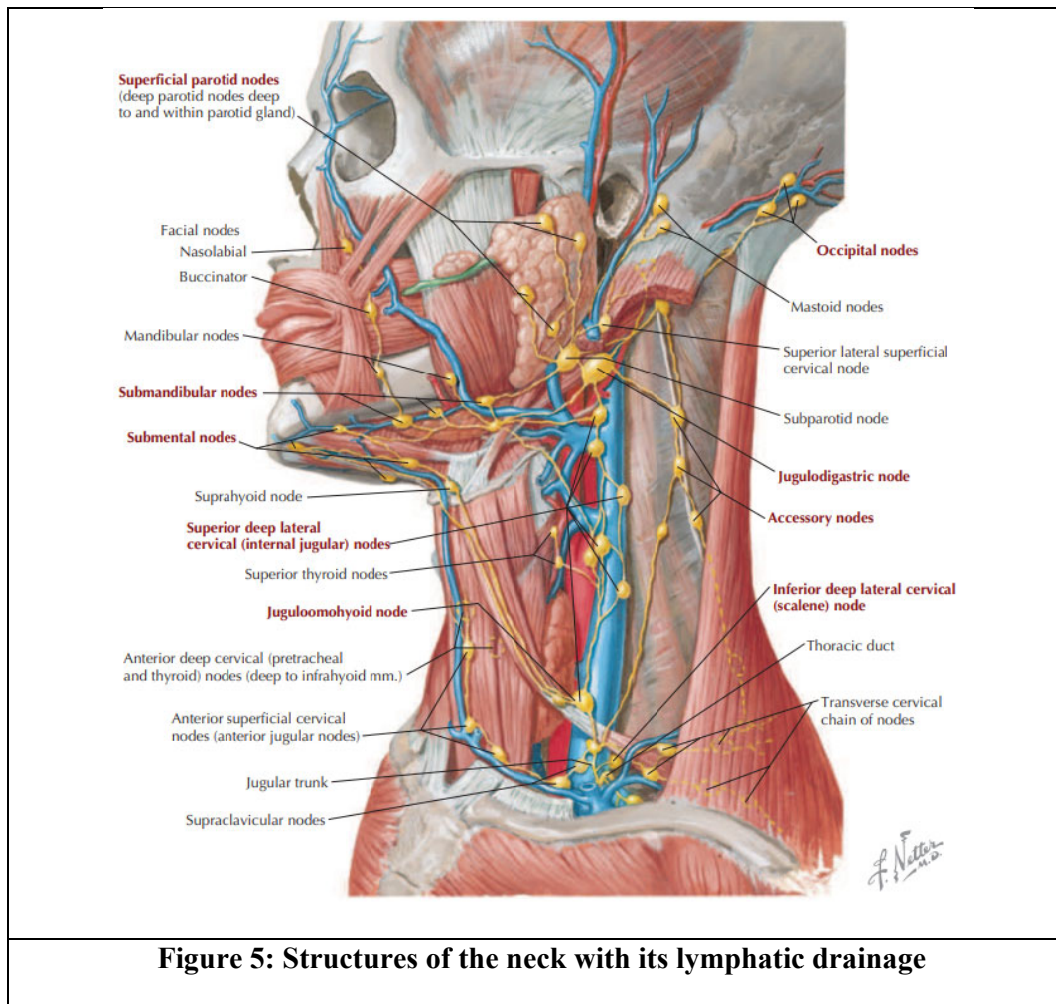
### **Arterial System:**

The main artery enters at the hilum and divides into further branches. In the outer cortical portion, the arterioles further branch into capillaries to terminate into lymphoid follicles. In the central medullary region, few arterioles run along the trabeculae up to the cortex whereas some end up supplying the capillaries.<sup>24</sup> (Figure 5)

---

## Venous System:

Venous and the arterial systems follow similar route through the hilus. In the cortex, number of venules converge and form a small vein which further converge and give rise to the main vein in medulla. The main draining vein exits through the hilus.<sup>24,25</sup>



---

## **FUNCTION OF LYMPH NODES**

Lymph is composed of tissue fluids, large extracellular molecules and cells. Lymph from interstitial spaces of tissues and organs is drained into lymphatic capillary vessels which eventually join to larger lymphatic channels. All organs of human body have lymphatic vessels other than brain, retina, and bone. Lymph nodes are present along these lymphatic vessels.<sup>26</sup>

Afferent vessels enter lymph node through hilum. Lymph from afferent lymphatic vessel traverses through sub capsular sinus and continues within the trabecular sinuses and joins medullary sinus. All the medullary sinuses of the lymph node drain lymph into efferent lymphatic vessel which exits lymph node through hilum. Efferent lymphatics drain lymph into thoracic or lymphatic ducts that subsequently join subclavian veins.<sup>26,27</sup>

During the process of circulating and filtering lymph through lymph node, B-cells and T-cells within the node are exposed to antigens present in the lymph. Antigen-presenting cells, dendritic cells, and follicular dendritic cells play a role in activating antigen specific B-cells and T cells. Lymph nodes form integral part of both adaptive and innate immune system of the body.<sup>27</sup>

Apart from being part of immune system, lymphatic system also plays a role in tissue fluid homeostasis, absorption of large molecules and lipids in the digestive systems, transportation of degraded extracellular molecules and cell debris.<sup>27</sup>

---

## LYMPHATIC SYSTEM OF HEAD AND NECK

Head and neck region lymph nodes are broadly classified into superficial and deep group of cervical lymph nodes.

Table 1: Classification of head and neck group of lymph nodes	
Superficial Lymph Nodes	Deep Lymph Nodes
1. Occipital Nodes	1. Deep Parotid
2. Mastoid or Post auricular Nodes	2. Deep Cervical : Pretracheal
3. Pre auricular Nodes	Prelaryngeal
4. Superficial parotid nodes	Infrahyoid
5. Submental Nodes	Retropharyngeal
6. Submandibular Nodes.	Jugulo-omohyoid
7. Facial Nodes : Maxillary, Buccinator	Jugulo-omohyoid
and supramandibular lymph nodes.	Supraclavicular nodes
8. Superficial cervical : Anterior and	
posterior superficial cervical nodes	

### Neck Anatomy

The cervical region contains an extensive lymphatic network bound by aponeuroses, a fibrous structure, that helps in binding them to the adjacent muscles, vasculature and peripheral nerves. The chains of lymphatic flow are strictly lateralized and usually do not mix with the contralateral system without any evidence of pathologic process. They

---

ideally drain either straight away into the vessels through the left jugular -subclavian vein confluence or in the thoracic lymphatic duct on left side. The flow terminates in the lymphatic duct on the contralateral side. Majority flow into ipsilateral chain, except the midline structures- that includes the laryngeal, nasopharyngeal & pharyngeal structures and tongue base. They are classified as IA, IB, IIA, IIB, III, IVA, IVB, VA, VB, VC, VIA, VIB, VIIA, VIIB, VIII, IX, XA and XB.<sup>28</sup> The boundaries of the lymph nodes are defined in reference to the patient lying in supine position with his/her head in a “neutral” position.

### **Level I**

**Level IA** (submental nodes) – Submental nodes are located anteriorly in the midline bounded by anterior belly of digastric muscle on either side, posteriorly by mylohyoid muscle, inferiorly by hyoid bone and superiorly by mandible. These lymph nodes drain lymph from lower lip, anterior mandibular alveolar ridge, floor of the mouth, and anterior 1/3rd of tongue.<sup>27, 28</sup>

**Level IB** (submandibular nodes) – Located in submandibular triangle bounded by anterior and posterior belly of the digastric muscles on either side, stylohyoid muscle and body of the mandible. Receives lymphatic drainage from submandibular gland, oral cavity and anterior nasal cavity.<sup>27, 28</sup>

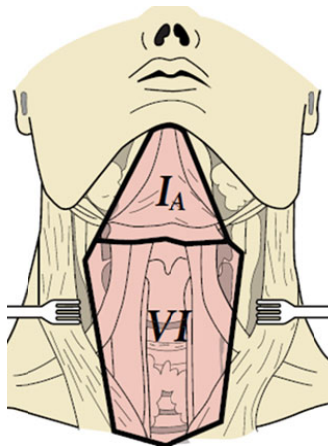


**Figure 6: Submental and anterior compartment group of lymph node**

### **Level II (Upper Jugular Group)**

They are found around the upper 1/3rd of the IJV. Extend from the level of skull base up to the level of lower margin of hyoid bone. Stylohyoid muscle and lateral border of the sternohyoid muscle form the antero-medial boundary, and posterior border of sternocleidomastoid muscle forms the postero-lateral boundary. Lymph nodes located in level II are further divided into level IIA (anterior) and IIB (posterior) by spinal accessory nerve. Nasal cavity, nasopharynx, oral cavity, oropharynx, hypopharynx, larynx and parotid glands drain lymph into upper jugular group of lymph nodes.<sup>27, 28</sup>

### **Level III (Middle Jugular Group)**

These are located along middle third of the Internal jugular vein between lower margin of the hyoid bone (superior border) and lower margin of the cricoid cartilage (inferior border). Lateral border of the sternohyoid muscle forms medial boundary and posterior border of the sternocleidomastoid muscle forms the lateral boundary. These lymph nodes drain lymph from nasopharynx, oropharynx, hypopharynx, oral cavity, and larynx.<sup>27, 28</sup>

---

#### **Level IV: Lower Jugular Group**

Lower jugular group of lymph nodes are located along lower 1/3rd of the IJV bounded superiorly by cricoid cartilage and inferiorly by clavicle. Medial and lateral borders are formed by lateral margin of the sternohyoid muscle and posterior margin of the sternocleidomastoid (SCM) muscle, respectively. This group also includes Virchow nodes. These lymph nodes drain lymph from larynx, hypopharynx and cervical esophagus.<sup>27, 28</sup>

#### **Level V (VA and VB)**

Posterior triangle group of lymph nodes are located along transverse cervical artery and spinal accessory nerve (lower half). Superior border is formed by the convergence of the sternocleidomastoid and trapezius muscle at the skull base and the inferior border is formed by clavicle. Medial and lateral boundaries are formed by posterior margin of the sternocleidomastoid muscle and the anterior margin of the trapezius muscle respectively. Level V is divided into VA and VB by horizontal plane along the inferior margin of cricoid cartilage. Level VA and VB group are located in the posterior triangle demarcated by the cricoids cartilaginous structure for oncologic dissections. Sublevel VA drains nasopharynx and oropharynx. Sublevel VB drains thyroid gland.<sup>27, 28</sup>

#### **Level VC**

They are called the lateral group of supraclavicular nodes which share common boundary with level IVA, inferior margin of level IVA marks the superior extent of VC. Anterior extent reaching up to the epidermis and postero-laterally the trapezius. Medially, reaching up to the lateral margin of SCM. Commonly involved in nasopharyngeal carcinomas.<sup>27, 28</sup>

---

## **Level VIA and VIB**

Anterior group of lymph nodes include perithyroid, Delphian (precricoid), pre- and paratracheal nodes, and lymph nodes along recurrent laryngeal nerves. Common carotid arteries form lateral boundaries, hyoid bone forms superior boundary and suprasternal notch forms inferior boundary. These lymph nodes drain larynx (glottis and subglottis), pyriform sinus, thyroid gland, and cervical esophagus.<sup>27, 28</sup>

## **Supraclavicular Group of Lymph Nodes**

Supraclavicular group of lymph nodes are bounded superiorly by the lower border of the cricoid cartilage and inferiorly by clavicle. Sternocleidomastoid muscle forms the medial border and trapezius muscle forms the lateral border. They belong to level VA (posterior triangle group).

Virchow node is located near venous confluence of IJV and subclavian vein and it is the most proximal supraclavicular lymph node on left side. Virchow node belongs to group IV.<sup>27</sup>

Breast, lung and upper oesophagus drain into right supraclavicular lymph nodes which eventually drain into right lymphatic duct. Left supraclavicular lymph nodes receive lymph from distant organs (kidney, cervix, testis, and pancreas) and they drain into the thoracic duct.<sup>28</sup>

---

## **Level VIIA and VIIB**

These are the retropharyngeal and retro-styloid nodes respectively. The first group lie in the retropharyngeal space extending from the atlas vertebrae to hyoid bone with lateral extension up to the internal carotids. Ventrally it extends up to the intrinsic pharyngeal musculature – the superior constrictor and dorsally up to the longus group of muscles.

Retropharyngeal node (VIIA) receives efferent lymphatics from the mucosa of the nasopharynx, Eustachian tube and soft palate. These nodes are at risk of harbouring metastases from cancers of the nasopharynx, posterior pharyngeal wall and oropharynx (mainly the tonsillar fossa and the soft palate).

Level VIIB contains the retro-styloid nodes, which are the cranial continuation of the level II nodes. They are located in the fatty space around the jugulo-carotid vessels up to the base of skull (jugular foramen). Retro-styloid nodes receive efferent lymphatics from the nasopharyngeal mucosa, and are at risk of harbouring metastases from cancers of the nasopharynx.<sup>27, 28</sup>

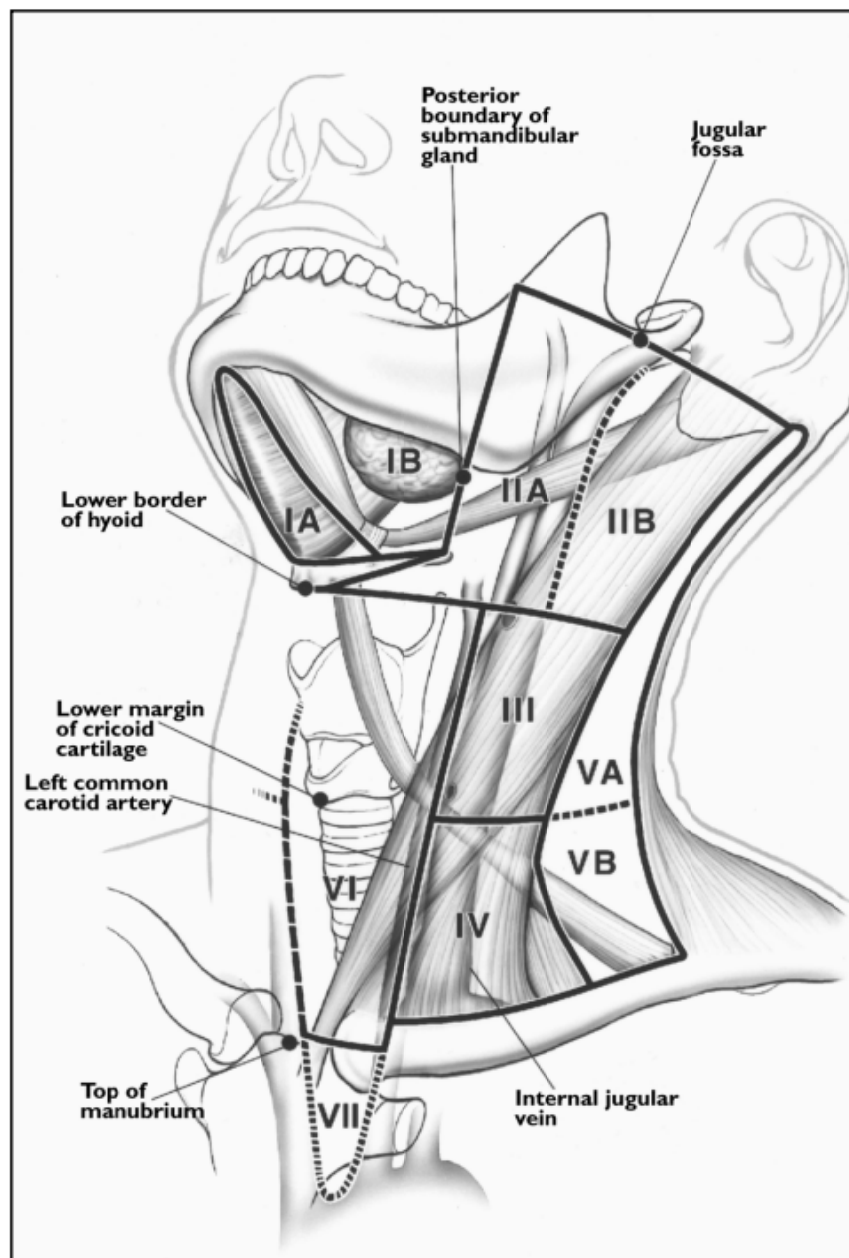


**Figure 7: Levels of cervical lymph nodes**

---

### **Level VIII**

They are called the parotid group; comprising of the sub and intraparotid nodes. They are suspended in the subcutaneous plane of pre-auricular region extending from lower margin of zygomatic bone up to the lower border of ramus of mandible. Anterior & posterior limits are the masticator space and digastric muscle respectively. Their extensions are from subcutaneous plane laterally to styloid bone medially. Anteriorly from the pterygoid and masseter muscles, to the SCM & digastric muscle (posterior belly) posteriorly. The parotid group nodes receive efferent lymphatic from the eyelids, conjunctiva, auricle, external acoustic meatus, tympanum, nasal cavities, root of the nose, nasopharynx, and Eustachian tube.<sup>27, 28</sup>

### **Level IX**

These are bucco-facial and malar groups, suspended in the subcutaneous plane of face and buccal fat pad covering the superficial face muscles like buccinators on its medial aspect and the masseter on the ventral aspect. They are mostly vulnerable to the primaries of face, nose, cheek and the maxillary air sinuses.<sup>27, 28</sup>

### **Level XA and XB**

XA are the retro auricular (also called mastoid) and subauricular groups that form a chain along the mastoid processes with extensions as mentioned below- plane passing along the external auditory meatus (superior margin) to inferior end of mastoid bone and anteriorly from the parotid space to the occiput posteriorly. These groups harbour the least metastases and are involved only in ear and occipital region primaries. XB is the occipital group, with anterior boundary being the lateral most SCM and posterior trapezius muscle. Again, these are involved in skin neoplasms of posterior occipital scalp region.<sup>27, 28</sup>

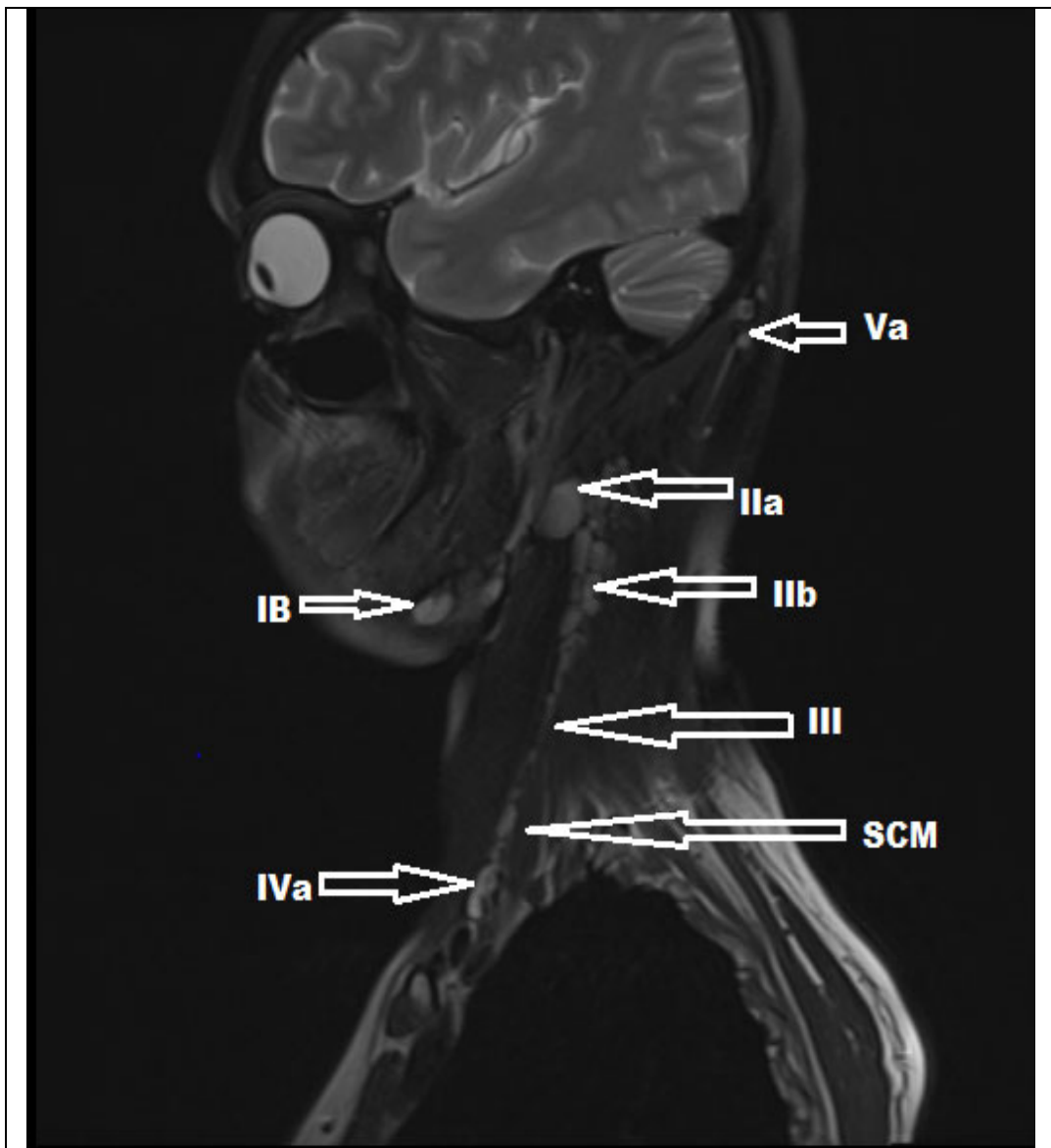


**Figure 8: Levels of lymph nodes on MRI sagittal section**

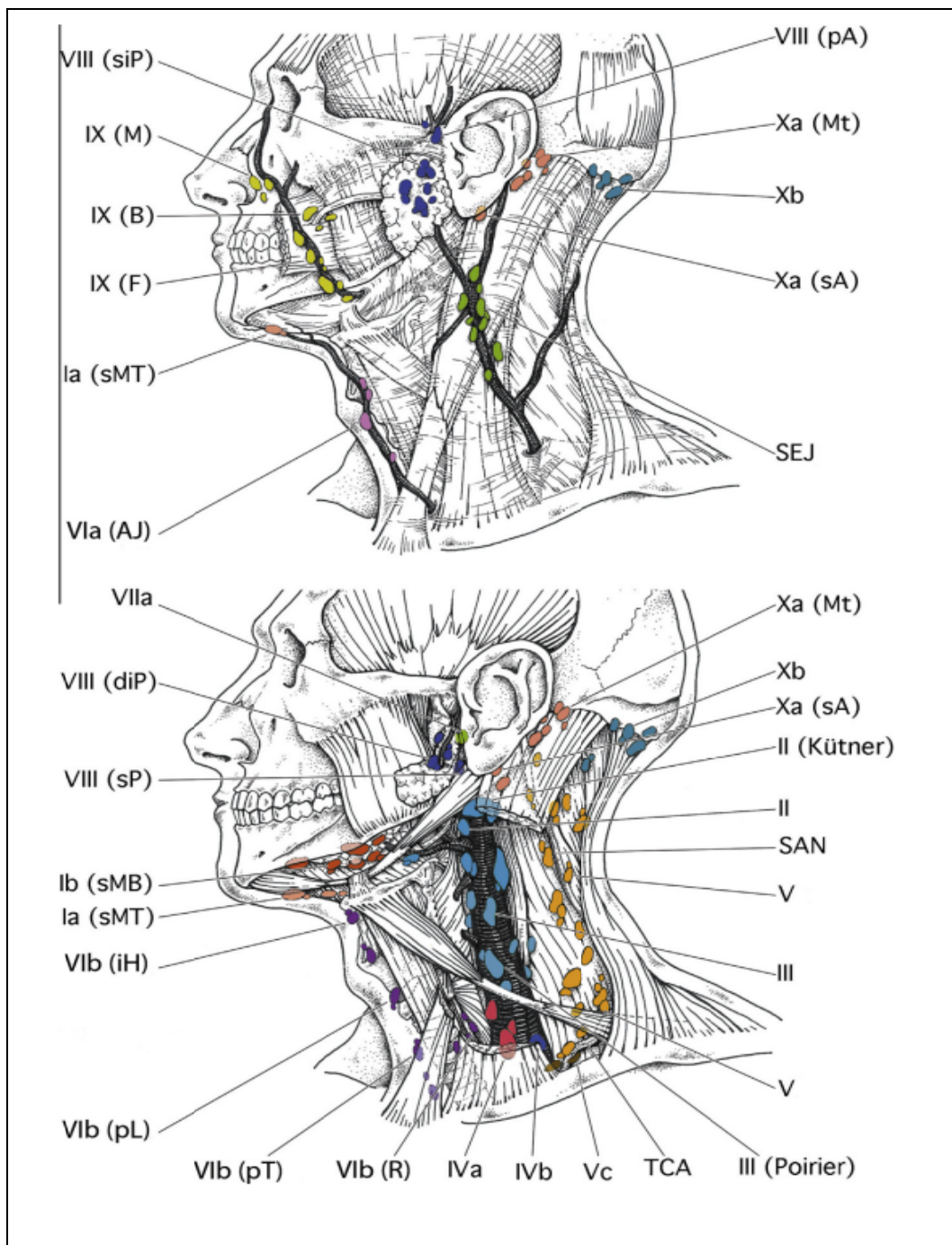


**Figure: 9 - Superficial (top) and deep (bottom) lymphatic node groups of the head and neck.** These groups are named according to the node levels modified from Robbins classification. AJ: anterior jugular; B: buccal; diP: deep intraparotid; F: facial; iH: infrahyoid; M: malar; Mt: mastoid; pA: preauricular; pL: prelaryngeal; pT: pretracheal; R: recurrent or paratracheal; sA: subauricular; SAN: spinal accessory nerve; SEJ: superficial external jugular; siP: superficial intraparotid; sMb: submandibular; sMT: submental; sP: subparotid; TCA: transverse cervical artery.

---

## CAUSES OF LYMPHADENOPATHY

### 1. Infective Causes:

Infections are the commonest aetiology for cervical nodal enlargement, especially in paediatric age group. In most of these cases, infective foci are usually in head and neck region (eg: tonsillitis, pharyngitis) or any other tissue/organ system. However, cervical lymph node enlargement can present even in cases with no evident primary site of infection. Infective causes of cervical lymph nodal enlargement can be further divided based on infective organism.

#### A. Viral:

Viral infections are the frequent etiological factor for cervical lymphadenitis in paediatric age group and result in mildly enlarged cervical lymph nodes on both sides without evidence of periadenitis. Recurrent upper respiratory tract viral infections (influenza virus, parainfluenza virus, adenovirus, etc) predispose to development of acute cervical lymphadenitis. Most common presentation is bilateral enlarged cervical lymph nodes.<sup>29</sup>

Chronic cervical lymphadenopathy is usually caused by Epstein Barr virus (EBV), cytomegalovirus (CMV), human immunodeficiency virus (HIV). Patients with HIV usually present with persistent generalized lymphadenopathy rather than isolated cervical lymphadenopathy. HIV also predisposes patients to opportunistic infections which can also cause cervical lymphadenopathy.<sup>29, 30</sup>

---

## **B. Bacterial:**

Bacteria usually cause unilateral cervical lymphadenopathy. Streptococcus is the most common bacteria causing cervical lymphadenitis, especially in children between 1 – 4 years of age. Bacterial cervical lymphadenitis is often associated with perinodal inflammatory changes and eventually necrosis may develop and result in lymph nodal abscess formation.<sup>30</sup>

Lymph nodes are the typical site for extra-pulmonary tubercular infection. Presence of necrosis, adjacent inflammatory changes/ soft tissue oedema and lymph node matting favour diagnosis of tubercular lymphadenitis. On CT, lymph nodes show peripheral rim enhancement, obliteration of surrounding fat plane with or without evidence of abscess formation. Long standing cases present with sinus tract extending to the skin surface. Calcification maybe present in chronic or healed cases of tuberculosis.<sup>30</sup>

## **C. Parasites/protozoa:**

Protozoal infections are secondary to consumption of contaminated water/ unpasteurized milk/meat or from animals. Infection of neck and throat region by protozoa results in cervical lymph nodal enlargement. Organisms like leishmaniasis, toxoplasmosis and microfilaria have predilection for lymphoreticular system and hence result in enlargement of lymph nodes.<sup>30</sup>

---

#### D. Fungi:

Fungal infections (histoplasmosis, coccidioidomycosis, etc) are secondary to inhalation of fungi or direct skin infection. Lung involvement results in reactive enlargement of supraclavicular lymphadenopathy. Isolated cervical lymphadenopathy is rare.<sup>30</sup>

Table 2: Infective causes of cervical lymphadenopathy	
<b>VIRAL</b>	EBV, CMV, HIV, varicella, rubella, measles, HSV II (Herpes Simplex Virus), enterovirus, rhinovirus, parvovirus B19.
<b>BACTERIAL</b>	Staphylococci, streptococci, tuberculosis, non-tuberculous mycobacteria, brucellosis, bartonellahenselae, tularemia, mycoplasma pneumoniae, yersiniapestis, pasteurellamultocida, cervical actinomycosis.
<b>PARASITES/ PROTOZOAN</b>	Toxoplasmosis, trypanosomes, toxocariasis, leishmaniasis, microfilaria.
<b>FUNGAL</b>	Dermatophytes (tinea), coocidiocomycosis, histoplasmosis, blastomycosis.

## 2. Immunological:

### A. Granulomatous Diseases:

Granulomatous diseases causing cervical lymphadenopathy have predilection for the posterior triangle and jugular chain lymph nodes groups. On imaging, they present either as necrotic lymph nodes or can have homogeneous echo texture in case of chronic granulomatous infiltration.<sup>30,31</sup>

---

Nearly 33 % of patients with sarcoidosis have cervical lymphadenopathy (intraparotid and supraclavicular lymph nodes are commonly involved) depending on stage of sarcoidosis. On imaging, they have homogeneous attenuation without evidence of necrosis and show homogenous enhancement on post-contrast study. In sarcoidosis patients, calcification is a frequent finding in mediastinal lymph nodes but is rarely seen in cervical lymph nodes.<sup>30, 31</sup>

#### **B. Rheumatoid Disorders:**

Cervical lymphadenopathy, enlargement of major salivary glands and sicca symptoms are most common presentations of rheumatoid disorders in head and neck region. Cervical lymphadenopathy is more common in childhood SLE (systemic lupus erythematosus) occurring in approximately 15 % of cases. Lymphoid involvement in rheumatoid arthritis causes generalised lymphadenopathy rather than isolated cervical lymphadenopathy.<sup>30, 31</sup>

#### **C. Lymphoproliferative and Histiocytic Disorders:**

Lymphadenopathy in cervical region can be the presenting feature in many patients with histiocytic disorders (Rosai- Dorfman disease, Langerhan's cell histiocytosis, hemophagocytic lymphohistiocytosis). Patients with Rosai- Dorfman disease (also known as sinus histiocytosis) present with significant lymphadenopathy, predominantly involving cervical region.<sup>32, 33</sup>

Castleman's disease (also called giant lymph node hyperplasia or angiofollicular lymph node hyperplasia) is a benign condition associated with lymph node enlargement in > 80 % of patients (mediastinal lymphadenopathy followed by cervical

lymphadenopathy). Autoimmune lymphoproliferative syndrome is another lymphoproliferative disease associated with cervical lymphadenopathy.<sup>32,33</sup>

Cervical lymphadenopathy is one among the five diagnostic criteria for Kawasaki disease and manifest as unilateral coalescent nodal mass. Kikuchi-Fujimoto disease occurs in young women and presents with cervical lymphadenopathy associated perinodal inflammatory change and intranodal necrosis.<sup>32, 33</sup>

<b>Table 3: Immunologic disorders causing cervical lymphadenopathy</b>	
<b>Granulomatous diseases</b>	<ul style="list-style-type: none"> <li>- Sarcoidosis</li> <li>- Common variable immunodeficiency</li> <li>- Hyper-IgM syndrome</li> <li>- Chronic granulomatous disease</li> </ul>
<b>Rheumatoid disorders</b>	<ul style="list-style-type: none"> <li>- Arthritis</li> <li>- Systemic lupus erythematosus</li> <li>- Dermatomyositis</li> </ul>
<b>Lymphoproliferative and histiocytic disorders</b>	<ul style="list-style-type: none"> <li>- Rosai-Dorfam disease</li> <li>- Castleman's disease</li> <li>- Autoimmune lymphoproliferative syndrome</li> <li>- Langerhans cell histiocytosis</li> <li>- Hemophagocytic lymphohistiocytosis</li> <li>- Kawasaki syndrome</li> <li>- Kikuchi-Fujimoto disease</li> </ul>

---

### 3. Metabolic Diseases:

#### A. Storage Disorders:

Niemann-Pick disease is an autosomal recessive lysosomal storage disease associated with accumulation of sphingomyelin in lysosomes present in the liver, spleen, lymph nodes and brain. Other storage disorders like Gaucher's disease and Tangier disease less frequently involve cervical lymph nodes.<sup>33, 34</sup>

#### B. Hypersensitivity:

Serum sickness is a type III hypersensitivity reaction to proteins from animal source. Apart from systemic symptoms, lymphadenopathy is seen predominately near site of injection and head & neck region. Allergic reaction to certain drugs can also result in lymphadenopathy, either as direct cause or secondary to serum sickness. DRESS syndrome (drug reaction with eosinophilia and systemic symptoms) is a special form of the drug-induced systemic reaction associated with lymphadenopathy.<sup>33,34</sup>

Table 4: Metabolic disorders causing cervical lymphadenopathy	
Storage disease	<ul style="list-style-type: none"><li>- Niemann-Pick disease</li><li>- Gaucher's disease</li><li>- Tangier disease</li><li>- Amyloidosis</li></ul>
Hypersensitivity	<ul style="list-style-type: none"><li>- Serum sickness</li><li>- Adverse drug reaction: Antiepileptic drugs, heparin, antituberculosis drugs (isoniazid), allopurinol, antibiotics (cephalosporins), pyrimethamines, hydralazine, etc.</li></ul>

---

## 4. Neoplastic Diseases:

### A. Lymphoma:

Lymphoma is malignancy of lymphocytes and lymphoblasts manifesting as nodal or extranodal disease. It is the most prevalent head and neck malignancy in paediatric age group (27 %). Hodgkin's lymphoma usually manifests as lymph nodal disease, involving either upper cervical or less frequently supraclavicular group of lymph nodes. Extranodal involvement with or without diffuse nodal involvement is a feature of non-Hodgkin's lymphoma.<sup>33,34</sup>

On ultrasound, lymphomatous lymph nodes appear diffusely hypoechoic with pseudocystic appearance secondary to reduced fat in lymph nodes. Lack of calcifications and necrosis helps in differentiating from tubercular/ metastatic etiology.<sup>33</sup>

Four patterns of head and neck lymphoma are described on CT (computed tomography): Type 1: Only nodal involvement, Type 2: Only extranodal involvement, Type 3: Combination of extranodal and nodal disease, and Type 4: Multifocal extranodal disease with or without nodal involvement. Non-Hodgkin's lymphoma usually presents as extranodal disease (type 2), followed by combination of extranodal and nodal disease (type 3). Waldeyer's ring, nasal cavity, and paranasal sinuses are the extranodal sites frequently affected in head and neck lymphomas.<sup>34</sup>

---

## **B. Metastasis:**

Lymph nodal metastasis in cervical region can either be from a known primary tumour or from clinically unidentified primary or from unknown/ occult primary tumour. Head and neck cancers account for bulk of cervical lymph node metastasis cases. Squamous cell carcinoma (SCC) constitutes majority of these malignant tumours. SCC spreads through lymphatic system hence have high incidence of lymph node metastasis. Rate of metastasis can even give a clue to nature of primary tumor.<sup>33,34</sup>

Cervical lymph node metastasis is a significant prognostic factor for head and neck tumours. 5-year survival rate decreases by 50 % in patients with nodal metastasis. Factors affecting prognosis are: size of lymph node, level and site of lymph node and extranodal extension.<sup>34</sup>

Malignant tumours can metastasize to either ipsilateral/contralateral or bilateral or midline lymph nodes. Other than thyroid cancer cases, midline cervical lymph nodes are considered as ipsilateral nodes. Bilateral and contralateral lymph nodal involvement indicates poor prognosis and is considered as N2c disease. Metastasis to lymph nodes in lower neck levels, i.e., level IV and level V (supraclavicular area) and metastasis to distant lymph nodal groups is considered as poor prognostic factor.<sup>33,34</sup>

## **OCCULT NODAL DISEASE**

Occult disease in cervical lymph nodes indicates presence of metastases in the neck nodes that cannot be identified either clinically or radiologically. Occult nodal disease can be further divided into two categories: occult metastases identified on light microscopy or micro metastases (less than 2 mm) identified on special histological techniques (immunohistochemistry/ step serial sectioning/ molecular analysis).<sup>34</sup>

---

## **CERVICAL LYMPH NODE METASTASIS FROM UNKNOWN ORIGIN (MUO)**

MUO is a disease entity characterized by the presence of pathologically proven cervical lymph node metastasis in the absence of clinically or radiologically obvious primary tumour. In a true MUO primary tumour is never identified in spite of extensive clinical, radiological and pathological investigation. Whereas in occult disease, primary tumour is present but not detected on initial investigation<sup>30</sup>

Most common histotypes in pathology proven malignant cervical lymph node is squamous cell carcinoma followed by adenocarcinoma, undifferentiated carcinoma and other malignancies. Management protocol, treatment guidelines and prognosis vary according to histopathological diagnosis.<sup>34,35</sup>

Lymph from each part of the human body drains into specific group of lymph nodes, hence level or group of lymph node affected can give a clue to possible site of primary tumour (Table 5). Level II and level III groups are most commonly involved as compared to lymph nodes of other neck levels. Head and neck region carcinoma tend to metastasize to upper and middle neck levels, whereas metastasis to level IV and supraclavicular nodes is usually from below the level of clavicle. Any malignancy from head and neck region, malignancy from thorax, abdomen and pelvis (including lung, breast, oesophageal, gastric, pancreatic, cervix, and prostate cancers) can present with metastasis to supraclavicular lymph nodes.<sup>35</sup>

---

Table 5: First echelon lymph nodes for various primary sites		
Level of lymph node		Primary drainage site
Level I	Submental (IA) and submandibular (IB)	Oral cavity, oropharynx
Level II	Upper jugular	Oral cavity, oropharynx, larynx, nose, hypopharynx, parotid, nasopharynx
Level III	Middle jugular	Oral cavity, oropharynx, larynx, hypopharynx, thyroid, nasopharynx
Level IV	Lower jugular	Larynx, thyroid, hypopharynx, oesophagus
Level V	Posterior compartment	Nasopharynx, hypopharynx, thyroid, oropharynx
Level VI	Anterior compartment	Thyroid, larynx, hypopharynx, cervical oesophagus

## STAGING

Staging is a process in oncology that allows health care providers to determine the extent of disease burden from its primary locations. It should be known that malignant lymphadenopathy can occur from both primary lymphomas or from metastatic cancer. Most, but not all, cancers use the tumour, node, and metastasis (TNM) staging system. A tumour refers to the primary involvement by the neoplasm and the depth of involvement. Node describes the local lymph nodes that are involved by the disease process, and metastasis defines distant sites of involvement.<sup>36</sup>

Extranodal extension beyond lymph node capsule indicates poor prognosis and thus considered as N3b stage in UICC/AJCC eighth edition (Table 6). Invasion of adjacent

soft tissue, skin, nerve and involvement of underlying muscle or adjacent structures are considered as extranodal extension. Pathological N staging system is based on histological assessment which takes into account total number of nodes in neck dissection specimen.<sup>37</sup>

Table 6: Clinical N staging: 8 <sup>th</sup> edition of AJCC cancer staging	
AJCC N Classification	Definition
N0	No regional LN metastasis
N1	Single ipsilateral node ≤3cm in greatest diameter
N2a	Single ipsilateral node >3cm but ≤6cm
N2b	Multiple ipsilateral nodes ≤6cm in greatest diameter
N2c	Bilateral or Contralateral nodes ≤6cm in greatest diameter
N3	Any positive nodes, at least one ≥6cm

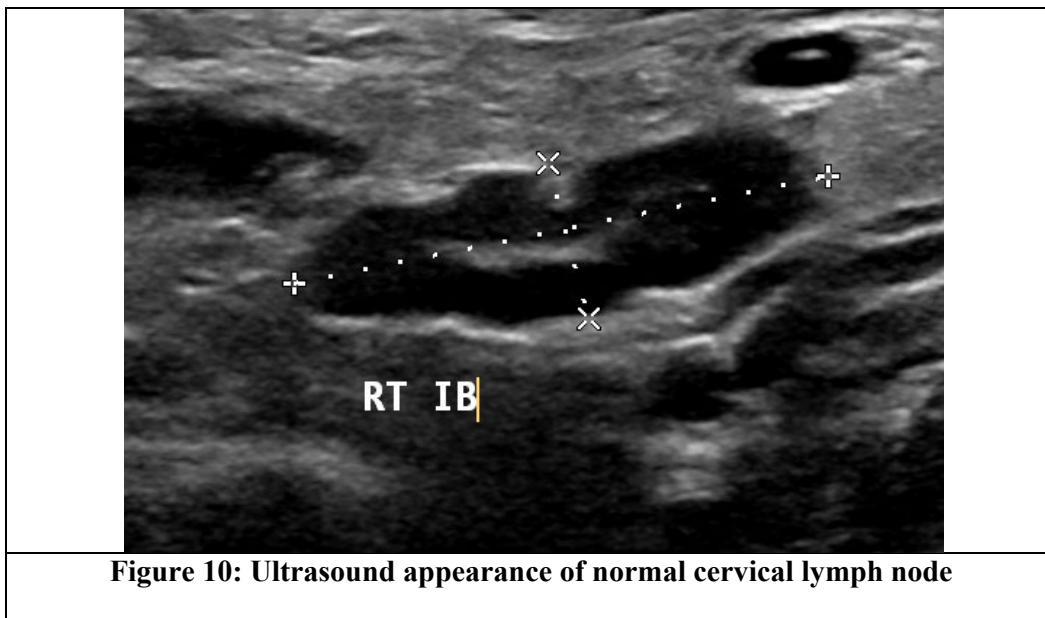
---

## CROSS SECTIONAL IMAGING

### ULTRASOUND (USG)

Ultrasound is usually the first imaging modality used to assess cervical lymph nodes. Ultrasound is widely accessible, cheaper, no effects of radiation and can even be used for guided FNAC of suspicious lymph nodes.<sup>38, 39</sup>

Normal lymph node has ovoid shape on USG and appears hypoechoic with a central echogenic hilum (figure 10). Ultrasound evaluation is based on various B-mode features and colour Doppler evaluation. B-mode parameters usually employed in nodal assessment are size, shape, echogenicity, border, hilum, matting and calcifications.<sup>40, 41</sup>



---

## COLOUR DOPPLER IMAGING (CDI)

Normal lymph nodes on CDI show hilar vascularity or appear avascular. Reactive lymph nodes also usually have hilar vascularity. Malignant lymph nodes have either mixed (peripheral and hilar) or peripheral vascularity. Development of peripheral vascularity in malignant lymph nodes is due to tumour angiogenesis and proliferation of capsular vessels.<sup>42, 43</sup>

Role of Doppler indices like, resistivity index (RI) and pulsatility index (PI) in differentiating malignant from benign nodes is still controversial. Doppler indices of malignant lymph nodes usually have higher value than benign and/ or normal lymph nodes. When tumour cells grow, they replace a large portion of the lymph node and compress intranodal blood vessels. This results in increase in vascular resistance and hence high RI and PI values in malignant lymph nodes. Studies have shown that Doppler indices have poor diagnostic accuracy in discriminating benign from malignant lymph nodes.<sup>42, 43</sup>

## ELASTOGRAPHY

Elasticity is the ability of the material to resume its original size and shape after applying a deforming force or stress. Pathological changes in the tissue lead to change in elasticity. Elastography is an imaging modality which can qualitatively and quantitatively assess the changes in elasticity of the tissue due to pathological process.<sup>44</sup>

Ultrasound elastography techniques are classified based on the measured physical quantity. They are strain and shear wave elastography (SWE) techniques. Strain imaging is a semi-qualitative technique which can assess the relative stiffness of lesion as compared to normal tissue. It can be further subdivided into strain elastography and

---

acoustic radiation force impulse (ARFI). SWE is a quantitative method to measure the tissue stiffness.<sup>44, 45</sup>

## **STRAIN IMAGING**

### **A. STRAIN ELASTOGRAPHY**

Strain elastography is one of the earliest elastography technique used with ultrasound. There are two excitation methods to induce tissue displacement. In first method, manual compression is applied by the operator using ultrasound transducer. This is usually used for superficial structures like lymph nodes, thyroid and breast. For deep seated organs like liver, ultrasound transducer is held steady and the displacement is produced by internal physiologic motion (ex: respiration, cardiac pulsations). This method is non-operator dependent and the results are easily reproducible as compared to first method.<sup>44.</sup>

In strain elastography, the amount of displacement produced in the lesion by transducer or the physiological movement of the patient is compared to that in normal surrounding tissue and is displayed as elastograms. Elastograms are colour maps laid on B-mode images. Low strain or hard tissue is displayed in blue colour, whereas high strain or softer tissue is displayed in red colour. Five patterns are described on elastograms for characterizing the lymph nodes based on the distribution and percentage of blue area (hard area).<sup>46</sup>

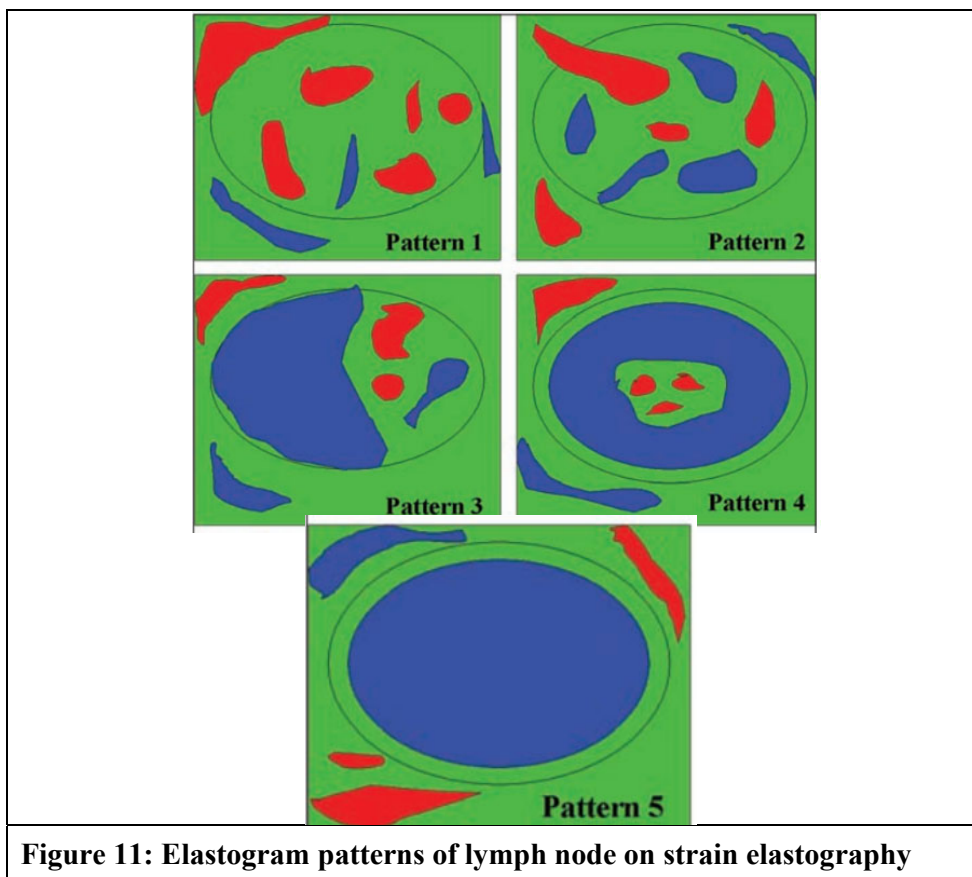


**Figure 11: Elastogram patterns of lymph node on strain elastography**

Five patterns on elastogram for lymph node characterisation.

Pattern 1	Absent or very small blue (hard) area(s).
Pattern 2	Small scattered blue (hard) areas, blue area < 45%.
Pattern 3	Large blue area(s), total blue area > 45%.
Pattern 4	Peripheral blue area and central green area, suggesting central necrosis.
Pattern 5	Blue area occupying entire lymph node with or without a green (soft) rim

---

Strain ratio is a semi-quantitative method to measure tissue stiffness. It is a ratio of strain measured in the ROI within the lesion and the strain ROI within adjacent normal tissue. Low strain ratio indicates that the lesion is more easily compressible and hence considered to be benign. Whereas, malignant lesions are less compressible and have high strain ratio. Cut-off value varies depending on the tissue assessed.<sup>47</sup>

### **ACOUSTIC RADIATION FORCE IMPULSE (ARFI) STRAIN IMAGING**

ARFI is a relatively new elastography technique used to measure strain. In ARFI strain imaging, short duration; high-intensity acoustic pulses produced by ultrasound transducer are used to displace tissue. Virtual touch tissue imaging (VTI) qualitatively assess the displacement of the tissue within a specified ROI and it can be displayed as an elastogram similar to strain elastography. Softer tissues have larger displacement and produce brighter image as compared to harder tissues which have smaller displacement and produce darker image. VTI images are graded (6 grades) depending on the proportion of dark and bright area in the lymph node.<sup>48</sup>

### **SHEAR-WAVE ELASTOGRAPHY**

Shear wave elastography (also called as dynamic elastography) is a newer technique which gives quantitative assessment of the elasticity of the tissue. Shear waves generated using focused acoustic radiation force from a linear US array, are used to cause local displacement in the tissue. Tissue displacement is used to calculate shear wave velocity (expressed in kPa or  $\text{m/sec}^2$ ) (quantitative measure of elasticity of the tissue). Shear waves propagate faster in stiffer tissues and have higher velocity. Hence, malignant lymph nodes have higher shear wave velocity as compared to benign lymph nodes.<sup>49</sup>

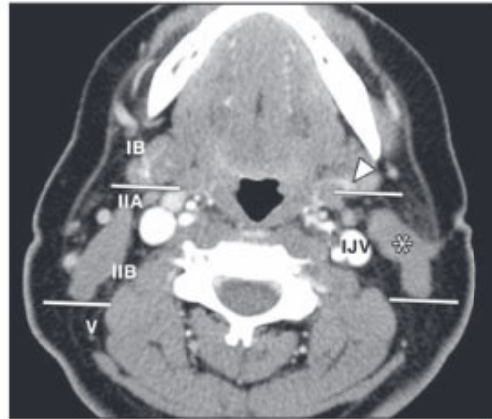
---

SWE is non-operator dependent and hence is reproducible and has less inter-observer variability. It provides quantitative measurements of tissue elasticity and is therefore considered superior to strain elastography.<sup>49</sup>

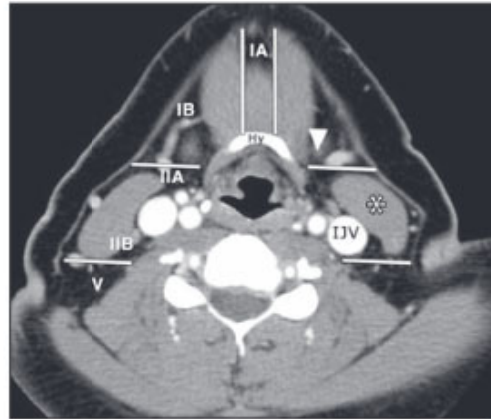
## **COMPUTED TOMOGRAPHY (CT)**

CT is done to assess the levels of lymph node involved (Figure 12), extent of lymph nodal disease, spread to adjacent structures and to identify primary pathology in case of metastatic disease. CT is also frequently used for follow-up of nodal status. Most of the parameters used in CT are same as those used in ultrasound like, size, shape (short/long axis ratio), border, presence of intranodal necrosis /cystic component or intranodal calcification.<sup>50</sup>

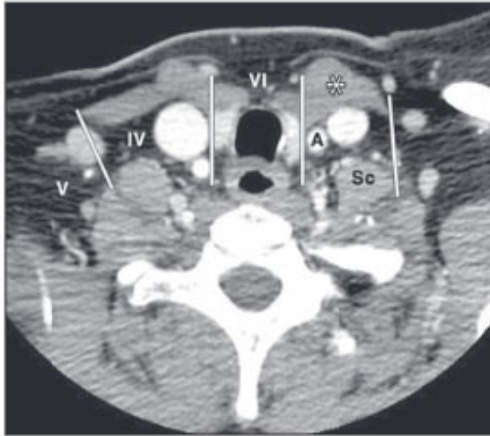
CT scan is also used to predict the prognosis of the disease. Extranodal spread of lymph nodal disease and invasion into adjacent structures indicates poor prognosis. Lymph nodal mass can invade adjacent structures like, muscle, bone and neurovascular structures.<sup>51</sup>



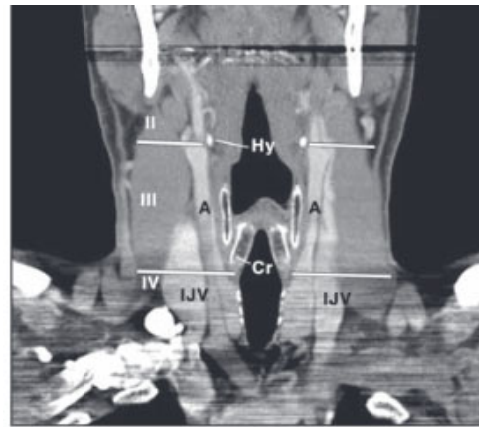
**A**



**B**



**C**



**D**

**Figure 12: Contrast-enhanced CT image at suprahyoid, hyoid and infrahyoid neck level**

- A. Contrast-enhanced CT image of suprahyoid neck shows level IB, IIA, IIB, and V sites, defined by horizontal lines through posterior border of submandibular gland (arrowhead) and posterior border of sternocleidomastoid muscle (asterisk). Levels IIA and IIB are divided by internal jugular vein (IJV).
- B. Contrast-enhanced CT image at level of hyoid shows level IA and IB sites, defined by medial border of anterior belly of digastric muscle.
- C. Contrast-enhanced CT image of infrahyoid neck shows level IV, V, and VI sites, defined by medial margin of common carotid artery (A) and oblique line from lateral anterior scalene muscle (Sc) to posterior border of sternocleidomastoid muscle (asterisk).
- D. Contrast-enhanced coronal CT image shows level II, III, and IV sites divided by body of hyoid bone (Hy) and inferior border of cricoid cartilage (Cr).

---

Presence of arterial invasion can lead to several complications like occlusion of vessel, pseudoaneurysm formation or carotid blowout. Loss of fat planes with adjacent artery is considered to be the most sensitive sign of arterial invasion, whereas narrowing or irregularity of the arterial wall is the most specific sign. Circumferential encasement ( $> 180 - 270^{\circ}$ ) of carotid artery can indicate adventitial invasion and is not operable.<sup>51</sup>(Figure 13)

Dual energy CT combines both morphological and functional changes in lymph nodes thus helps in better evaluation. Studies have shown that dual energy CT scan characterize metastatic cervical lymphadenopathy based on qualitative analysis (monochromatic data) and quantitative analysis (iodine concentration and the slope of the spectral HU curve).<sup>51</sup>

CT perfusion imaging (CTP) is a functional imaging technique which can quantitatively and qualitatively assess the enhancement in the lymph node. Blood flow (BF), blood volume (BV), and mean transit time (MTT) will be calculated and depicted in a colour-coded display. Metastatic lymph nodes have higher BF and BV and lower MTT as compared to benign lymph nodes.<sup>52</sup>

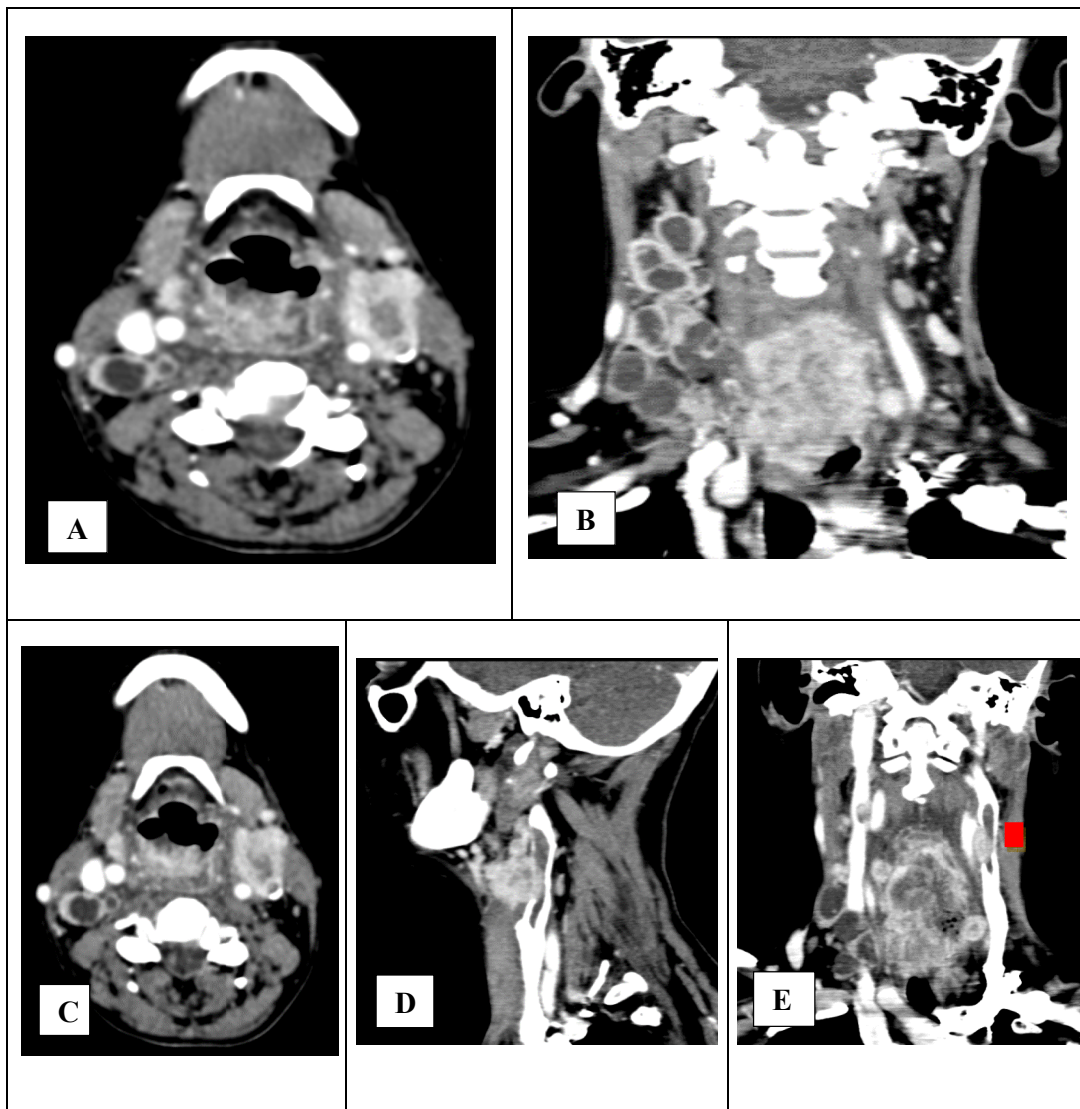


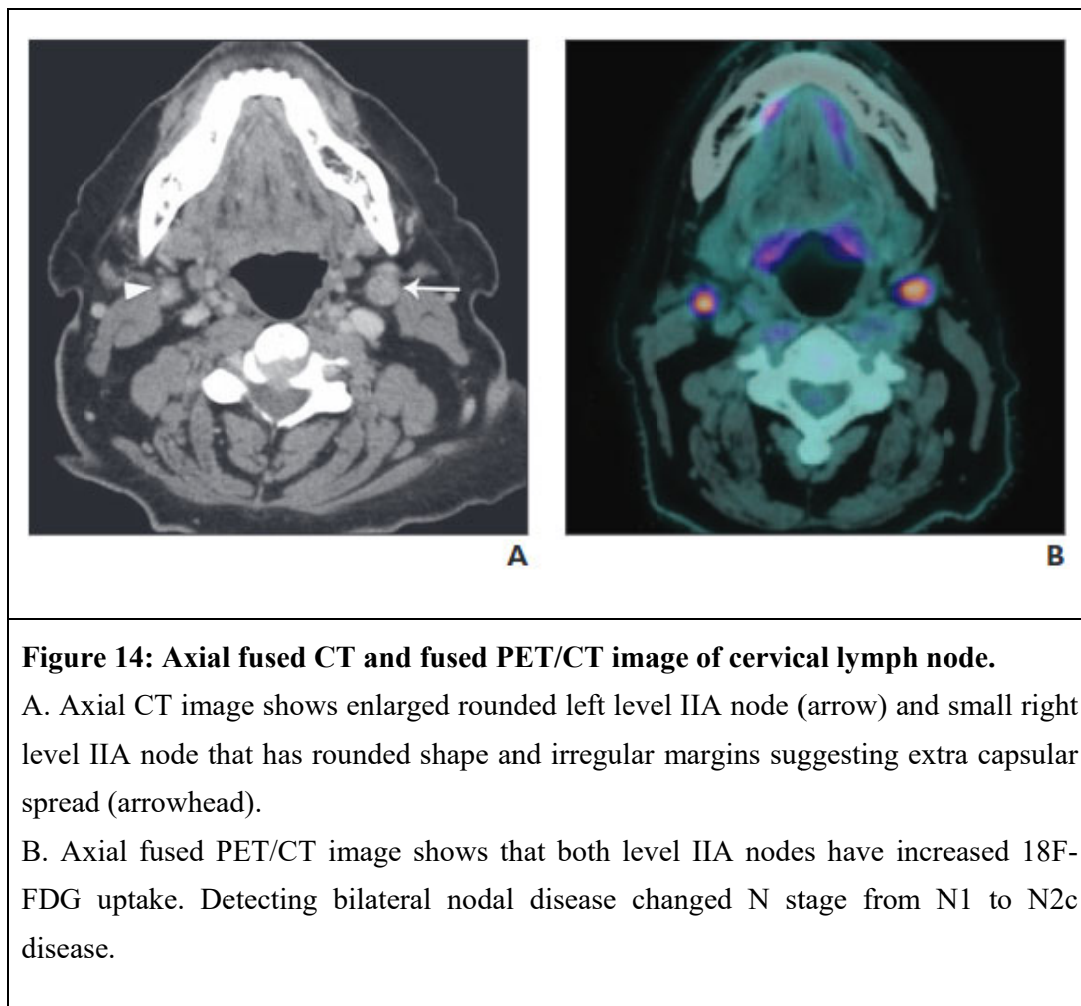
**Figure 13: CECT neck axial, coronal & sagittal section of metastatic cervical lymph nodes with vascular invasion.**

Multiple heterogeneously enhancing lymph nodes with central necrosis in right level II, III, & IV (A & B). The left level III lymph node (Axial, sagittal and coronal) shows extra capsular spread with  $> 180^{\circ}$  encasement and infiltrating left internal jugular vein with resultant enhancing tumour thrombus (Red Box) within the lumen (C,D&E)

---

## FDG-PET/CT

PET scan is a functional imaging technique used to identify metabolic changes in the tissue and can detect changes earlier than the other imaging methods. PET scan is found to have better diagnostic accuracy in differentiating cervical lymph nodes with sensitivity of 89 % and specificity of 98 %. It is used for tumour staging (including N staging), treatment response assessment, and to look for recurrence. PET- CT provides better anatomical localization of the lymph nodes.<sup>53</sup>



---

## MAGNETIC RESONANCE IMAGING (MRI)

MRI has high intrinsic soft-tissue discrimination and thus is preferred for evaluating the head and neck soft tissues. Morphological features assessed in conventional MRI are similar to those in CT and ultrasound and include size, shape, border, vascularity, extranodal extension and other ancillary findings like presence of calcifications, necrosis or cystic components, extranodal spread of tumour and involvement of carotid artery. Presence of homogenous signal intensity on contrast-enhanced T1 and T2 weighted images favours benign etiology.<sup>54</sup>

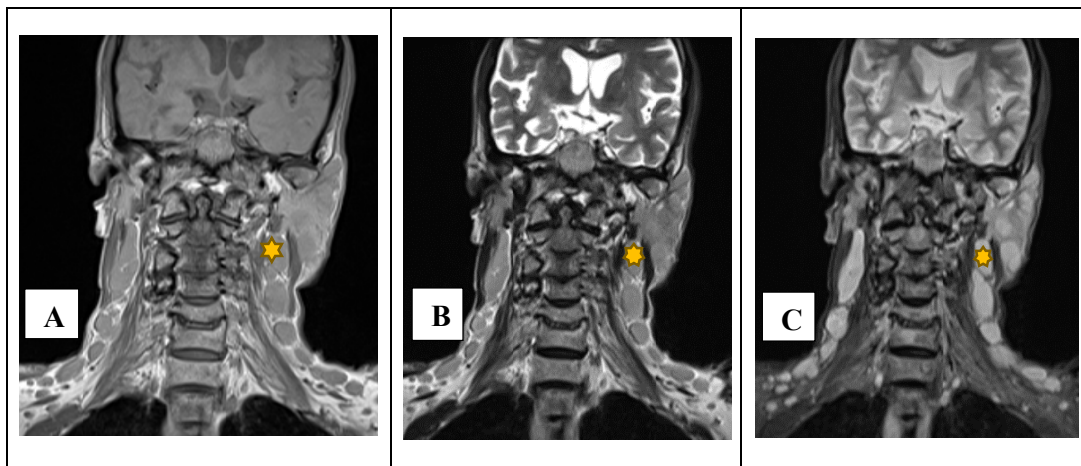


**Figure 15: MRI coronal T1,T2 & STIR images of cervical lymph nodes:**

Multilevel enlarged cervical lymph nodes (Yellow stars), appears Iso intense on T1WI (A) heterogeneously hyper intense on T2WI (B) & STIR (C) images.

---

## DIFFUSION-WEIGHTED MAGNETIC RESONANCE IMAGING

DWI is a non-invasive MRI based sequence that works on the principle of the tissue characterization depending on tissue microenvironment. The basic principle involved in DWI is the motion of water molecules across the membranes of cells. It is named as the “Brownian motion”. The analysis of the lesions is largely dependent on the water motion across the cell membranes as micro structural changes in tissues will result in alteration of the movement of molecules, thus resulting in altered signal intensities.<sup>54</sup> The amount of restriction in a given biologic tissue is inversely related to the membrane intactness and tissue cellularity. The degree to which there is seen restriction of movement of molecules containing protons is directly proportional to the cellularity of the tumour containing tissues.<sup>55,56</sup>

The sensitivity of detection on DWI sequence is dependent on three parameters - the ‘time duration’ for which the gradient is applied, the ‘amplitude of the gradient’ for that particular tissue and ‘interval of time’ for the area of interest for the applied pair of gradients. For clinical purposes, the sensitivity of detecting the minute anatomic alteration can be changed by applying different “values of b”, which is subjective to the above mentioned parameters.<sup>57, 58</sup>

The alteration in b value results in alteration in amplitude rather than altering the time factors. b values range from 0, 50, 500, 1000 and 2000 sec/mm<sup>2</sup>. Higher b values can pick up signals from the short diffusion distances. A human cell measures 10 µm and the mean of root square displacement of diffusion is calculated to be 8 µm. Hence, DWI is proven as an excellent imaging modality to determine the micro structural changes in the cancerous tissue.<sup>59</sup>

---

Differentiation of treatment-induced tissue changes, especially after chemo and/or radiotherapy, and persistent or recurrent cancer, is another area in which DWI may be very helpful. As DWI allows differentiation between inflammatory and neoplastic tissues, another possible application could be the monitoring of tumour response during radiotherapy: this could have prognostic importance and possibly influence the management of the patient.<sup>60</sup>

---

## APPARENT DIFFUSION COEFFICIENT VALUES

DWI is sensitive to the diffusion of water molecules in tissue, which can make subtle abnormalities more obvious.<sup>10</sup> The contrast of DWI depends principally on the degree to which water molecules are free to move within tissues and pass-through cell membranes.<sup>61,62</sup>

Diffusion is expressed as an ADC, which reflects the diffusion properties unique to each type of tissue. Hypercellular tissue, such as occurring within malignant tumours, will show low ADC values. Non-tumoral tissue changes such as oedema, inflammation, fibrosis, and necrosis are expected to show low cellularity, in strong contrast with viable tumour, resulting in high ADC values. An inverse correlation between the ADC value and tumour cellularity in experimental models has been shown, and this has been clinically validated.<sup>60, 61, 62</sup>

Several studies have reported the ability of DWI to discriminate malignant from benign lymph nodes in the neck with the ADC value of metastatic nodes is significantly lower than that of benign nodes.<sup>62</sup>

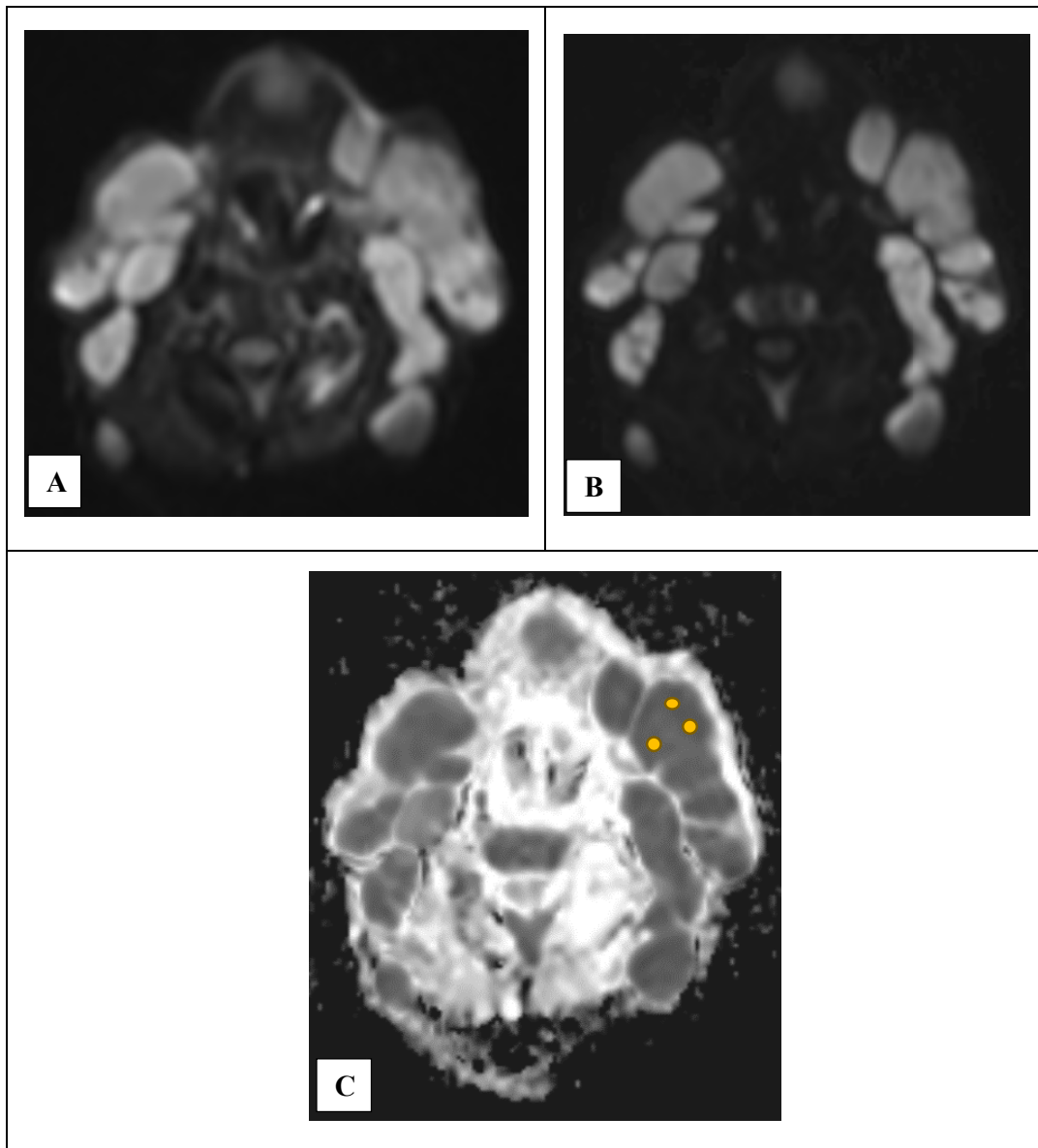


**Figure 16: MRI axial DWI and ADC images of enlarged lymph nodes.**

Multiple well-defined multilevel enlarged lymph nodes shows diffusion restriction (A&B) with ADC image (C) demonstrating multiple ovoid ROIs (Yellow circles), each measuring  $\sim 25 \text{ mm}^2$  in the areas of restricted diffusion for calculation of mean ADC value.

---

## CLINICAL STUDIES

**Zhang A et al.** conducted a study in 133 patients to assess the diagnostic value of apparent diffusion coefficient (ADC) for discriminating different-sized metastatic lymph nodes in patients with cervical cancers. They concluded that diffusion-weighted imaging can be used to differentiate enlarged metastatic lymph nodes from benign lymph nodes, and  $ADC_{min}$  can be further used to identify micro-metastasis in normal-sized lymph nodes.<sup>55</sup>

**Sharma P et al.** conducted a study in 40 patients and assessed the role of MRI with the help of DWI and ADC to differentiate infective from tuberculous lymph nodes and calculated the statistical parameters in the differentiation of infective and tuberculous lymph nodes of neck using diffusion weighted imaging (DWI) and apparent diffusion coefficient (ADC) values with histopathological examination as the gold standard. They found that the range of ADC values for tuberculous cervical lymph nodes was between  $0.99 - 1.01 \times 10^{-3} \text{mm}^2/\text{s}$  in the solid portion of the lymph node and  $1.27 - 1.31 \times 10^{-3} \text{mm}^2/\text{s}$  in the necrotic portion of the lymph node. The mean of ADC values for infective cervical lymph nodes was between  $1.0 - 1.2 \times 10^{-3} \text{mm}^2/\text{s}$  in the solid portion and in the necrotic portion the values. The study demonstrated that the ADC values of both the necrotic and solid portions of the lymph nodes are useful in differentiation between the causes of cervical lymphadenopathy. The ADC value of necrosis is especially helpful in discriminating infective from tuberculosis.<sup>56</sup>

---

**Chen C et al.** conducted a study in 40 patients to assess the utility of apparent diffusion coefficient (ADC) determined on diffusion-weighted MR imaging (DWI) to differentiate between benign and malignant parotid area lymph nodes (PLN) in nasopharyngeal carcinoma (NPC) patients. They found that the mean ADC value for benign PLNs was markedly higher than malignant PLNs. A threshold ADC of  $1.01 \times 10^{-3} \text{ mm}^2/\text{s}$  was associated with a sensitivity of 85.7 % and a specificity of 72.7 % (area under the curve: 0.84). Therefore, the study concluded that DWI may be a promising technique to differentiate metastatic from benign PLNs.<sup>57</sup>

**Ustabasioglu FE et al.** conducted a study in 63 patients to prospectively assess the diagnostic value of apparent diffusion co-efficient (ADC) measurement in the differentiation of benign and malignant lymphadenopathies. They found that the mean ADC value of malignant lymphadenopathy ( $1.030 \pm 0.245 \times 10^{-3} \text{ mm}^2/\text{s}$ ) was significantly lower ( $P < 0.05$ ) when compared to benign lymphadenopathies ( $1.571 \pm 0.559 \times 10^{-3} \text{ mm}^2/\text{s}$ ). For differentiating malignant from benign lymphadenopathy, the best result was obtained when an ADC value of  $1.334 \times 10^{-3} \text{ mm}^2/\text{s}$  was used as a threshold value; area under the curve 0.848, accuracy 78.4 %, sensitivity 66 %, specificity of 86 %, positive predictive value 76.7 %, and negative predictive value of 79.2 %. Based on the study results it was concluded that interobserver agreement was excellent for ADC measurements. Hence, ADC measurements could be considered an important supportive method in differentiating benign from malignant lymphadenopathies.<sup>58</sup>

---

**De Boer P et al.** conducted a study to evaluate change in ADC of the primary tumour and pathologic lymph nodes during treatment and to correlate this with clinical outcome. Twenty patients were included who received chemo radiation. They concluded that ADC is a predictor for response to EBRT. However, the correlation in this study was not statistically significant.<sup>59</sup>

**Serour DK et al.** conducted a study to evaluate the diagnostic value of diffusion-weighted as a part of the magnetic resonance imaging in patients with head and neck cancer to allow differentiation of lymph nodes, cancer staging, assessment of recurrence, and evaluation of the effects of oncologic therapy. They found that the ADC value for benign LNs ranged from  $1.26 \times 10^{-3}$  to  $2.49 \times 10^{-3} \text{ mm}^2/\text{s}$  (mean  $1.98 \times 10^{-3} \pm 0.32 \times 10^{-3}$ ), and malignant LNs from  $0.608 \times 10^{-3}$  to  $2.1 \times 10^{-3} \text{ mm}^2/\text{s}$  (mean  $0.971 \times 10^{-3} \pm 0.305 \times 10^{-3}$ ) ( $P < 0.001$ ) with sensitivity and a specificity of 94 % and 100 % respectively. The ADC value for metastatic LNs ranged from  $0.70 \times 10^{-3}$  to  $2.10 \times 10^{-3}$  ( $1.08 \times 10^{-3} \pm 0.31 \times 10^{-3}$ ) while lymphomatous nodes ranged  $0.608 \times 10^{-3}$  to  $1.16 \times 10^{-3}$  ( $0.78 \times 10^{-3} \pm 0.17 \times 10^{-3}$ ). In this study, a significant statistical difference was also observed between the ADC value of the SCC and lymphomatous LN ( $P = 0.0034$ ) with sensitivity and a specificity of 90 % and 75 % respectively. Hence, the study concludes that diffusion-weighted MR imaging is an effective assist in differentiating benign and malignant lymph nodes. It acts as an indicator for recovery or recurrence after chemotherapy and radiotherapy.<sup>60</sup>

---

**Kanmaz L et al. 2018** conducted a study in 32 patients to evaluate the value of diffusion-weighted MRI (DW-MRI) in differentiating benign and malignant head and neck masses by comparing their apparent diffusion coefficient (ADC) values. They found that the mean ADC values of benign and malignant neck masses were  $1.57 \times 10^{-3} \text{ mm}^2/\text{s}$  and  $0.90 \times 10^{-3} \text{ mm}^2/\text{s}$ , respectively. The difference between mean ADC values of benign and malignant neck masses was significant ( $P < 0.01$ ). Diffusion-weighted MRI with ADC measurements can be useful in the differential diagnosis of neck masses.<sup>61, 62</sup>

Therefore, with this background, this study was aimed to evaluate the role of DWMRI and ADC cut-off values in differentiating benign from malignant cervical lymph nodes.

# **MATERIALS AND METHODS**



---

## MATERIALS AND METHODS

### Source of data:

This was a hospital based cross-sectional study conducted in the department of Radio-Diagnosis, R.L. Jalappa Hospital and Research Center attached to Sri Devaraj Urs Medical College, Tamaka, Kolar over a period of 18 months from Jan 2021 to June 2022. The study included patients with enlarged cervical lymph nodes referred for MRI who fulfilled the inclusion criteria.

### Study Design: A cross sectional analytical study.

### Sample Size:

Sample was calculated based on sensitivity of DWMRI as 97 % in a study by Parihar et al.<sup>62</sup> with 95 % confidence interval and absolute error of 5 %. The formula used to calculate the sample size is as follows:

$$\text{Sample size} = \frac{Z_{1-\alpha/2}^2 p(1-p)}{d^2}$$

Where  $Z_{1-\alpha/2} = 1.96$  at 5 % error alpha.

As in majority of studies  $p$  values are considered significant below 0.05 hence 1.96 is used in formula.

$p$  = Expected proportion in population based on previous studies or pilot studies.

$d$  = Absolute error or precision – Has to be decided by researcher.

---

$$p = 97 \text{ or } 0.97$$

$$1 - p = 10 \text{ or } 0.1$$

$$d = 5 \%$$

Using the above values at 95 % confidence level a sample size calculated was 45 subjects with enlarged cervical lymph nodes.

**Inclusion Criteria:**

1. Patients with enlarged cervical lymph nodes.

**Exclusion Criteria:**

1. Patients who have recently received radiotherapy/chemotherapy.
2. Patients who underwent recent cervical lymph node FNAC/Biopsy in last 3 weeks.

**Method of collection of data (including sampling procedure if any):**

Baseline data of the patients participating in the study were recorded. Individuals having clinically palpable lymph nodes or diagnosed on ultrasonography and/or CT-Neck. MRI of Neck was performed on 1.5 Tesla, 18 channel, MR Scanner (Siemens® Magnetom Avanto®) using dedicated surface coil. The patients were made to lie down in supine position and following sequences was performed:

- T1WI (axial & coronal)
- T2WI (axial & coronal)
- STIR (axial & coronal)
- DWI will be acquired with b values 50,400 and 800 mm<sup>2</sup>/s with corresponding ADC values.

---

Imaging characteristics were interpreted based on morphological changes size, shape, margins; DWI along with its ADC values were used in assessing enlarged cervical lymph nodes and their corresponding ADC values were calculated.

Initially, T1, T2 & STIR axial & coronal sequences are acquired within a total time of 15-20 minutes. Next DWI sequences at 50, 400 and 800 s/mm<sup>2</sup> b values are taken followed by its ADC sequence is acquired. Both the sequences; i.e. DWI at 800 s/mm<sup>2</sup> b value and ADC sequence are compared to assess the presence or absence of restricted diffusion within the lymph nodes.

For derived ADC values, in case of malignant lesions, multiple oval shaped region of interest (ROI) each measuring ~25 mm<sup>2</sup> are drawn over the areas of restricted diffusion. Value of each ROI is measured and mean of all the ROIs is taken as the final ADC value for malignant lymph nodes. In case of benign lymph nodes, multiple ROIs each measuring ~25 mm<sup>2</sup> are drawn throughout the lesion and the lymph nodes show no restricted diffusion. Mean of all the ROIs are taken as final ADC value for benign lymph node.



**Figure 17: 1.5 Tesla, 18 channel, MR Scanner (Siemens® Magnetom Avanto®)**

#### **Data Analysis:**

The data were entered in Microsoft excel sheet. The measurable variables were analyzed and interpreted between them by the student's t test and the ordinal and categorical variables between them were interpreted by Chi-square ( $\chi^2$ ) test. The predictive value of DWMRI for differentiating benign and malignant lymph nodes was estimated. The statistical procedures were performed with the help of an SPSS statistical package (ver 21) and OpenEpi ver 3.01. P value less than 0.05 ( $P < 0.05$ ) was considered as statistically significant. Sensitivity, specificity, positive predictive value, negative predictive value and diagnostic accuracy was calculated and compared with pathological findings, which is used as gold standard.



# RESULTS

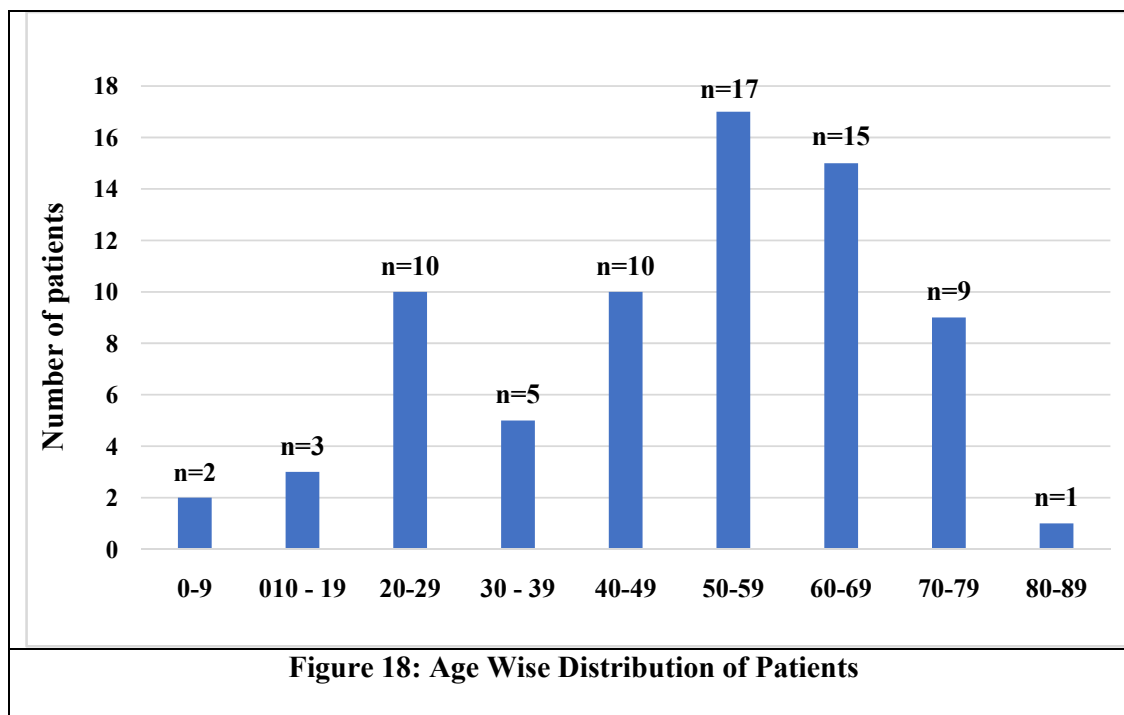


## RESULTS

In the present study, out of 72 (100 %), majority of the patients were in the age group of 50 - 59 (17/23.6 %) years followed by 60 - 69 years (15/20.8 %). (Table 7 and Figure 18)

**Table 7: Age Wise Distribution of Patients**

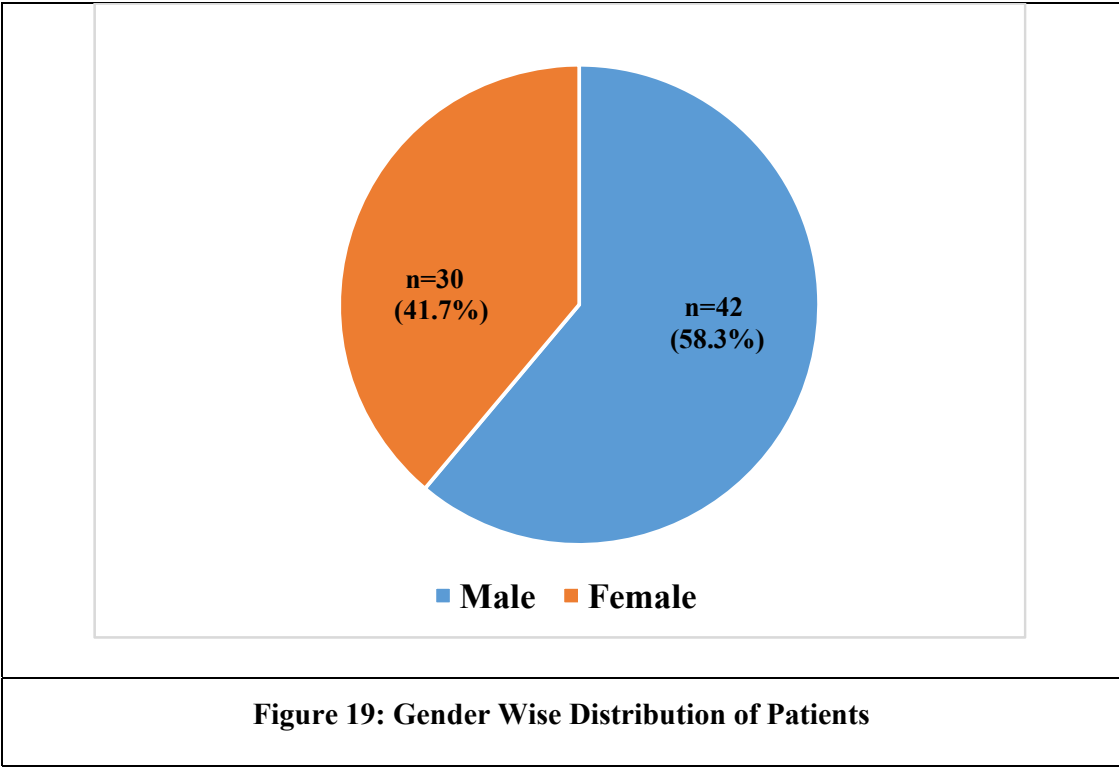
Age Group	Number	Percentage (%)
0 - 9	2	2.8 %
10 - 19	3	4.2 %
20 - 29	10	13.9 %
30 - 39	5	6.9 %
40 - 49	10	13.9 %
50 - 59	17	23.6 %
60 - 69	15	20.8 %
70 - 79	9	12.5 %
80 and above	1	1.4 %
Total	72	100.0 %



Among 72 (100 %) patients, most of the patients were males (44/61.1 %) compared to females (628/38.9 %). (Table 8 and Figure 19)

**Table 8: Gender Wise Distribution of Patients**

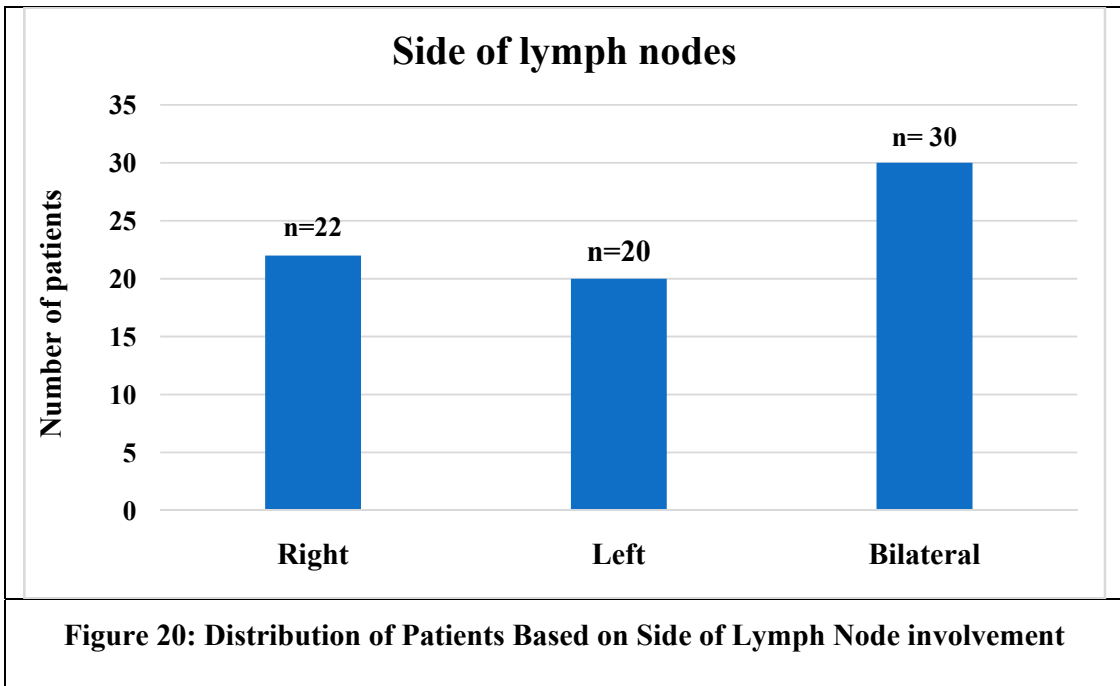
Gender	Number	Percentage (%)
Male	30	41.6 %
Female	42	58.4 %
Total	72	100.0 %



Out of 72 (100 %), 30 (41.7 %) patients had bilateral lymph node involvement, about 22 (30.6 %) of the patients had right side involvement and about 20 (27.8 %) of the patients had left side involvement. (Table 9 and Figure 20)

**Table 9: Distribution of Patients Based on Side of Lymph Node**

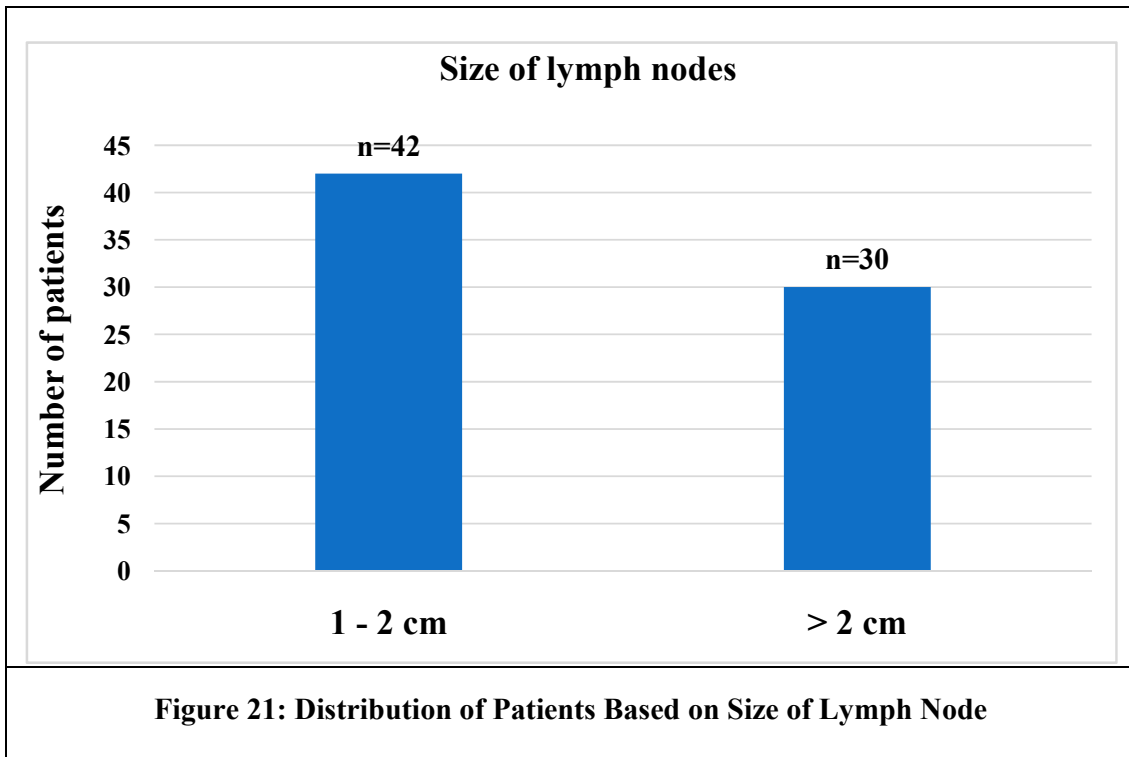
Side	Number	Percentage (%)
Right	22	30.6 %
Left	20	27.8 %
Bilateral	30	41.7 %
Total	72	100.0 %



Majority of the patients had lymph node size measuring 1 – 2 cm (42/58.3 %) and about 30 (41.7 %) patients had lymph node measuring > 2 cm. (Table 10 and Figure 21)

**Table 10: Distribution of Patients Based on Size of Lymph Node**

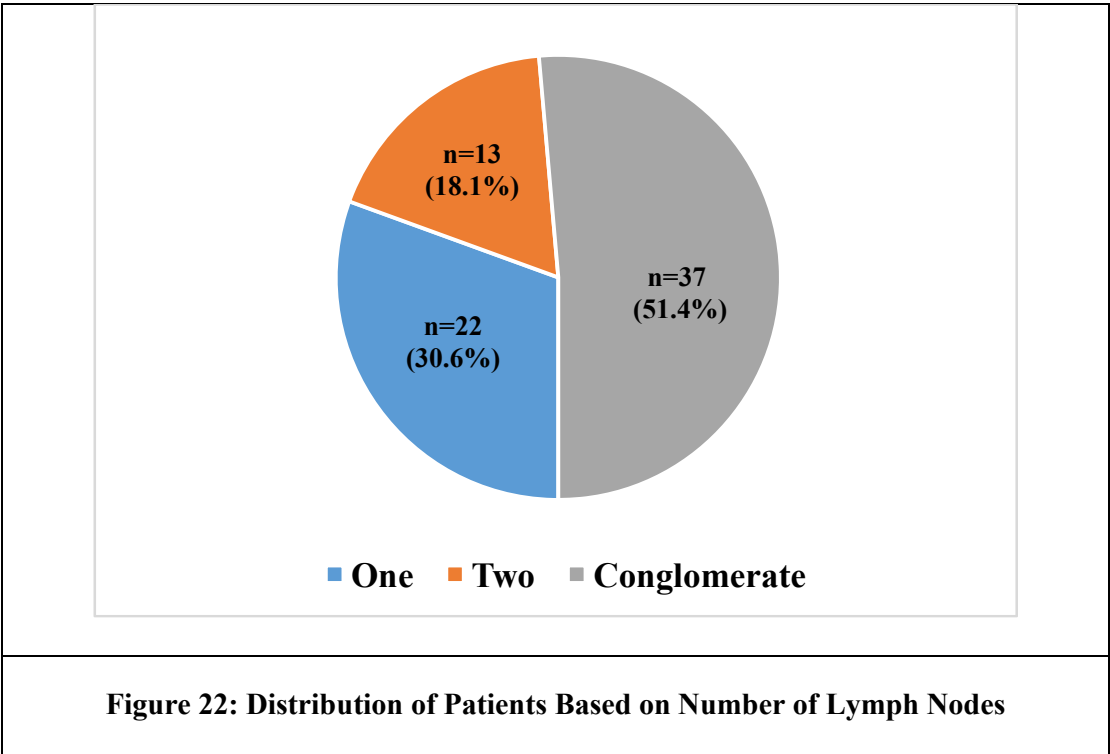
Size	Number	Percentage (%)
1 - 2 cm	42	58.3 %
> 2 cm	30	41.7 %
Total	72	100.0 %



Most of the patients i.e., 37 (51.4 %) of patients had conglomerate lymph nodes followed by 1 lymph node in 22 (30.6 %) of the patients and about 13 (18.1 %) of the patients had 2 lymph nodes. (Table 11 and Figure 22)

**Table 11: Distribution of Patients Based on Number of Lymph Node**

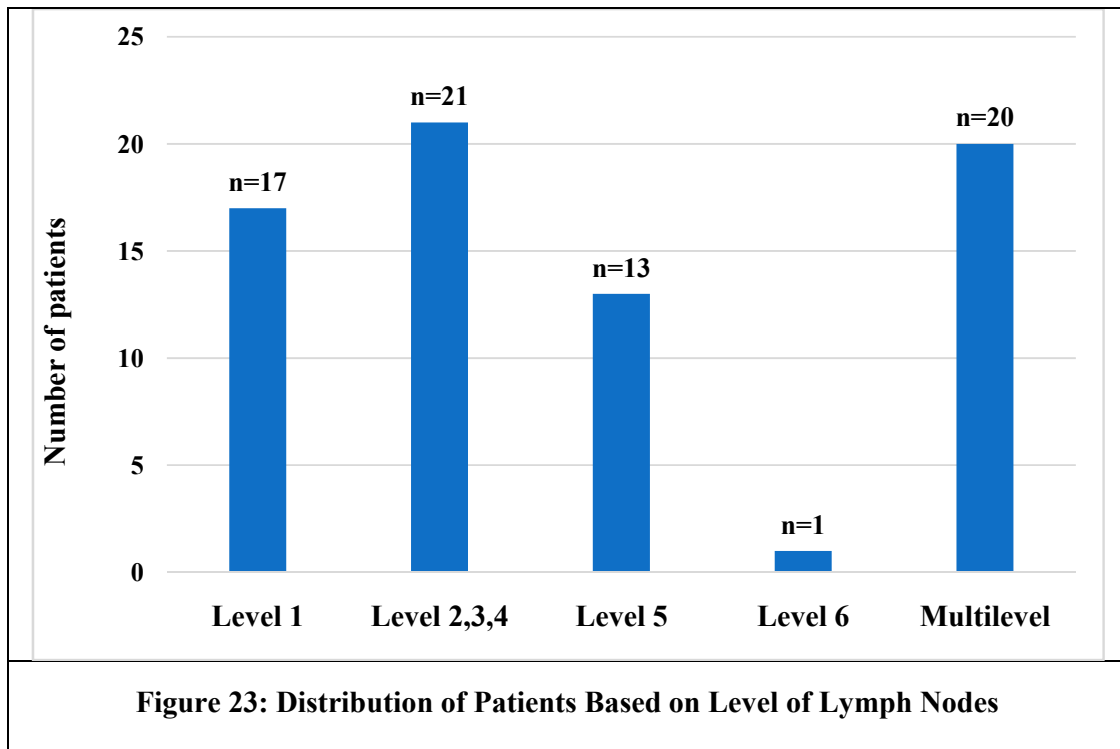
Number of Lymph Nodes	Number	Percentage (%)
One	22	30.6 %
Two	13	18.1 %
Conglomerate	37	51.4 %
Total	72	100.0 %



Majority, 21 (29.2 %) of patients had level 2, 3, 4 lymph nodes, followed by 20 (27.8 %) had multilevel involvement, about 17 (23.6 %) had level 1, about 13 (18.1 %) had level 5 and only 1 patient (1.4 %) had level 4 lymph node. (Table 12: and Figure 23)

**Table 12: Distribution of Patients Based on Level of Lymph Nodes**

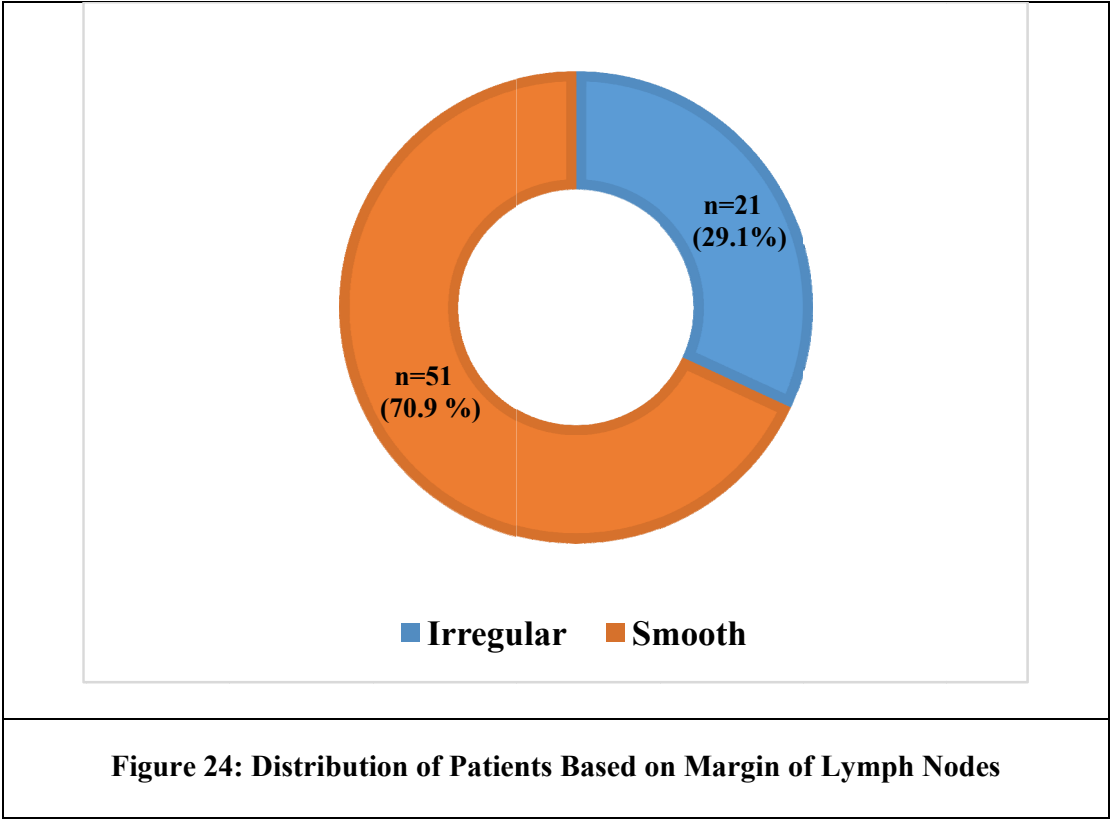
Level	Number	Percentage (%)
Level 1	17	23.6 %
Level 2,3,4	21	29.2 %
Level 5	13	18.1 %
Level 6	1	1.4 %
Multilevel	20	27.8 %
Total	72	100.0 %



Out of 72 (100 %) patients, most of the patients, 49 (68.1 %) had smooth margin in lymph nodes followed by irregular margin in 23 (31.9 %) of the patients. (Table 13 and Figure 24)

**Table 13: Distribution of Patients Based on Margin of Lymph Nodes**

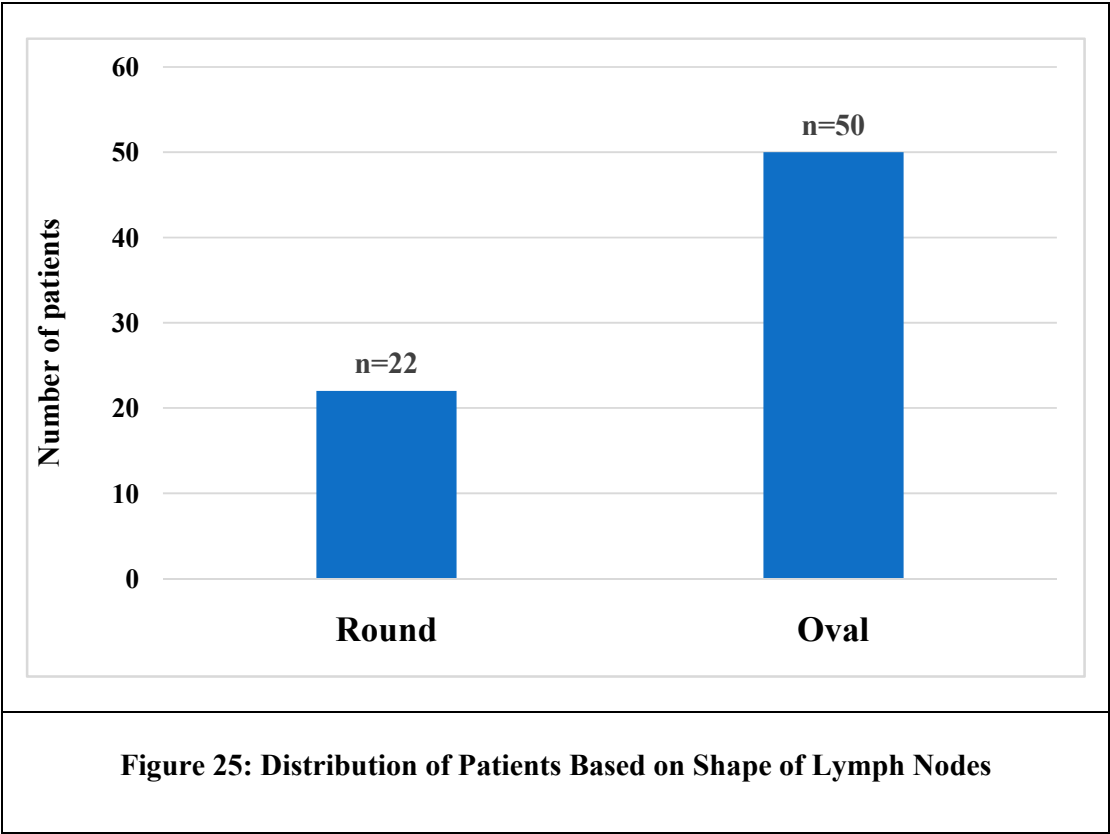
Margin	Number	Percentage (%)
Irregular	51	70.9 %
Smooth	21	29.1 %
Total	72	100.0 %



Majority, 50 (69.4 %) of the patients had lymph nodes in oval shape and remaining 22 (30.6 %) of the patients had lymph node round in shape. (Table 14 and Figure 25)

**Table 14: Distribution of Patients Based on Shape of Lymph Nodes**

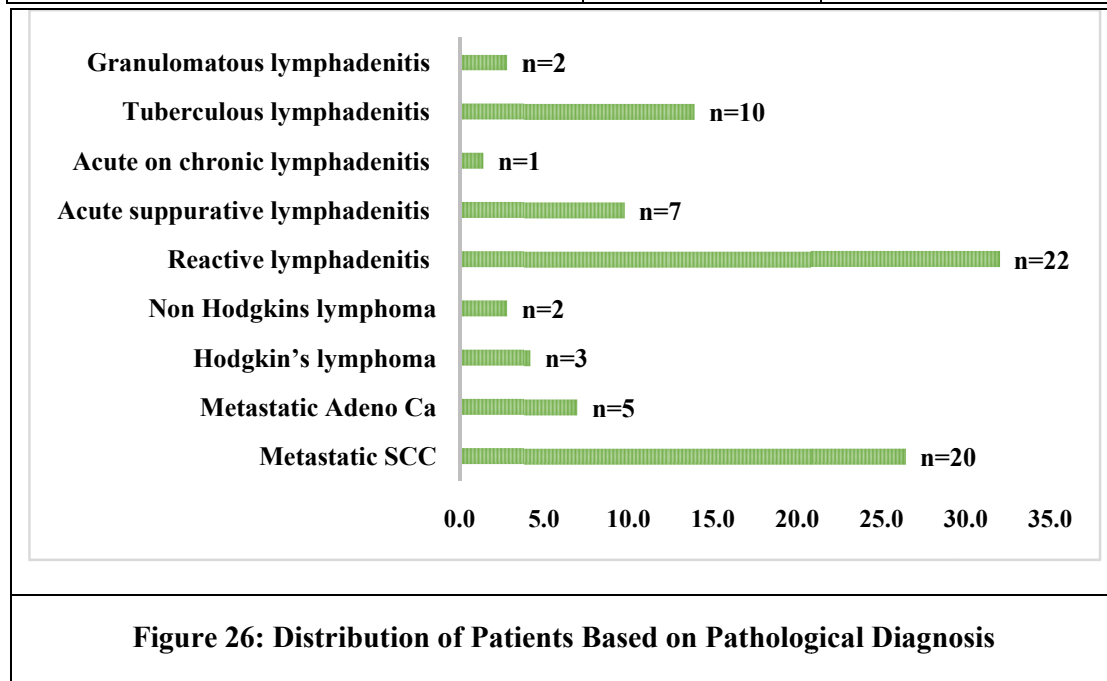
Shape	Number	Percentage (%)
Round	22	30.6 %
Oval	50	69.4 %
Total	72	100.0 %



The reactive lymphadenitis 23 (31.9 %) was the commonest pathological diagnosis followed by 19 (26.4 %) metastatic SCC, tuberculous lymphadenitis in 10 (13.9 %) of the patients, 7 (9.7 %) acute suppurative lymphadenitis, 5 (6.9 %) metastatic adeno Ca, 3 (4.2 %) Hodgkin's lymphoma, 2 (2.8 %) non-Hodgkin's lymphoma, 2 (2.8 %) granulomatous lymphadenitis and 1 (1.4 %) acute chronic lymphadenitis respectively. (Table 15 and Figure 26)

**Table 15: Distribution of Patients Based on Pathological Diagnosis**

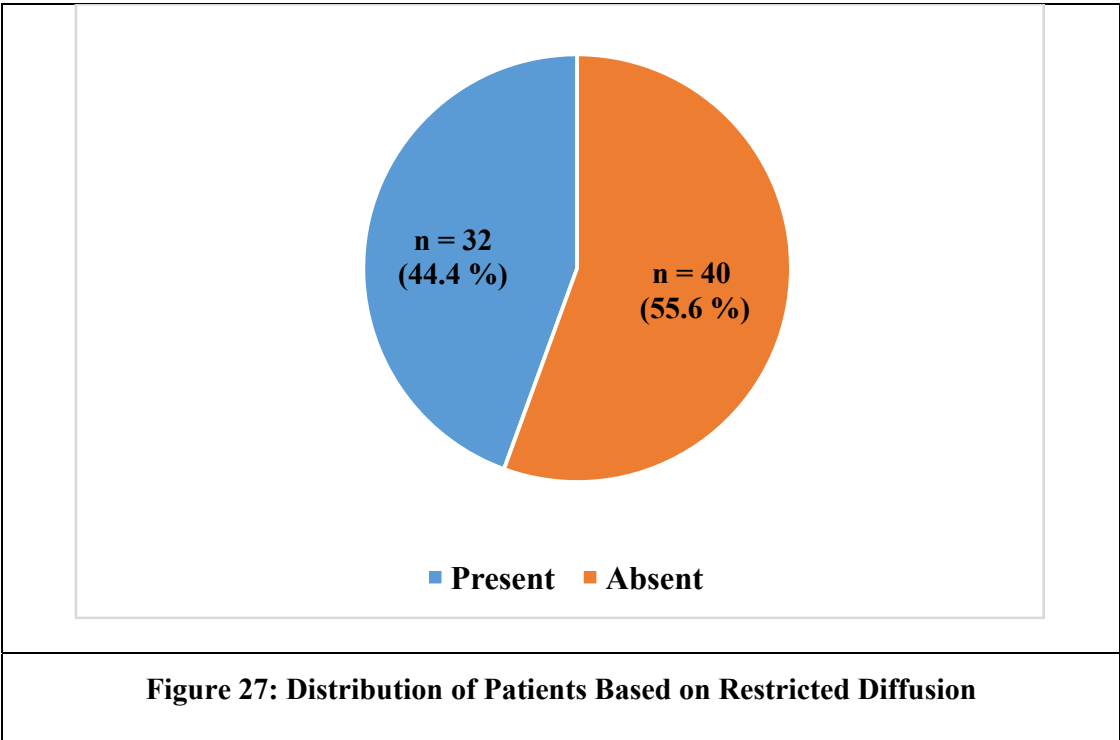
<b>Pathological Diagnosis</b>	<b>Number</b>	<b>Percentage (%)</b>
Metastatic SCC	20	27.7 %
Metastatic Adeno Ca	5	6.9 %
Hodgkin's lymphoma	3	4.2 %
Non-Hodgkin's lymphoma	2	2.8 %
Reactive lymphadenitis	22	30.5 %
Acute suppurative lymphadenitis	7	9.7 %
Acute on chronic lymphadenitis	1	1.4 %
Tuberculous lymphadenitis	10	13.9 %
Granulomatous lymphadenitis	2	2.8 %
Total	72	100.0 %



Among 72 (100 %) patients, about 32 (44.4 %) of the patients had restricted diffusion. (Table 16 and Figure 27)

**Table 16: Distribution of Patients Based on Restricted Diffusion**

Restricted Diffusion	Number	Percentage (%)
Present	32	44.4 %
Absent	40	55.6 %
Total	72	100.0 %



---

Out of 72 (100 %), about 30 pathologically proven malignant cases had ADC value of  $< 1.0 \times 10^{-3} \text{ mm}^2/\text{s}$ , among 42 pathologically proven benign cases, 40 cases have ADC value of  $> 1.0 \times 10^{-3} \text{ mm}^2/\text{s}$ , 2 discrepancies cases showed ADC value of  $< 1.0 \times 10^{-3} \text{ mm}^2/\text{s}$  and given as malignant, but pathologically proven as benign case of tuberculous abscess. There was a statistically significant association between ADC and pathological findings. Hence, findings with ADC cut-off value as  $1.0 \times 10^{-3} \text{ mm}^2/\text{s}$  for differentiating benign from malignant cervical lymph nodes were corresponding with histopathological findings. (Table 17).

**Table 17: Comparison of ADC and Pathological Findings**

ADC	Pathology		Total	X <sup>2</sup>	p
	Malignant	Benign			
$< 1.0 \times 10^{-3}$	30 (100.0 %)	2 (4.8 %)	32 (44.4 %)	60.22	0.0001
$> 1.0 \times 10^{-3}$	0 (0.0)	40 (95.2 %)	40 (55.6 %)		
Total	30	42	72		

Overall sensitivity, specificity, positive predictive value, negative predictive value and accuracy were 100 %, 95.2 %, 93.7 5%, 100 % and 97.22 % respectively.

---

**Table 18: Validity of ADC**

Sensitivity	100 %
Specificity	95.24 %
Positive predictive value	93.75 %
Negative predictive value	100 %
Accuracy	97.22 %

**Table 19: Validity of DWMRI, ADC and Pathology Diagnosis**

	Type of Nodes	Number	Sensitivity	Specificity	Accuracy
<b>DWMRI</b>	Benign	40	100 %	100 %	100 %
	Malignant	32			
<b>ADC</b>	Benign	40	100 %	100 %	100 %
	Malignant	32			
<b>Pathology Diagnosis</b>	Benign	42	100 %	95.24 %	97.22 %
	Malignant	30			

Our study found that for discriminating between benign and malignant cervical lymph nodes below are the range of: -

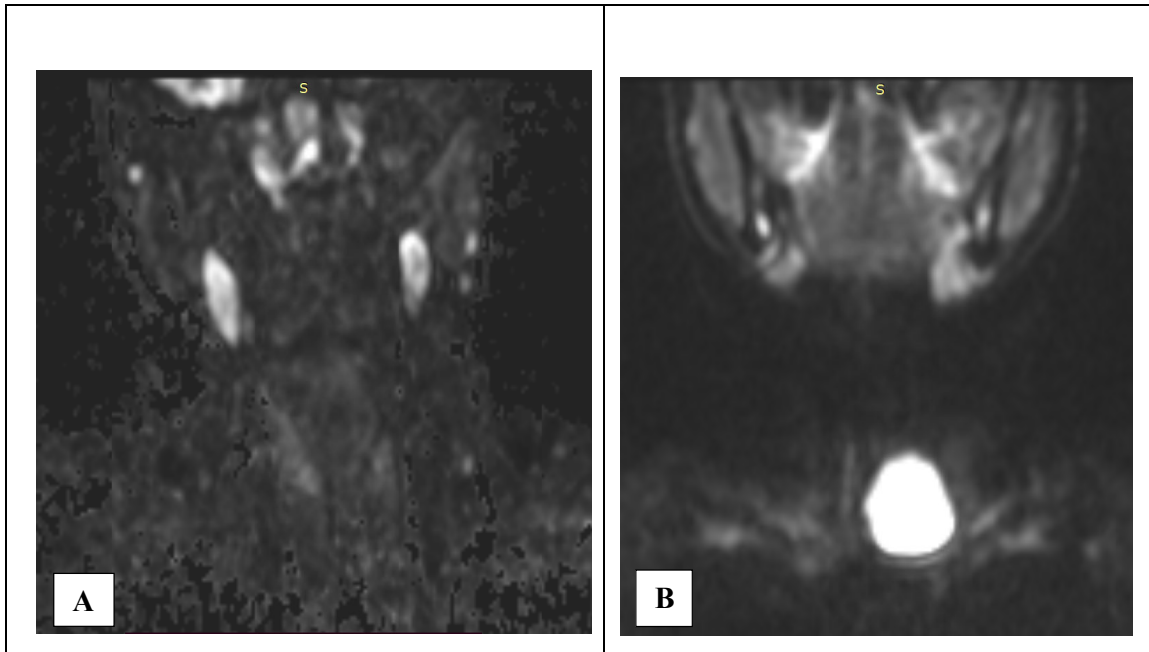
- ADC cut-off value  $-1.0 \times 10^{-3} \text{ mm}^2/\text{s}$
- Diagnostic accuracy – 97.22 %
- Sensitivity – 100 %
- Specificity - 95.24 %
- Positive predictive value – 93.75 %
- Negative predictive value – 100 %

**IMAGES**



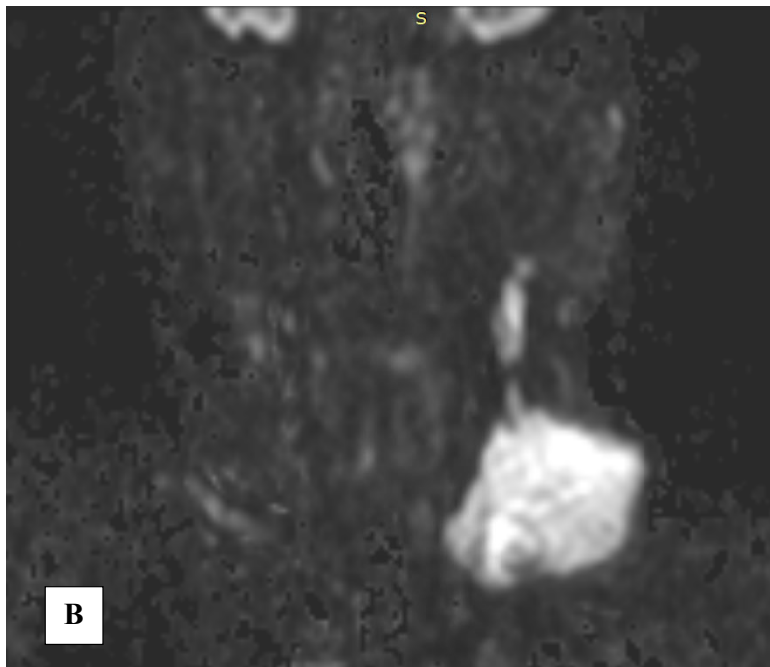
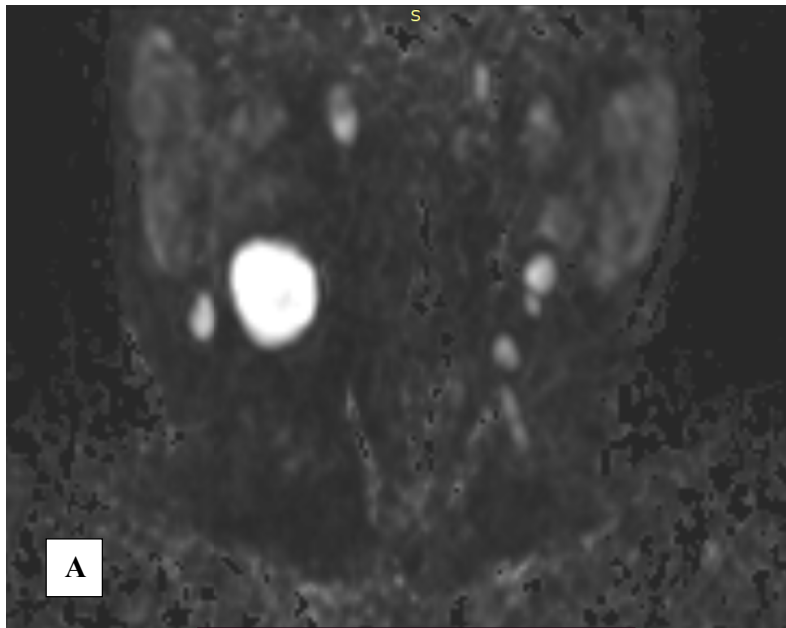
---

## IMAGES

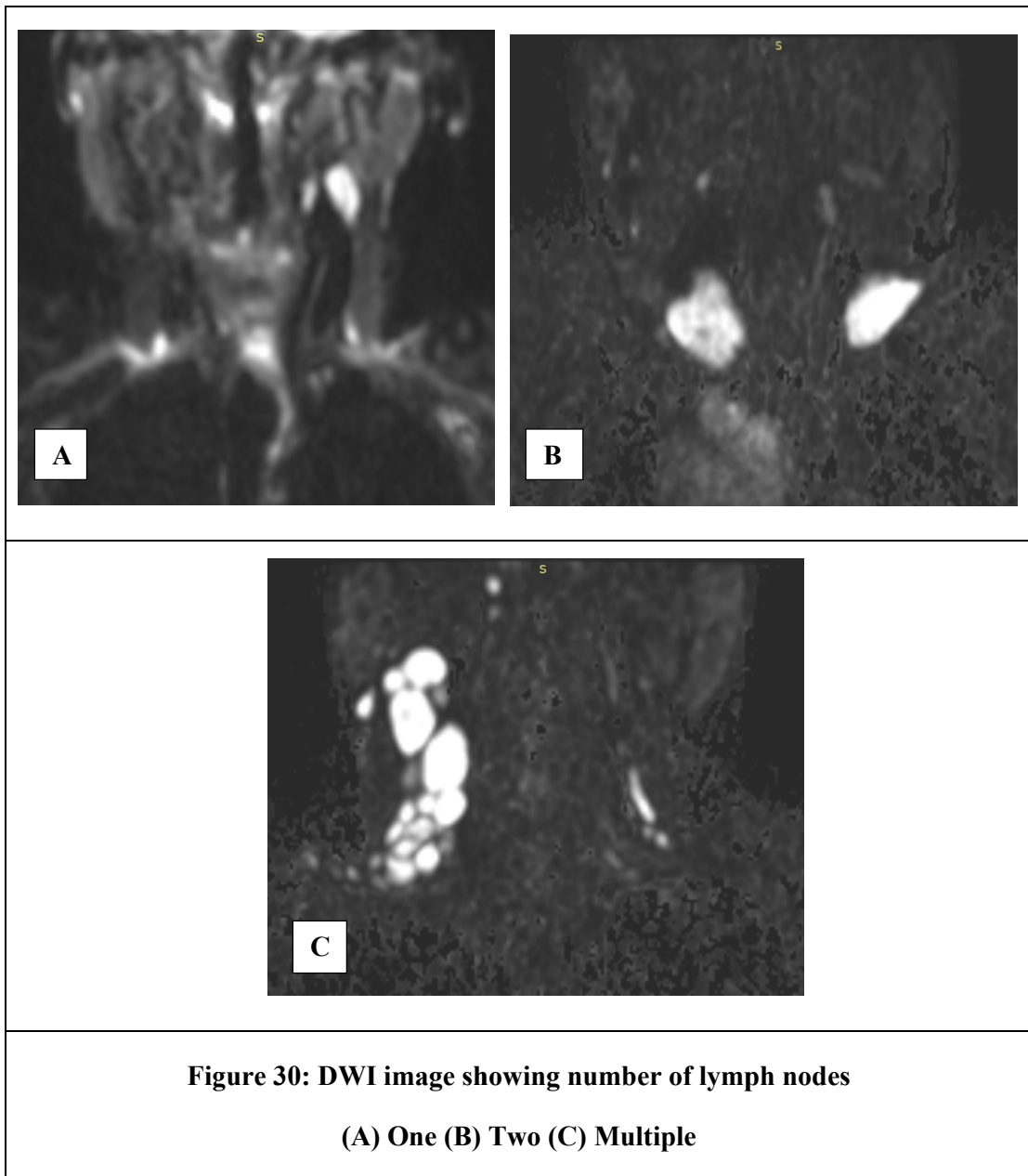


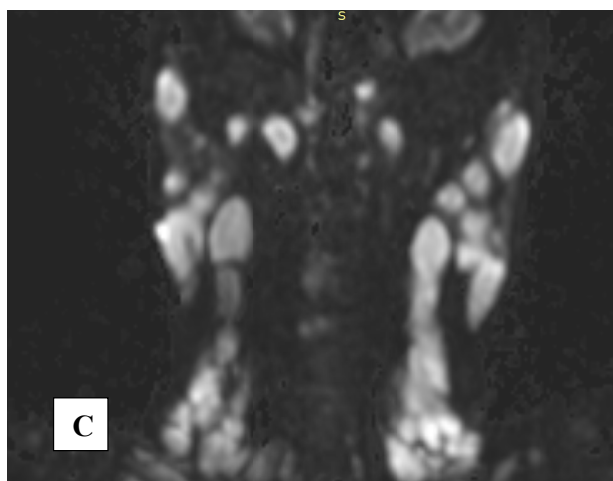
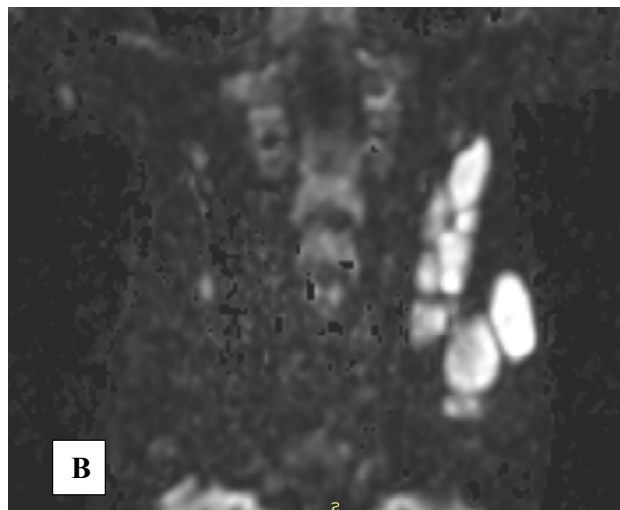
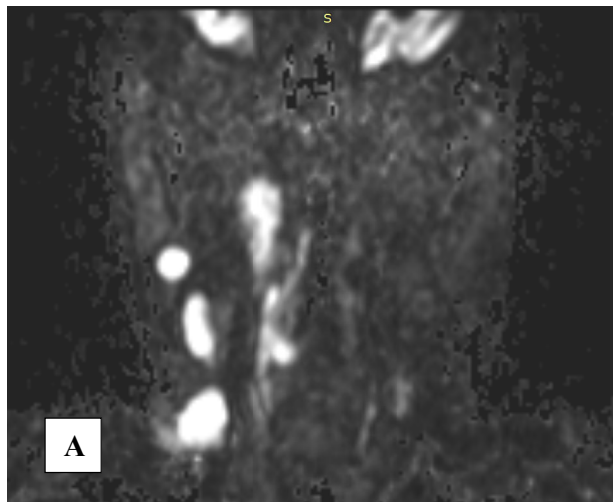
**Figure 28: DWI image showing shapes of lymph nodes:**

**(A) Oval (B) Round**



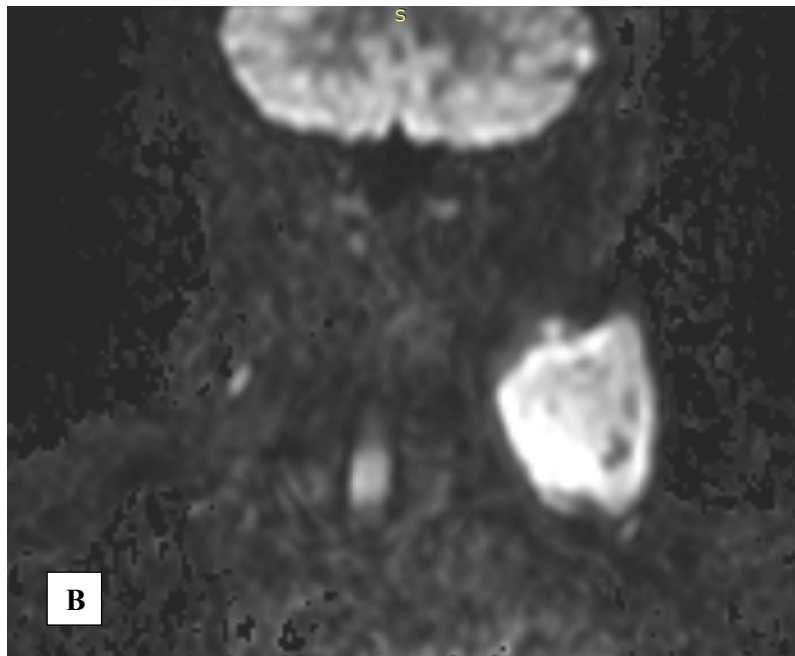
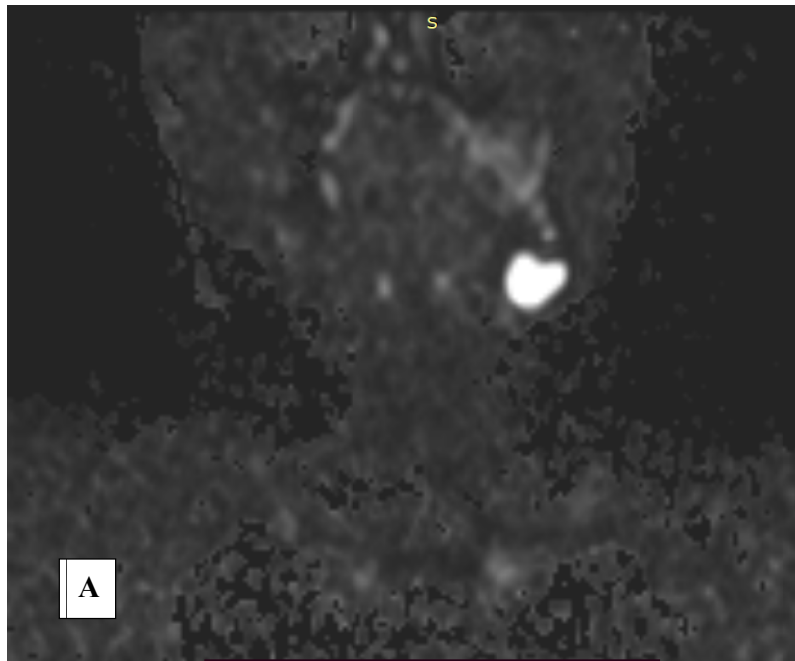
**Figure 29: DWI image showing margins of lymph nodes**  
**(A) Smooth (B) Irregular**





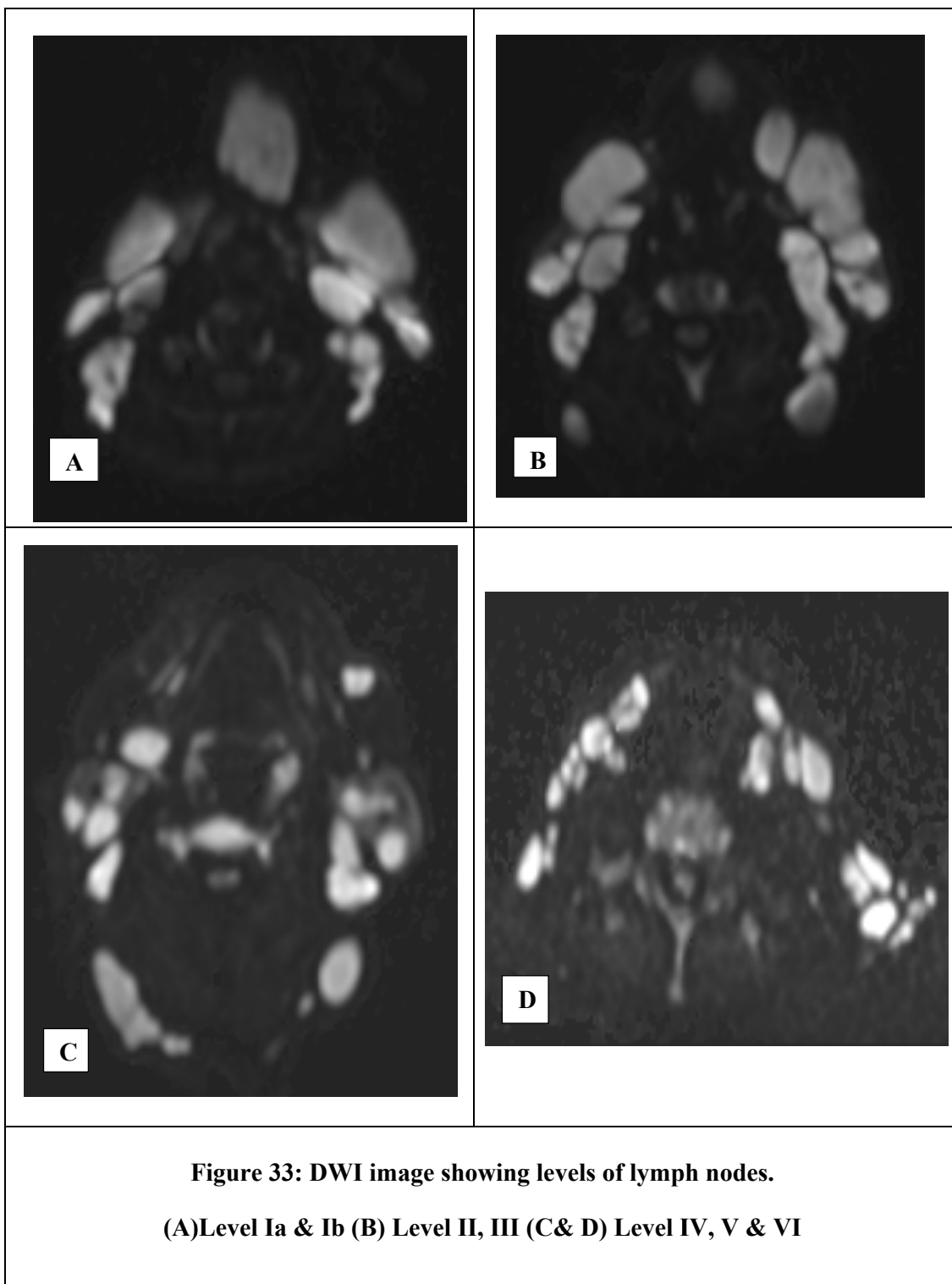
**Figure 31: DWI image showing sides of lymph node involvement.**

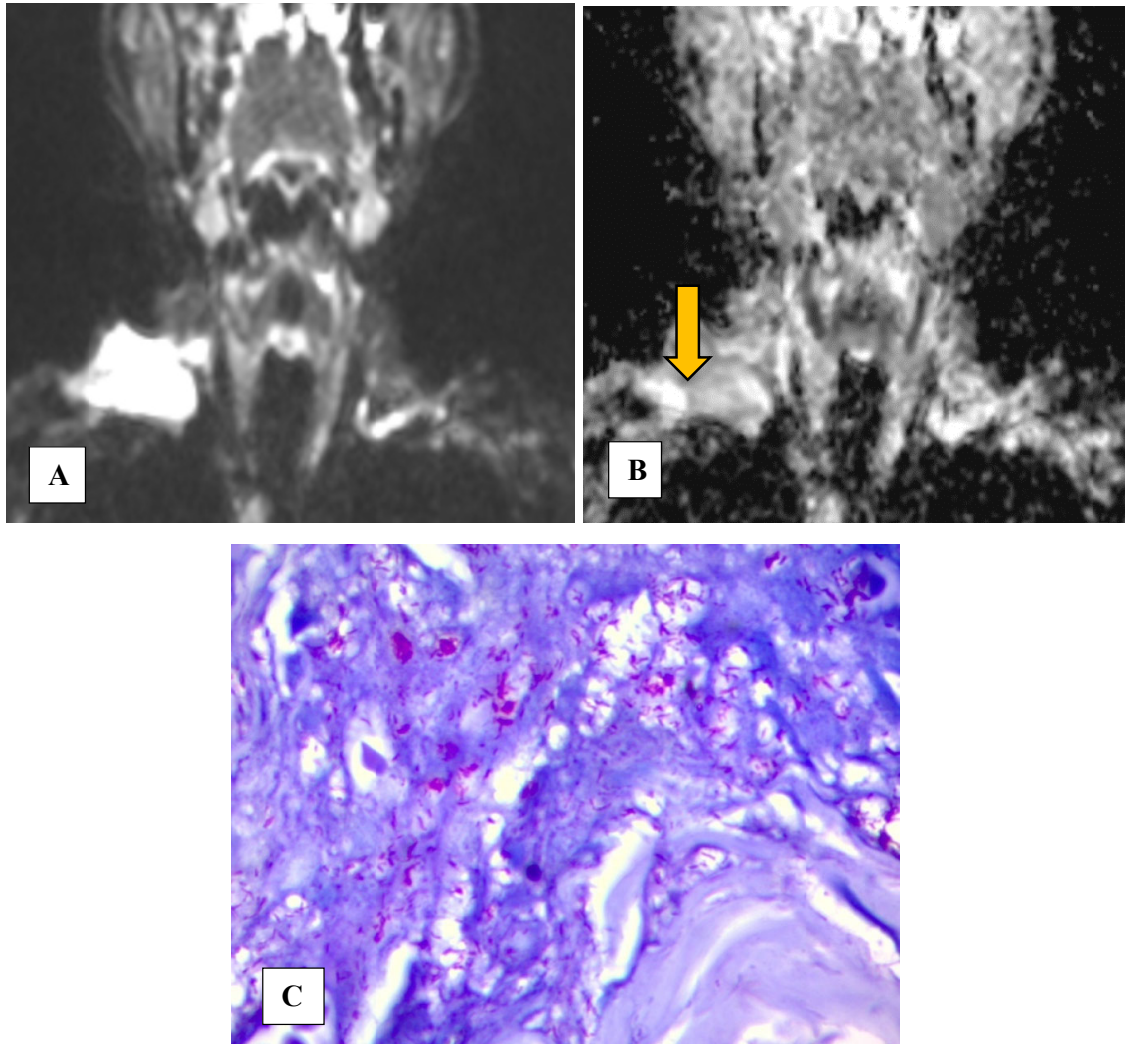
**(A)Right (B) Left (C) Bilateral**



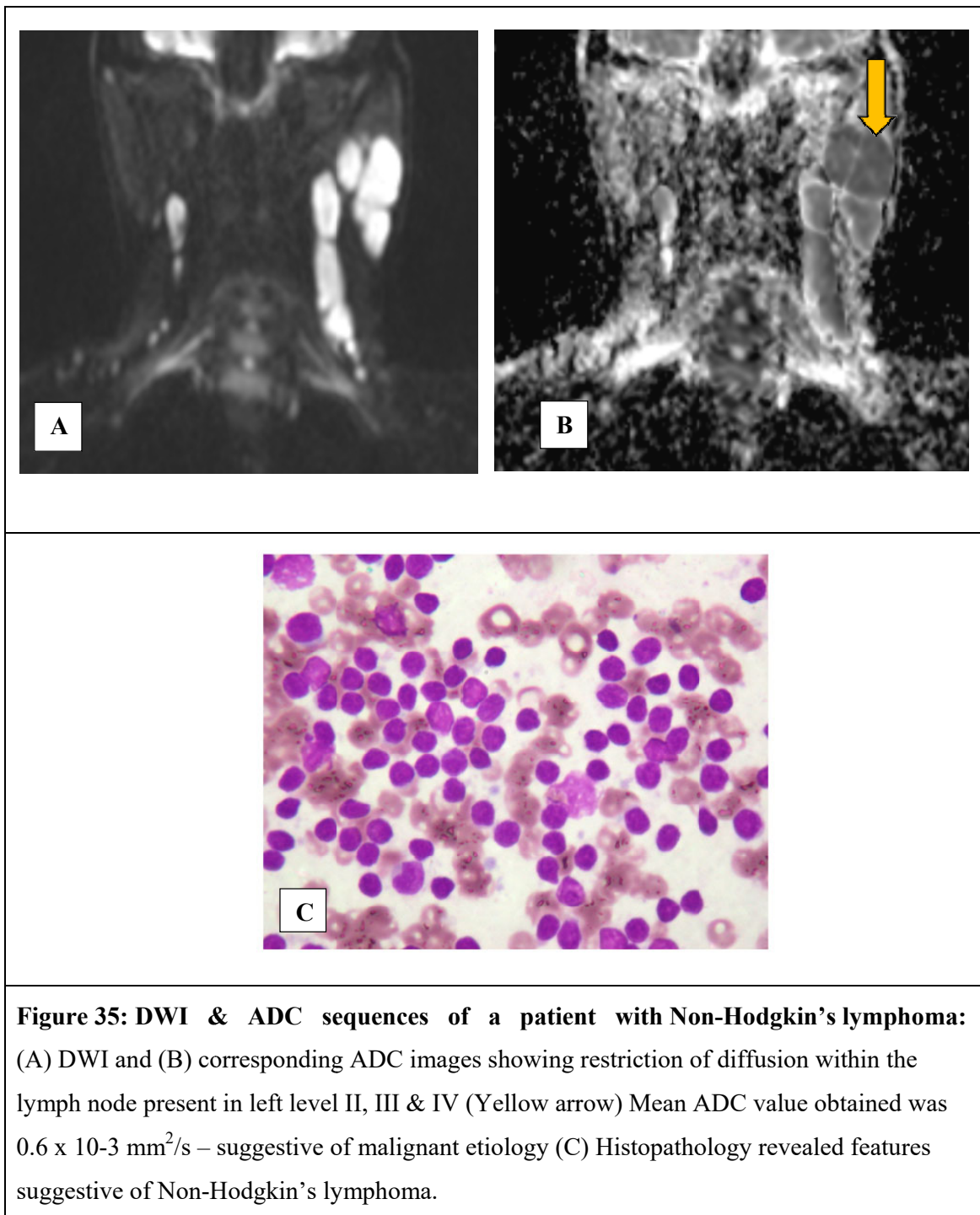
**Figure 32: DWI image showing size of lymph node.**

**(A) 1 - 2 cm (B) > 2 cm**





**Figure 34 :DWI & ADC sequences of a patient with tuberculous lymphadenitis:** (A) DWI and (B) corresponding ADC images showing no restriction of diffusion within the lymph node present in left supraclavicular region (Yellow arrow) Mean ADC value obtained was  $1.4 \times 10^{-3} \text{ mm}^2/\text{s}$ . – suggestive of benign etiology (C) Histopathology revealed features suggestive of tuberculous lymphadenitis.



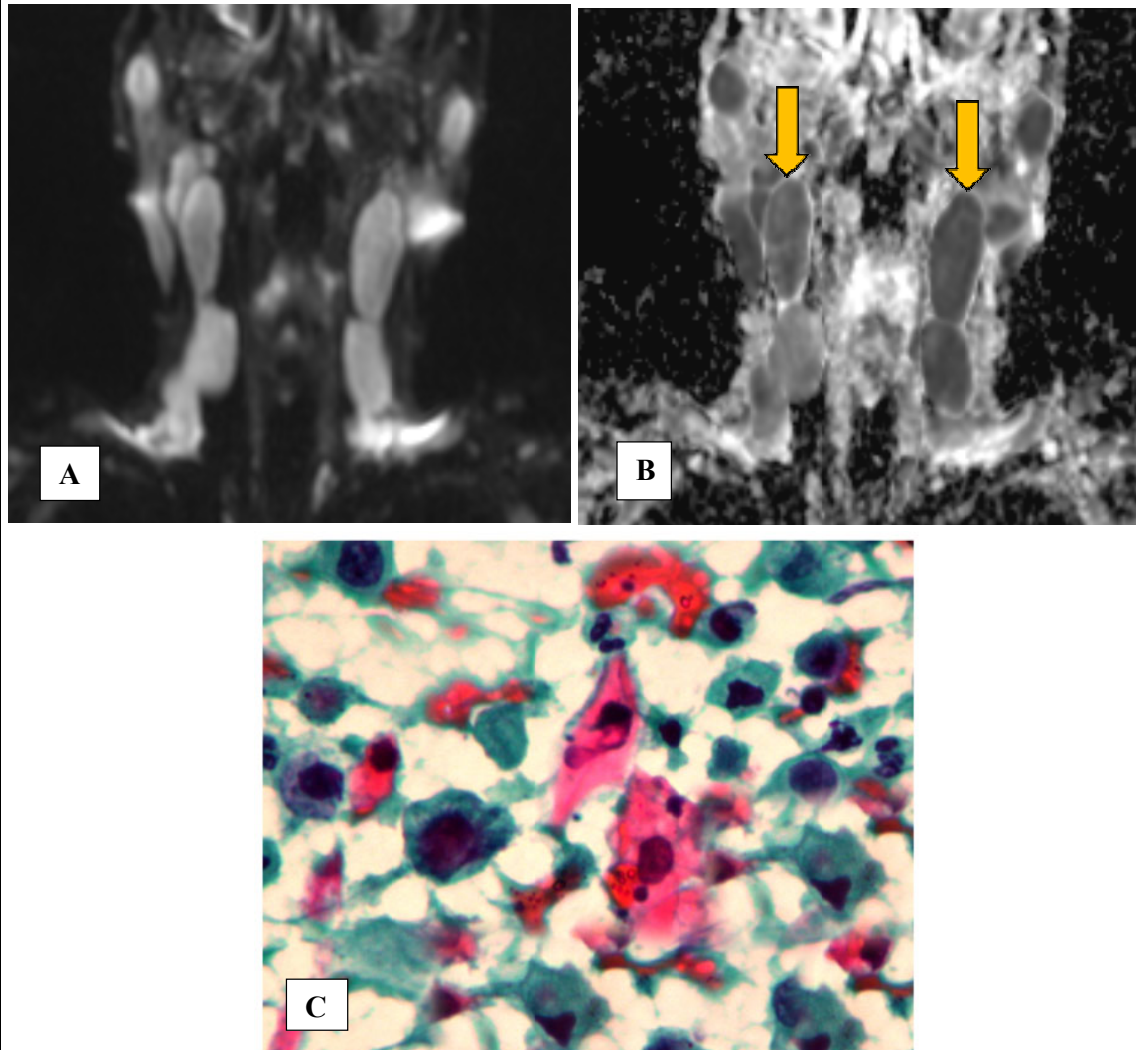


**Figure 36: DWI & ADC sequences of a patient with metastatic squamous cell carcinoma:**(A) DWI and (B) corresponding ADC images showing no restriction of diffusion within the lesion present in bilateral level Ib, II, III & IV (Yellow arrows). Mean ADC value obtained was  $0.8 \times 10^{-3} \text{ mm}^2/\text{s}$ – suggestive of malignant etiology (C).Histopathology revealed features suggestive of metastatic squamous cell carcinoma.

# DISCUSSION



---

## DISCUSSION

Diffusion weighted imaging, a well-known MRI technique which is reliable non-invasive imaging technique for tissue characterization. DWI exploits the random motion of water in the targeted tissue, which reflects the tissue specific diffusion capacity. In biologic tissues, the diffusivity of water molecules is confined by the intra-cellular and inter-cellular spaces. Hyper cellular tissue, such as malignant tumours, results in decreased mobility of water protons and consequently in a restricted diffusion capacity of the tissue. Thus, tumours present with increased signal on DWI and low ADC values. Non-tumoral tissues such as oedema, inflammation, fibrosis, and necrosis are expected to show low cellularity in strong contrast with viable tumour. In these tissues the diffusion capacity is not restricted. This results consecutively in a signal loss on DWI and high ADC.<sup>63,64</sup>

The evaluation of cervical lymphadenopathies is important as they serve as an excellent clue to underlying problems. They could be due to infections, autoimmune disorders or malignancies (metastatic or lymphomas).<sup>65</sup> Ultrasound image, contrast-enhanced computed tomographic and contrast-enhanced MRI allow the detection of cervical lymphadenopathies. None of these methods reach the ideal accuracy in diagnosis. These imaging methods use standard parameters (shape, size, internal architecture, extranodal diffusion and vascular features). The size is the most used criterion for the diagnosis.<sup>66</sup> The criterion of a short-axis diameter of 10 mm has gained widespread acceptance and thus used in our study.<sup>67</sup> To date, the diagnosis of lymph node metastases is based mainly on size criteria; however, non-enlarged nodes may harbour malignancy and also reactive nodes may be enlarged. Promising results with DW imaging to help detect cervical lymph node metastases and differentiate between benign and malignant enlarged nodes have been reported by Theony et al.<sup>68</sup>

---

Our hospital based cross-sectional study was conducted on 72 patients. Commonest age group with lymphadenopathy was 50 - 59 (17/23.6 %) years followed by 60 - 69 years (15/20.8 %). Mean age of the patients was  $45.13 \pm 17.08$  years and age range was 9 – 78 years. There was an increasing number of malignant lymph nodes with increase in age group, 79.1 % in > 30-year age group as opposed to 20.9 % in < 30-year age group. Similar observation was also made by Elsaid et al. where the age of patients ranged from 6 – 76 years, mean age being  $45 \pm 18.8$  years.<sup>70</sup>

We found that among 72 (100 %) patients, majority of the patients were males (44/61.1%) as compared to females (28/38.9 %). We did not find any statistically significant association between aetiology and gender of the patients. A similar observance was made by Ragheb et al. where majority of subjects were males (M - 70 %, F - 30 %).<sup>69</sup>

We recognized that there was higher lymphoma: metastatic lymph node ratio in < 30 years age group as compared to middle and older age groups. All malignant lymph nodes (100%) in younger age group (<30 years) were lymphoma cases and all of the malignant nodes in middle age group (30-60 years) and elderly age group were metastatic. This observation was consistent with study by Serour et al<sup>71</sup>. They also observed that, lymphoma cases were predominantly found in younger age group as opposed to middle and elderly age groups, which showed predominantly metastatic lymph nodes. Among malignant cervical lymph nodes, both Hodgkin's lymphoma (HL) and Non-Hodgkin's lymphoma (NHL) showed male predominance. An Indian study conducted by Mondal SK et al on 455 patients with lymphoma observed that, male: female ratio was 3.1:1 and NHL: HL ratio was 3.2:1<sup>72</sup>.

Considering the location of the lymph nodes among study population, we observed out of 72 patients, majority of patients, that is, 30 patients (41.7 %) had bilateral lymph nodal

---

involvement, about 22 patients (30.6 %) had right side involvement and about 20 patients (27.8 %) had left side involvement. In our study we found that laterality had significant correlation with nodal staging in head and neck carcinoma with nodal metastasis which is in agreement with study by Hoang et al.<sup>73</sup>

In our study, out of 72 cases, 42 cases (58.3 %) had lymph node size measuring 1 – 2 cm and about 30 cases (41.7 %) had size of lymph node > 2 cm. Among 30 malignant lymph nodes 10 cases had lymph nodes size between 1 - 2 cm, whereas among 42 benign cases 10 cases had lymph nodes size > 2 cm. In our study we found that size is not a reliable marker of malignancy. Small nodes can harbour small metastases that do not expand the node, and, conversely, benign nodes can commonly be enlarged due to hyperplasia or inflammation. A study by Curtin et al found that the radiologist's choice of size cut-off simply changes sensitivity and specificity for detection of nodal metastases. A 1.0 cm size cut-off in the largest axial diameter achieved 88% sensitivity and 39% specificity, whereas a 1.5-cm cut-off resulted in 56% sensitivity and 84% specificity which is in concordance with our study.<sup>74</sup>

In our study majority of the patients i.e., 37 patients (51.4%) had Conglomerate/multiple lymph nodes, 22 patients (30.6 %) had 1 lymph node and 13 patients (18.1 %) had 2 lymph nodes. We found that the majority, 21 cases (29.2 %) had level 2,3,4 lymph nodes, followed by multilevel involvement in 20 cases (27.8 %), 17 cases (23.6 %) had level 1 lymph nodes, about 13 cases (18.1 %) had level 5 and only 1 patient (1.4 %) had level 4 lymph node. These morphological characteristics observation was consistent with study by Serour et al.<sup>71</sup> In a study by Liu Z et al on 138 patients concluded that MRI is more sensitive than ultrasonography in diagnosis of central lymph nodal metastases, whereas there is no significant difference between the sensitivity of MRI & USG in differentiating lateral cervical lymph nodes.<sup>75</sup>

---

In our study, in 49 cases (68.1 %), the lymph nodes had smooth margins whereas irregular margin in lymph nodes was noted in 23 patients (31.9 %). Nodular contour can have a greater discriminatory value. ; Ill-defined irregular margins in a lymph node are a sign of malignancy secondary/due to extracapsular spread of tumor. This has been shown to be more accurate than nodal size<sup>71</sup>.

Out of 72 cases, 50 cases (69.4 %) of had oval shaped lymph nodes and remaining 22 cases (30.6 %) had rounded lymph nodes. Among 42 benign cases 20 cases had oval shaped lymph nodes and 10 cases had rounded lymph nodes. Among 30 malignant cases, 20 cases had oval shaped lymph nodes and 10 cases had rounded lymph nodes. Metastatic disease can change the shape of the node by infiltrating nodal tissue and expanding the nodal capsule. Thus, rounded rather than oval nodes are suspicious. Subcentimetric small oval nodes can harbor small metastases that do not expand the node, and conversely, benign nodes can commonly be enlarged due to hyperplasia or inflammation. In our study we found that shape of the lymph node has not much significance in differentiating benign and malignant lymph nodes which is in agreement with study by Hoang et al.<sup>73</sup>

In the present study, reactive lymphadenitis was the commonest pathological diagnosis seen in 23 cases, (31.9 %) followed by 19 cases (26.4 %), metastatic SCC, 10 cases (13.9 %) of tuberculous lymphadenitis, 7 cases (9.7%) of Acute suppurative lymphadenitis, 5 cases (6.9%) of Metastatic Adeno Carcinoma in Hodgkin's lymphoma in 3 cases (4.2 %), 2 (2.8 %) non-Hodgkin's lymphoma, 2 (2.8 %) granulomatous lymphadenitis and 1 (1.4 %) acute chronic lymphadenitis. In a study done by Ragheb et al, pathological examination of the studied lymph nodes in the examined 30 patients revealed: benign cases (5 cases of inflammatory, 3 cases

---

granulomatous), 12 lymphomatous cases including 9 cases of Non-Hodgkin lymphoma and 3 cases of Hodgkin lymphoma and 9 metastatic cases.<sup>69</sup>

In our research, malignant lymph nodes had been subdivided into subgroups of metastatic lymph nodes and lymphoma based upon the histopathology. An attempt was made to distinguish between them according to their ADC values. The mean ADC value for metastatic lymph nodes ( $0.93 \times 10^{-3} \text{ mm}^2/\text{s}$ ) was little higher than that of the lymphoma ( $0.65 \times 10^{-3} \text{ mm}^2/\text{s}$ ) which is in agreement with study by Serour et al.<sup>71</sup>

Among 72 (100 %) patients, restricted diffusion was present in about 32 cases (44.4 %). Restriction of diffusion was present in all 30 pathologically proven malignant cases. Similar observation was made in a study done by Elsaid et al. where all malignant cases showed restricted diffusion<sup>70</sup>. Out of 72 cases (100 %), 30 pathologically proven malignant cases had ADC value of  $< 1.0 \times 10^{-3} \text{ mm}^2/\text{s}$ . Out of 42 pathologically proven benign cases, 40 cases had ADC value of  $> 1.0 \times 10^{-3} \text{ mm}^2/\text{s}$ , however 2 cases with ADC value of  $< 1.0 \times 10^{-3} \text{ mm}^2/\text{s}$  which were considered to be malignant turned out to be pathologically proven benign cases of tuberculous abscess. In spite of this discrepancy, there was a statistically significant association between ADC and pathological findings noted in this study. These findings were in concordance with a study done by Ragheb et al which showed similar results.<sup>69</sup>

In our study, ADC value of  $1.0 \times 10^{-3} \text{ mm}^2/\text{s}$  was taken as cut-off in differentiating benign from malignant cervical lymph nodes. These values were found to be corresponding with histopathological findings. The ADC cut-off value of  $1.0 \times 10^{-3} \text{ mm}^2/\text{s}$  had an overall sensitivity, specificity, positive predictive value, negative predictive value and diagnostic accuracy of 100 %, 95.2 %, 93.7 %, 100 % and 97.2 % respectively. Hence, it was proven that the use of ADC values in combination with the other MRI criteria significantly improves the

---

discrimination between malignant and benign lymph nodes. Similar results were shown in a study done by Ragheb et al wherein optimal ADC cut off value of  $1.0 \times 10^{-3} \text{ mm}^2/\text{s}$  had an accuracy of 96.7 %, sensitivity 100 %, specificity 88.9 %, PPV 95.4 % and NPV 100 % for differentiation between benign and malignant lymph nodes.<sup>69</sup>

Holzapfel et al. and De Bondt et al showed that an ADC cut off value of  $1.02 \times 10^{-3} \text{ mm}^2/\text{s}$  had diagnostic accuracy of 94 %, sensitivity of 100 % and specificity of 87.0 % of in differentiating benign and malignant cervical lymph nodes.<sup>76,77</sup> A study done by Sumi et al. reported a low ADC threshold for metastatic nodes ( $> 0.400 \times 10^{-3} \text{ mm}^2/\text{s}$ ) which yielded a moderate negative predictive value (71 %) and high positive predictive value (93 %), which did not match with our results.<sup>78</sup>

Razek et al. reported slightly higher threshold (ADC =  $1.38 \times 10^{-3} \text{ mm}^2/\text{s}$ ) for reliably characterizing suspected malignant lymph nodes with an accuracy of 96 %, sensitivity of 98 % and specificity of 88 %.<sup>79</sup> Kanmaz et al Showed that an ADC value of  $1.13 \times 10^{-3} \text{ mm}^2/\text{s}$  had a sensitivity of 93.33 %, specificity of 82.35 %, positive predictive value of 82.35 %, and a negative predictive value of 93.33 % in differentiating malignant from benign lymph nodes.<sup>61</sup>

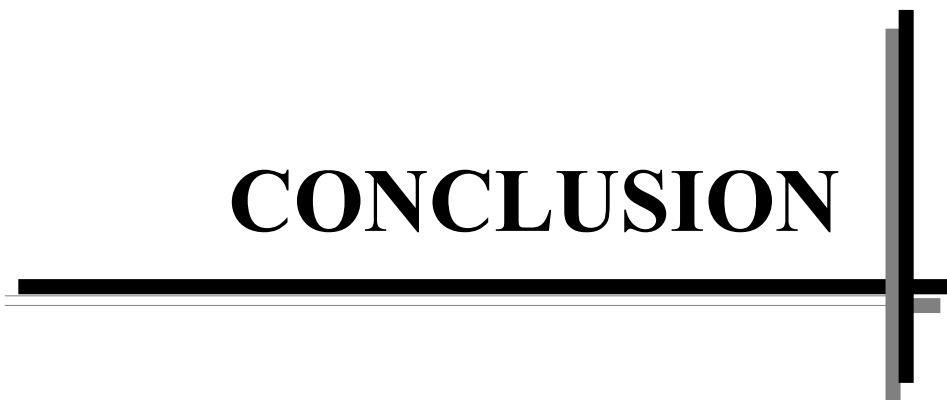
Serour et al concluded that mean ADC value of  $0.9 \times 10^{-3} \text{ mm}^2/\text{s}$  as a cut-off value in differentiation between benign and malignant cervical lymph nodes with accuracy, sensitivity and specificity of 97%, 90% and 75 % which is concordance with our study<sup>71</sup>.

A recent study conducted by Eldabry et al in 2022 concluded that ADC value of  $1.13 \times 10^{-3} \text{ mm}^2/\text{s}$  as a cut-off value in differentiation between benign and malignant cervical lymph nodes, with resultant accuracy, sensitivity and specificity of 94%, 100% and 87 % which is in agreement with our study.<sup>80</sup>

Hence, in our study it has been concluded that by using the combination of conventional MRI features of lymph node such as size, shape, characteristics and site of lymph nodes and DWMRI with ADC cut-off value of  $1.0 \times 10^{-3} \text{ mm}^2/\text{s}$  further improve the diagnostic accuracy of benign and malignant cervical lymph nodes. Hence it can be concluded that, using histopathological examination as the standard reference; we found that diffusion weighted MRI with ADC cut-off value of  $1.0 \times 10^{-3} \text{ mm}^2/\text{s}$  had excellent predictive validity (P - value < 0.001) in differentiating benign and malignant cervical lymph nodes.

<b>Author</b>	<b>Publication year</b>	<b>ADC Cut-off value (<math>\text{mm}^2/\text{s}</math>)</b>	<b>Diagnostic Accuracy</b>	<b>Sensitivity</b>	<b>Specificity</b>
Razek et al	2006	$1.3 \times 10^{-3}$	96 %	98 %	88 %
Holzapfel et al	2009	$1.0 \times 10^{-3}$	94 %	100 %	87 %
Ragheb et al	2014	$1.0 \times 10^{-3}$	96 %	100 %	88 %
Elsaid et al	2014	$1.0 \times 10^{-3}$	89 %	100 %	62 %
Kanmaz et al	2018	$1.1 \times 10^{-3}$	93 %	82 %	82 %
Serour et al	2020	$1.3 \times 10^{-3}$	97 %	90 %	75 %
Recent study (Eldabry et al)	2022	$1.3 \times 10^{-3}$	96 %	100 %	88 %

# CONCLUSION



---

## CONCLUSION

DWI is an MRI technique, which is non-invasive and helps in differentiating benign and malignant characteristics of the tissue. ADC is an objective parameter derived from DWI techniques, which helps to evaluate the tissue-specific diffusion capacity and, in turn, determine its malignant potential. Hence the present study was performed to evaluate the role of DWI and ADC in differentiating benign and malignant lesions and to determine other imaging features that can help in identifying neoplastic etiology.

This study was a hospital based cross-sectional study involving 72 subjects, with male subjects in the majority. The difference in the proportion of pathological findings between ADC values of the lymph nodes was statistically significant (P-value <0.001). The ADC cut off value of  $1.0 \times 10^{-3} \text{ mm}^2/\text{s}$  for cervical lymph nodes had a sensitivity of 100 %, specificity of 95.24 %, with total diagnostic accuracy of 97.22 % in predicting benign and malignant lymph nodes. Hence from our study results, the ADC value obtained had an excellent predictive value in predicting malignancy and correlated well with pathological diagnosis.

# SUMMARY



---

## SUMMARY

This study was a hospital based observational study involving 72 subjects (100%), of which male participants (44/61.1 %) were majority and females were (28/38.9 %). Considering the location of the lymph node among study population, out of 72 (100 %), majority of them that is, 30 (41.7 %) subjects had bilateral lymph node involvement, about 22 (30.6 %) subjects had right side involvement followed by 20 (27.8 %) subjects had left side involvement.

The majority of the subjects had lymph node size measuring 1 – 2 cm (42/58.3 %) and about 30 (41.7 %) of the patients had lymph node measuring > 2 cm. Among 72 subjects, majority 37 (51.4 %) of the subjects had Conglomerate lymph nodes followed by 1 lymph node in 22 (30.6 %) of the subjects and about 13 (18.1 %) subjects had 2 lymph nodes.

Majority 21 (29.2 %) of subjects had level II, III & IV lymph nodes involvement, 20 (27.8 %) of subjects had multilevel involvement, about 17 (23.6 %) had level I, about 13 (18.1 %) had level V and only 1 patient (1.4 %) had level IV lymph node involvement.

Most of the lymph nodes 49 (68.1 %) exhibited smooth margin and 23 (31.9 %) had irregular margins. Irregular margins and pericapsular spread were more commonly seen in malignant lymph nodes. Tuberculous lymph nodes may also show these features. Out of 72 subjects, majority 50 (69.4 %) of the subjects had oval shaped lymph nodes and 22 (30.6 %) had round shaped lymph nodes. Benign lymph nodes predominantly appeared oval in shape and malignant lymph nodes were round in shape.

---

In our study, benign lymph nodes predominantly appeared homogenous iso-intense on T1 weighted and homogenous hyperintense on T2 weighted and STIR images. However, malignant lymph nodes commonly appeared heterogeneous on T1 weighted, T2 weighted and STIR images.

Among 72 (100 %) subjects, 32 (44.4 %) subjects had lymph nodes showing restricted diffusion and 40 (55.6 %) subjects had lymph nodes which were not showing restricted diffusion on DWI with ADC. As per MRI diagnosis, 32 (44.4 %) were malignant, and 40 (55.6 %) were benign lymph nodes. As per HPE diagnosis, 30 (41.6%) were malignant, and 42 (58.4 %) were benign lymph nodes.

On pathological correlation, reactive lymphadenitis 23 (31.9 %) was the commonest pathological diagnosis followed by metastatic SCC 19 (26.4 %), tuberculous lymphadenitis 10 (13.9 %), acute suppurative lymphadenitis 7 (9.7 %), metastatic adenocarcinoma 5 (6.9 %), Hodgkin's lymphoma 3 (4.2 %), non-Hodgkin's lymphoma 2 (2.8 %), granulomatous lymphadenitis 2 (2.8 %) and acute chronic lymphadenitis 1 (1.4 %).

Among 72 (100 %) subjects, 30 pathologically proven malignant cases had ADC value of  $< 1.0 \times 10^{-3} \text{ mm}^2/\text{s}$  and 42 pathologically proven benign cases, 40 cases have ADC value of  $> 1.0 \times 10^{-3} \text{ mm}^2/\text{s}$  with 2 discrepancy cases showed ADC value of  $< 1.0 \times 10^{-3} \text{ mm}^2/\text{s}$  and were given as malignant, but were pathologically proven as benign case of tuberculous abscess. There was a statistically significant association (P-value  $< 0.001$ ) between ADC and pathological findings.

---

The ADC cut-off value of cervical lymph nodes as  $1.0 \times 10^{-3} \text{ mm}^2/\text{s}$  had overall sensitivity, specificity, positive predictive value, negative predictive value and accuracy of 100 %, 95.24%, 93.75 %, 100 % and 97.22 % respectively.

Therefore, the ADC value of cervical lymph nodes obtained had excellent predictive validity in predicting malignancy (P - value < 0.001).

---

## **LIMITATIONS AND RECOMMENDATIONS**

The present single center study was performed on a relatively small study population. Increasing the sample size would improve the statistical power of the results. Extracapsular spread, intranodal necrosis, irregular margins, heterogeneous appearance commonly observed in malignant lymph nodes can be seen in benign etiology like tuberculosis and granulomatous lymphadenitis.

ADC value is influenced by factors like cellularity, vascularity and matrix of lymph nodes, there may be some overlap between benign and malignant cervical lymph nodes.

Necrotic areas in metastatic lymph nodes show restricted diffusion with false low ADC values, hence ROI for calculating ADC values should be accurately placed in non-necrotic portion of lymph nodes.

# BIBLIOGRAPHY



---

## BIBLIOGRAPHY

1. Gupta A, Rahman K, Shahid M, Kumar A, Qaseem SMD, Hassan S, et al. Sonographic assessment of cervical lymphadenopathy: role of high-resolution and color Doppler imaging. *Head and Neck* 2011;33:297–302.
2. Adibelli ZH, Unal G, Gul E, Uslu F, Kocak U, Abali Y. Differentiation of benign and malignant cervical lymph nodes: value of B-mode and color Doppler sonography. *Eur J Radiol* 1998;28:230–4.
3. Castelijns JA, Van den Brekel MW. Imaging of lymphadenopathy in the neck. *Eur Radiol* 2002;12:727–38.
4. Warach S, Chien D, Li W, Ronthal M, Edelman RR. Fast magnetic resonance diffusion-weighted imaging of acute human stroke. *Neurology*. 1992;42:1717.
5. Sumi M, Sakihama N, Sumi T, Morikawa M, Uetani M, Kabasawa H, Shigeno K, Hayashi K, Takahashi H, Nakamura T. Discrimination of metastatic cervical lymph nodes with diffusion-weighted MR imaging in patients with head and neck cancer. *Am J Neuroradiol* 2003;24:1627-34.
6. Sumi M, Van Cauteren M, Nakamura T. MR microimaging of benign and malignant nodes in the neck. *Am J Roentgenology*. 2006;186:749-57.
7. Razek AA, Soliman NY, Elkhamary S, Alsharaway MK, Tawfik A. Role of diffusion-weighted MR imaging in cervical lymphadenopathy. *Eur Radiol* 2006;16:1468–77.
8. Kwee TC, Takahara T, Ochiai R, Nieuvelstein RA, Luijten PR. Diffusion-weighted whole-body imaging with background body signal suppression (DWIBS): features and potential applications in oncology. *Eur radiol* 2008;18:1937-52.

- 
9. Ishikawa M, Anzai Y. MR imaging of lymph nodes in the head and neck. *Neuroimaging Clinics*. 2004;14:679-94.
  10. King AD, Tse GM, Ahuja AT, Yuen EH, Vlantis AC, To EW, Van Hasselt AC. Necrosis in metastatic neck nodes: diagnostic accuracy of CT, MR imaging, and US. *Radiology*. 2004;230:720-6.
  11. Chong VF, Fan YF, Khoo JB. MRI features of cervical nodal necrosis in metastatic disease. *Clinical radiology*. 1996;51:103-9.
  12. Ferreira T. Comments on Castelijns and van den Brekel: Imaging of lymphadenopathy in the neck. *Eur radiol*. 2003;13:2236.
  13. Singh V. Development of blood vessels. *Textbook of clinical embryology*. Chapter 19. 2<sup>nd</sup> edition. Elsevier Limited; 2017:228-9.
  14. George AJT. Blood, lymphoid tissues and haemopoiesis. In: Standring S, editor. *Gray's Anatomy: The Anatomical Basis of Clinical Practice*. Chapter 4. 41<sup>st</sup> edition. Elsevier Limited. 2016:68-81.
  15. Young B, O'Dowd G, Woodford P. Immune system. *Wheater's functional histology: a text and colour atlas* Chapter 11 6<sup>th</sup> edition; Elsevier 2013:209-10.
  16. Bujoreanu I, Gupta V. Anatomy, Lymph Nodes. [Updated 2020 Aug 10]. In: StatPearls [Internet]. Treasure Island (FL): StatPearls Publishing; 2020.
  17. Singh I. Lymphatics and Lymphoid Tissue. In: Vasudeva N, Mishra S, editor. *Textbook of Human Histology*. Chapter 9 7<sup>th</sup> edition; Jaypee Brothers 2014: Pg 127-34.
  18. Choi I, Lee S, Hong YK. The New Era of the Lymphatic System: No Longer Secondary to the Blood Vascular System. *Cold Spring Harb Perspect Med* 2012;2006-445.
  19. Blum KS, Pabst R. Keystones in lymph node development. *J Anat* 2006;209:585-95.
-

- 
20. Dubey A, Jethani SL, Mehrotra N, Singh D. Development of the Human Lymph Nodes- A Histological Study. J Clin Diagn Res 2012;6:1155-7.
  21. Singh I. Cardiovascular System. In: Devi VS, editor. Human embryology. Chapter 15. 11<sup>th</sup> edition. Jaypee. 2018: Pg 59-60.
  22. Sadler TW. Cardiovascular system. Medical embryology. Chapter 13. 14<sup>th</sup> edition. Wolters Kluwer. 2019: Pg 219.
  23. Dubey A, Jethani SL, Mehrotra N, Singh D. Development of the Human Lymph Nodes- A Histological Study. J Clin Diagn Res 2012;6:1155-7.
  24. Dhingra PL, Dhingra S. Clinical methods in ENT. Diseases of Ear, Nose and Throat & Head and Neck Surgery. Chapter 76. 7<sup>th</sup> edition. 2018. Pg 374-90.
  25. Lo WC, Cheng PW, Wang CT, Liao LJ. Real-time ultrasound elastography: an assessment of enlarged cervical lymph nodes. Eur Radiol 2013;23:2351-7.
  26. Choi I, Lee S, Hong YK. The New Era of the Lymphatic System: No Longer Secondary to the Blood Vascular System. Cold Spring Harb Perspect Med 2012; 2006-445.
  27. Bujoreanu I, Gupta V. Anatomy, Lymph Nodes. [Updated 2020 Aug 10]. In: StatPearls [Internet]. Treasure Island (FL): StatPearls Publishing; 2020.
  28. Banjar FK, Wilson AM. Anatomy, Head and Neck, Supraclavicular Lymph Node. StatPearls Publishing 2019.
  29. Lang S, Kansy B. Cervical lymph node diseases in children. GMS Curr Top Otorhinolaryngol Head Neck Surg 2014;13:1-27.
  30. Nag D, Dey S, Nandi A, Bandyopadhyay R, Roychowdhury D, Roy R. Etiological study of lymphadenopathy in HIV-infected patients in a tertiary care hospital. J Cytol 2016; 33:66-70.
-

- 
31. Nwawka OK, Nadgir R, Fujita A, Sakai O. Granulomatous disease in the head and neck: developing a differential diagnosis. *Radiographics* 2014;34:1240-56.
  32. Ludwig BJ, Wang J, Nadgir RN, Saito N, Castro-Aragon I, Sakai O. Imaging of cervical lymphadenopathy in children and young adults. *AJR Am J Roentgenol* 2012; 199:1105-13.
  33. Radhakrishnan R, Kline-Fath BM. The Pediatric Head and Neck. Diagnostic ultrasound. Chapter 48. 5<sup>th</sup> edition. Elsevier. 2018. Pg 1628-71.
  34. Arora N, Singh J, Davessar JL. Evaluation of Cervical Lymph Node Metastasis in Head and Neck Cancers. *J Otolaryngol ENT Res* 2017;7:00219.
  35. Calabrese L, Jereczek-Fossa BA, Jassem J, Rocca A, Bruschini R, Orecchia R et al. Diagnosis and management of neck metastases from an unknown primary. *ActaOtorhinolaryngol Ital* 2005;25:2-12.
  36. Gaddey HL, Riegel AM. Unexplained Lymphadenopathy: Evaluation and Differential Diagnosis. *Am Fam Physician*. 2016;94:896-903.
  37. Roland NJ. Staging of head and neck cancer. In: Watkinson JC, Clarke RW, editor. *Scott-Brown's Otorhinolaryngology Head and Neck Surgery*. Chapter 4. 8<sup>th</sup> edition. CRC Press. 2019: Pg 35-47.
  38. Johns ME, Moscinski LC, Sokol L. Phenytoin-associated lymphadenopathy mimicking a peripheral T-cell lymphoma. *Mediterr J Hematol Infect Dis*. 2010;2:e2010028.
  39. Mohseni S, Shojaiefard A, Khorgami Z, Alinejad S, Ghorbani A, Ghafouri A. Peripheral lymphadenopathy: approach and diagnostic tools. *Iran J Med Sci*. 2014;39:158-70.

- 
40. Sumi M, Ohki M, Nakamura T. Comparison of sonography and CT for differentiating benign from malignant cervical lymph nodes in patients with squamous cell carcinoma of the head and neck. *AJR Am J Roentgenol.* 2001;176:1019-24.
  41. Mackenzie K, Watson M, Jankowska P, Bhide S, Simo R. Investigation and management of the unknown primary with metastatic neck disease: United Kingdom National Multidisciplinary Guidelines. *J LaryngolOtol* 2016;130:170-5.
  42. Pattanayak S, Chatterjee S, Ravikumar R, Nijhawan VS, Sharma V, Debnath J. Ultrasound evaluation of cervical lymphadenopathy: Can it reduce the need of histopathology/cytopathology? *Med J Armed Forces India* 2018;74:227-34.
  43. Ahuja A, Ying M. Sonography of neck lymph nodes. Part II: abnormal lymph nodes. *Clin Radiol* 2003;58:359-66.
  44. Sigrist RMS, Liao J, Kaffas AE, Chammas MC, Willmann JK. Ultrasound Elastography: Review of Techniques and Clinical Applications. *Theranostics* 2017;7:1303-29.
  45. Dietrich CF, Barr RG, Farrokh A, Dighe M, Hocke M, Jenssen C et al. Strain elastography- How to do it? *Ultrasound Int Open* 2017;3:e13-49.
  46. Alam F, Naito K, Horiguchi J, Fukuda H, Tachikake T, Ito K. Accuracy of sonographic elastography in the differential diagnosis of enlarged cervical lymph nodes: Comparison with conventional B-mode sonography. *AJR Am J Roentgenol.* 2008;191:604-10.
  47. Lo WC, Cheng PW, Wang CT, Liao LJ. Real-time ultrasound elastography: an assessment of enlarged cervical lymph nodes. *Eur Radiol.* 2013;23:2351-7.
-

- 
48. Zhang F, Zhao X, Ji X, Han R, Li P, Du M. Diagnostic value of acoustic radiation force impulse imaging for assessing superficial lymph nodes. *Medicine (Baltimore)*. 2017;96:e8125.
  49. Taljanovic MS, Gimber LH, Becker GW, Latt LD, Klauser AS, Melville DM et al. Shear-Wave Elastography: Basic Physics and Musculoskeletal Applications. *Radiographics*. 2017;37:855–70.
  50. Hoang JK, Vanka J, Ludwig BJ, Glastonbury CM, Benjamin J. Evaluation of Cervical Lymph Nodes in Head and Neck Cancer with CT and MRI: Tips, Traps, and a Systematic Approach. *AJR*. 2013;200:17–25.
  51. Yang L, Luo D, Li L, Zhao Y, Lin M, Guo W et al. Differentiation of malignant cervical lymphadenopathy by dual-energy CT: a preliminary analysis. *Sci Rep* 2016;6:31020.
  52. Zhong J, Lu Z, Xu L, Dong L, Qiao H, Hua R et al. The diagnostic value of cervical lymph node metastasis in head and neck squamous carcinoma by using diffusion-weighted magnetic resonance imaging and computed tomography perfusion. *Biomed Res Int* 2014;26:38-59.
  53. Çaylaklı F, Yılmaz S, Özer C, Reyhan M. The Role of PET-CT in Evaluation of Cervical Lymph Node Metastases in Oral Cavity Squamous Cell Carcinomas. *Turk Arch Otorhinolaryngol* 2015;53:67-72.
  54. Choure AA, Khaladkar SM, Jain S. Differentiation of benign and malignant cervical lymph nodes on MRI with special emphasis on DWI. *Int J Radiol Diagn Imaging* 2019;2:96-105.
-

- 
55. Zhang A, Song J, Ma Z, Chen T. Application of apparent diffusion coefficient values derived from diffusion-weighted imaging for assessing different sized metastatic lymph nodes in cervical cancers. *ActaRadiologica*. 2020;61(6):848-55.
  56. Sharma P, Rege RN, Renuka A, Kulasekaran DM. The Potential Role of Apparent Diffusion Coefficient Values In the Differentiation of Infective and Tuberculous Lymph Nodes of Neck-In Correlation with Histopathology. 2017.
  57. Chen C, Lin Z, Xiao Y, Bai P, Yue Q, Chen Y, Chen L. Role of diffusion-weighted imaging in the discrimination of benign and metastatic parotid area lymph nodes in patients with nasopharyngeal carcinoma. *Scientific Reports*. 2018 Jan 10;8:1-8.
  58. Ustabasioglu FE, Samanci C, Alis D, Samanci NS, Kula O, Olgun DC. Apparent diffusion coefficient measurement in mediastinal lymphadenopathies: differentiation between benign and malignant lesions. *Journal of Clinical Imaging Science*. 2017;7.
  59. de Boer P, Mandija S, Werensteijn-Honingh AM, van den Berg CA, de Leeuw AA, Jürgenliemk-Schulz IM. Cervical cancer apparent diffusion coefficient values during external beam radiotherapy. *Physics and imaging in radiation oncology*. 2019;9:77-82.
  60. Serour DK, Mahmoud BE, Daragily B, Elkholy SF. Lymph nodes in the head and neck cancer: would diffusion-weighted magnetic resonance imaging solve the diagnostic dilemma?. *Egyptian Journal of Radiology and Nuclear Medicine*. 2020;51:1-10.
  61. Kanmaz L, Karavas E. The role of diffusion-weighted magnetic resonance imaging in the differentiation of head and neck masses. *Journal of Clinical Medicine*. 2018 May 29;7:130.
-

- 
62. Parihar P, Goel V. Differentiating benign and malignant metastatic cervical lymph nodes by diffusion weighted MRI sequence. *Int J Anat Radiol Surg*. 2015;4:47-50.
  63. Herneth AM, Mayerhoefer M, Schernthaner R, Ba-Ssalamah A, Czerny C, Fruehwald-Pallamar J. Diffusion weighted imaging: lymph nodes. *European journal of radiology*. 2010;76(3):398-406.
  64. Sambandan T, ChristefiMapel R. Review of cervical lymphadenopathy. *JIADS*. 2011;2(1):31.
  65. Esen G. Ultrasound of superficial lymph nodes. *Eur J Radiol* 2006;58:345–59.
  66. Perronea A, Guerrisia Pietro, Izzob Luciano, et al. Diffusion weighted MRI in cervical lymph nodes: differentiation between benign and malignant lesions. *Eur J Radiol* 2011;77:281–6.
  67. Vandecaveye V, De Keyzer F, Vander Poorten V, Dirix P, Verbeken E, Nuyts S, Hermans R. Head and neck squamous cell carcinoma: value of diffusion-weighted MR imaging for nodal staging. *Radiology*. 2009; 251(1):134-46.
  68. Theony Harriet C, Keyzer Frederik De, King Ann D. Diffusion weighted MR imaging of head and neck. *Radiology*. 2012; 263(1):9–32.
  69. Ragheb AS, Rahman HM, Ismail AA, Nawar N. Can diffusion weighted image and apparent diffusion coefficient (ADC) differentiate benign from malignant cervical adenopathy? *The Egyptian Journal of Radiology and Nuclear Medicine*. 2014; 45(2): 377-86.

- 
70. ElSaid NA, Nada OM, Habib YS, Semeisem AR, Khalifa NM. Diagnostic accuracy of diffusion weighted MRI in cervical lymphadenopathy cases correlated with pathology results. *The Egyptian Journal of Radiology and Nuclear Medicine*. 2014; 45(4):1115-25.
  71. Serour DK, Mahmoud BE, Daragily B, Elkholy SF. Lymph nodes in the head and neck cancer: would diffusion-weighted magnetic resonance imaging solve the diagnostic dilemma?. *Egyptian Journal of Radiology and Nuclear Medicine*. 2020; 51(1):1-10.
  72. Mondal SK, Mandal PK, Samanta TK, Chakaborty S, Roy SD, Roy S. Malignant lymphoma in Eastern India: A retrospective analysis of 455 cases according to World Health Organization classification. *Indian J Med Paediatr Oncol* 2013;34:242-6.
  73. Hoang JK, Vanka J, Ludwig BJ, Glastonbury CM. Evaluation of cervical lymph nodes in head and neck cancer with CT and MRI: tips, traps, and a systematic approach. *Am J Roentgenology*. 2013;200: 17-25.
  74. Curtin HD, Ishwaran H, Mancuso AA, Dalley RW, Caudry DJ, McNeil BJ. Comparison of CT and MR imaging in staging of neck metastases. *Radiology* 1998; 207:123–130
  75. Liu Z, Xun X, Wang Y, Mei L, He L, Zeng W, Wang CY, Tao H. MRI and ultrasonography detection of cervical lymph node metastases in differentiated thyroid carcinoma before reoperation. *Am J Translational Research*. 2014;6:147.
  76. Holzapfel K, Duetsch S, Fauser C, Eiber M, Rummeny EJ, Gaa J. Value of diffusion-weighted MR imaging in the differentiation between benign and malignant cervical lymph nodes. *Eur j radiol*. 2009;72(3):381-7.
-

- 
77. De Bondt RB, Nelemans PJ, Hofman PA, Casselman JW, Kremer B, van Engelshovenet al. Detection of lymph node metastases in head and neck cancer: a meta-analysis comparing US, USgFNAC, CT and MR imaging. *Eur j radiol.* 2007;64(2):266-72.
  78. Sumi M, Sakihama N, Sumi T, Morikawa M, Uetani M, Kabasawa H, Shigeno K, Hayashi K, Takahashi H, Nakamura T. Discrimination of metastatic cervical lymph nodes with diffusion-weighted MR imaging in patients with head and neck cancer. *Am J Neuroradiol.* 2003;24 (8):1627-34.
  79. Abdel Razek AA, Soliman NY, Elkhamary S, Alsharaway MK, Tawfik A. Role of diffusion-weighted MR imaging in cervical lymphadenopathy. *Eur radiol.* 2006;16 (7):1468-77.
  80. Elbadry MS, Mohammad MA. Benign Versus Malignant Cervical Lymph Nodes; Differentiation by Diffusion Weighted MRI. *Benha Medical Journal.* 2022; Radiology: 194-209.

# ANNEXURE



---

## **PROFORMA FOR DISSERTATION**

### **Demographic details:**

Name:

Age:

Address:

### **Clinical History:**

### **Local Examination:**

### **Conventional MRI Findings:**

1.Size	
2.Shape	
3. Margin	
4.Signal intensity on T2/T1 images	
5.Ancillary findings	

### **DWMRI/ADC findings:**

<b>DWI</b>	<b>ADC Values</b>	<b>DIAGNOSIS</b>

### **DWMRI/ADC diagnosis:**

### **Pathological Diagnosis:**

---

## **PATIENT CONSENT FORM**

**Chief researcher/ PG guide's name: Dr. ANIL KUMAR SAKALECHA**

**Principal investigator: Dr. K.N.MADAN KUMAR**

Name of the subject:

Age:

Gender:

- a.** I have been informed in my own language that this study involves MRI Neck as part of procedure. I have been explained thoroughly and understand the procedure.
- b.** I understand that the medical information produced by this study will become part of institutional record and will be kept confidential by the said institute.
- c.** I understand that my participation is voluntary and may refuse to participate or may withdraw my consent and discontinue participation at any time without prejudice to my present or future care at this institution.
- d.** I agree not to restrict the use of any data or results that arise from this study provided such a use is only for scientific purpose(s).
- e.** I confirm that Dr. K.N.Madan Kumar / Dr. Anil Kumar Sakalecha (chief researcher/ name of PG guide) has explained to me the purpose of research and the study procedure that I will undergo and the possible risks and discomforts that I may experience, in my own language. I hereby agree to give valid consent to participate as a subject in this research project.

**Participant's signature/thumb impression**

**Signature of the witness:**

**Date:**

1)

2)

*I have explained to ----- (subject) the purpose of the research, the possible risk and benefits to the best of my ability.*

**Chief Researcher signature/Guide signature**

**Date:**

---

## **PATIENT INFORMATION SHEET**

**Principal Investigator: Dr. K.N.MADAN KUMAR / Dr. ANIL KUMAR SAKALECHA**

I, Dr. K.N.Madan Kumar., post-graduate student in Department of Radio-Diagnosis at Sri Devaraj Urs Medical College. I will be conducting a study titled “Role of Diffusion Weighted MRI and Apparent Diffusion Coefficient values in differentiating benign from malignant cervical lymph nodes” for my dissertation under the guidance of Dr. Anil Kumar Sakalecha, Professor & HOD, Department of Radio-Diagnosis. In this study, we will assess the role of MR mammography in differentiating benign from malignant breast mass. You will not be paid any financial compensation for participating in this research project.

All of your personal data will be kept confidential and will be used only for research purpose by this institution. You are free to participate in this study. You can also withdraw from the study at any point of time without giving any reasons whatsoever. Your refusal to participate will not prejudice you to any present or future care at this institution

**Name and Signature of the Principal Investigator**

**Signature of the Guide**

**Date:**

# MASTER CHART



---

## ABBREVIATIONS

M: Male

F: Female

B/L: Bilateral

R: Right

L: Left

Iso: Isointense

Hyper: Hyperintense

Hetero-hyper: Heterogeneously hyperintense

R: Restricted diffusion – present

NR: No restricted diffusion

ReacLym: Reactive lymphadenitis

Acute supplymadenitis: Acute suppurative lymphadenitis

Mets SCC: Metastatic squamous cell carcinoma

TB: Tuberculous lymphadenitis

Acute suppgranulL.adenitis: Acute suppurative granulomatous lymphadenitis

1	NAME	AGE	SEX	side	NO.	SIZE	SHAPE	MARGINS	LEVELS	INTENSITY( T1 & T2)	DWI	ADC	Pathological findings	Benign/malignant	
2	ANJINAPPA	66	M	B/L	1	> 1 cm	oval	irregular	supra clavicular	iso	hetero hyper	NR	1.6	reactive lym	BENIGN
3	ANUPAMA	24	F	B/L	multiple	> 1 cm	oval	smooth	level 2, 3	iso	hetero hyper	NR	1.1	Reac lym	BENIGN
4	BHAVAN SAI	18	M	B/L	Multiple	> 1 cm	oval	smooth	level 2, 3,4	iso	hetero hyper	NR	1.2	Reac lym	BENIGN
5	CHANDRAMMA	35	F	B/L	2	> 1 cm	oval	smooth	level 2	iso	hetero hyper	R	0.9	Reac lym	BENIGN
6	VISHWAMURTHY	59	M	R	2	> 1 cm	Round	smooth	level 2, 3	iso	hyper	NR	2.2	Acute supp lymadenitis	BENIGN
7	SIDDHAYELLAPPA	47	M	B/L	Multiple	> 2 cm	oval	smooth	level 2, 3,4	iso	hyper	NR	1.3	Reac lym	BENIGN
8	RAGHUNATHA RAO	67	M	R	1	> 2 cm	Round	irregular	level 5	iso	hyper	NR	1.7	Acute on chronic lymadenitis	BENIGN
9	GEETHA	25	F	B/L	2	> 1 cm	oval	smooth	level 2	iso	hetero hyper	NR	1.4	Reac lym	BENIGN
10	HARISH KUMAR	56	M	B/L	2	> 1 cm	oval	smooth	level 2	iso	hetero hyper	NR	1.5	Reac lym	BENIGN
11	KALLAMMA	57	F	R	Multiple	> 1 cm	Round	smooth	level 2, 3,4	iso	hetero hyper	NR	1	Reac lym	BENIGN
12	MANJUNATHA	35	M	B/L	Multiple	> 1 cm	Round	smooth	level 1B, 2, 3,4	iso	hetero hyper	NR	1.1	Reac lym	BENIGN
13	RAMA DEVI	55	F	R	2	> 1 cm	Round	smooth	level 1B	iso	hetero hyper	NR	1.3	Reac lym	BENIGN
14	SAROJAMMA	56	F	R	1	> 1 cm	oval	smooth	level 2	iso	hetero hyper	R	1.2	Reac lym	BENIGN
15	SPANDANA	5	F	B/L	Multiple	> 1 cm	oval	smooth	level 1B	iso	hetero hyper	R	0.9	Acute supp lymadenitis	BENIGN
16	VENKATRONAPPA	55	M	L	1	> 1 cm	oval	smooth	level 4	iso	hetero hyper	NR	1.2	Reac lym	BENIGN
17	VISHWANATH	45	M	B/L	Multiple	> 1 cm	Round	smooth	level 1B	iso	hetero hyper	R	1.2	Reac lym	BENIGN
18	CHIKKAMMAYA	45	F	B/L	multiple	> 1 cm	oval	smooth	level 1B,2	iso	hetero hyper	NR	1	Reac lym	BENIGN
19	GIDEON	46	M	B/L	2	> 1 cm	Round	smooth	level 1B	iso	hetero hyper	R	0.9	Reac lym	BENIGN
20	GOWRAMMA	40	F	R	multiple	> 2 cm	oval	irregular	level 1B, 2, 3,4,5	iso	hetero hyper	NR	1.2	Acute supp lymadenitis	BENIGN
21	LAVANYA	18	F	L	1	> 1 cm	oval	smooth	level 1B	iso	hetero hyper	R	0.9	Reac lym	BENIGN
22	SUMANA	52	F	L	multiple	> 1 cm	oval	smooth	level 1B	iso	hetero hyper	R	0.8	Reac lym	BENIGN
23	ARUNA	28	F	B/L	multiple	> 1 cm	oval	smooth	level 1B	iso	hetero hyper	R	0.7	Reac lym	BENIGN
24	JAYAMMA	58	F	L	multiple	> 2 cm	Round	irregular	level 5	iso	hetero hyper	R	0.9	Mets scc	MALIGNANT
25	MOHAMMED HUSSAN	66	M	B/L	multiple	> 1 cm	Round	smooth	level 2, 3,4,5	iso	hetero hyper	R	0.8	Mets scc	MALIGNANT
26	MUNIYAMMA	65	F	L	multiple	> 2 cm	Round	irregular	level 5	iso	hetero hyper	R	1	Mets scc	MALIGNANT
27	MUNIYAPPA	67	M	L	2	> 1 cm	oval	smooth	level 1B	iso	hetero hyper	R	0.8	Reac lym	BENIGN
28	PAPAMMA	65	F	L	1	> 1 cm	Round	irregular	level 1B	iso	hetero hyper	R	0.7	scc	MALIGNANT
29	PILAPPA	72	M	B/L	multiple	> 1 cm	oval	irregular	level 6	iso	hetero hyper	NR	0.9	SCC	MALIGNANT
30	RAJANNA	50	M	B/L	multiple	> 2 cm	oval	irregular	level 1B,2, 3,4,5	iso	hetero hyper	R	1.2	SCC	MALIGNANT
31	RANJITH KUMAR	27	M	L	multiple	> 2 cm	Round	smooth	level 1B,2, 3,4,5	iso	hyper	R	0.7	Hodgkins Lymphoma	MALIGNANT
32	RASOOL SAB	50	M	B/L	multiple	> 2 cm	oval	irregular	level 1B,2, 3,4,5	iso	hetero hyper	R	0.8	Poorly diff scc	MALIGNANT
33	REDDAPPA	41	M	L	multiple	> 1 cm	oval	smooth	level 5	iso	hetero hyper	R	0.9	Lymphoma	MALIGNANT
34	VENKATRAMAIAH	62	M	L	multiple	> 2 cm	oval	irregular	level 1B,2, 3,4	iso	hetero hyper	R	0.8	SCC	MALIGNANT
35	VENKATAMMA	63	F	L	multiple	> 2 cm	Round	irregular	level 5	iso	hetero hyper	R	1	Mets scc	MALIGNANT
36	NIRANJAN	60	M	L	2	> 1 cm	oval	smooth	level 5	iso	hetero hyper	R	0.9	CA STOMACH METS	MALIGNANT
37	SEENAPPA	60	M	R	1	> 1 cm	Round	irregular	level 1B	iso	hyper	R	0.6	Non Hodgkins	MALIGNANT
38	RAVI	38	M	B/L	2	> 1 cm	oval	smooth	level 1B	iso	hetero hyper	R	0.7	Well def scc	MALIGNANT
39	paravathamma	25	f	R	multiple	> 2 cm	oval	irregular	level 2, 3,4,5	iso	hetero hyper	R	1.5	Papillary ca thyroid mets	MALIGNANT
40	SEENAPPA	70	M	B/L	MULTIPLE	> 2 cm	oval	irregular	level 2, 3,4,5	iso	hetero hyper	R	0.6	Lymphoma	MALIGNANT

41	GOPAL	61	M	B/L	MULTIPLE	>1 cm	Round	Smooth	level 1B,2,3,4,5	iso	hetero hyper	NR	1.6	Reac lym	BENIGN
42	RAJENDRA REDDY	45	M	B/L	2	>1 cm	oval	Smooth	level 2	iso	hyper	NR	1.8	Cervical lymphadenitis	BENIGN
43	KRISHNAPPA	76	M	L	MULTIPLE	> 2 cm	oval	irregular	Level 2, 3,4,5	iso	hetero hyper	NR	1.9	Reac lym	BENIGN
44	srinivas	51	M	L	1	>1 cm	oval	Smooth	level 2	iso	hyper	R	0.9	SCC	MALIGNANT
45	Nagamma	58	F	L	1	> 2 cm	oval	Smooth	supra clavicular	iso	hyper	NR	2.3	TB	BENIGN
46	Mahadevappa	75	M	B/L	MULTIPLE	> 2 cm	oval	Smooth	level 1B,2,3,4,5	iso	hyper	R	0.6	Granulomatous lymphadenitis	BENIGN
47	Siddha yellappa	65	M	B/L	MULTIPLE	> 2 cm	oval	irregular	level 1B,2,3,4,5	iso	hetero hyper	R	0.8	SCC	MALIGNANT
48	LAKSHMAMMA	70	F	R	1	> 2 cm	oval	Smooth	level 2	iso	hyper	NR	1.5	Acute supp lymadenitis	BENIGN
49	HEMAVATHI	33	F	B/L	2	> 1 CM	Round	Smooth	level 1A	iso	hyper	R	0.8	Cervical lymphadenitis	BENIGN
50	SNEHA	21	F	R	1	> 1 CM	oval	Smooth	level 2	iso	hyper	NR	1.2	Reac lym	BENIGN
51	NARAYANA REDDY	80	M	B/L	MULTIPLE	> 2 cm	oval	Smooth	level 1B,2,3,4,5	iso	hyper	R	0.6	Lymphoma	MALIGNANT
52	CHANDRASEKAR	22	M	R	1	>1 CM	oval	Smooth	level 1B	iso	hyper	NR	1.2	Reac lym	BENIGN
53	LAKSHMI DEVAMMA	43	F	R	1	>1 CM	oval	Smooth	level 1B	iso	hyper	NR	1.6	Reac lym	BENIGN
54	MEGHNA	23	F	B/L	MULTIPLE	>1 CM	oval	Smooth	level 1B,2,3,4	iso	hyper	R	1	Cervical lymphadenitis	BENIGN
55	MOHAMMAD ALI	50	M	R	MULTIPLE	> 2 cm	oval	Smooth	level 1B,2,3,4,5	iso	hyper	R	0.7	CA STOMACH METS	MALIGNANT
56	GOVINDAPPA	59	M	R	MULTIPLE	> 2 cm	oval	Smooth	level 1B,2,3,4,5	iso	hyper	R	0.7	SCC	MALIGNANT
57	MUGILAPPA	62	M	R	2	> 2 cm	oval	Smooth	level 5	iso	hyper	R	0.7	SCC	MALIGNANT
58	NAGARAJ	37	M	L	1	>1 CM	Round	Smooth	level 1B	iso	hyper	NR	1.2	Acute supp lymadenitis	BENIGN
59	JAYARAM REDDY	70	M	B/L	1	>1 CM	oval	Smooth	level 4	iso	hyper	NR	1.6	TB	BENIGN
60	GANGAPPA	68	M	R	1	>1 CM	oval	Smooth	level 1B	iso	hyper	R	0.9	SCC	MALIGNANT
61	KRISHNA SHETTY	74	M	B/L	MULTIPLE	> 2 cm	Round	Smooth	supra clavicular	iso	hyper	R	0.8	CA STOMACH METS	MALIGNANT
62	DINESH	19	M	L	MULTIPLE	>1 CM	oval	Smooth	Level 2,3,4	iso	hyper	NR	1.3	Cervical lymphadenitis	BENIGN
63	RAMAPPA	70	M	R	1	> 2 cm	Round	irregular	supra clavicular	iso	hyper	R	0.8	CA STOMACH METS	MALIGNANT
64	VENKATAMMA	63	F	L	1	> 2 cm	oval	irregular	supra clavicular	iso	hyper	R	1.2	CA STOMACH METS	MALIGNANT
65	MUNIRATHNAMMA	51	F	R	1	> 2 cm	oval	Smooth	Level 3	iso	hyper	NR	2	Reac lym	BENIGN
66	VENKATESH	40	M	L	MULTIPLE	> 2 cm	oval	irregular	level 1B,2,3,4,5	iso	hetero hyper	R	0.8	Mets scc	MALIGNANT
67	SHALET	20	F	R	MULTIPLE	>1 CM	oval	Smooth	Level 2,3,4 & S.C	iso	hyper	NR	1.1	Acute supp lymadenitis	BENIGN
68	SUBBANNA	73	M	B/L	MULTIPLE	> 2 cm	Round	Smooth	Level 2,3,4 & S.C	iso	hyper	NR	2	Acute supp lymphadenitis	BENIGN
69	DADHAN	4	M	R	2	>1 CM	Round	Smooth	Level 2	iso	hyper	NR	1.4	Reac lym	BENIGN
70	SARWARI BEGUM	50	F	R	1	> 2 cm	oval	irregular	Level 2,3,4	iso	hyper	R	0.6	Hodgkins Lymphoma	MALIGNANT
71	NARAYANSWAMY	47	M	R	1	> 2 cm	oval	irregular	Level 2	iso	hyper	R	0.8	Mets scc	MALIGNANT
72	GOVINDAPPA	50	M	B/L	MULTIPLE	>1 CM	Round	irregular	Level 2,3,4	iso	hyper	R	0.7	Mets scc	MALIGNANT
73	THULASAMMA	26	F	L	1	> 2 cm	oval	irregular	supra clavicular	iso	hyper	NR	1.6	Acute supp granul l.adenitis	BENIGN